



THE SPECIAL ISSUE
IIOAB
JOURNAL

VOLUME 7 : NO 3 : AUGUST 2016 : ISSN 0976-3104

**Institute of Integrative Omics and
Applied Biotechnology Journal**

Dear Colleagues and Visionaries,

It is my distinct honor and privilege to extend a warm welcome to all contributors and enthusiasts joining our scientific journal, dedicated to exploring the frontiers of Advances in Pattern Recognition, Soft Computing, and Machine Learning.

As the Editor of this esteemed IIOAB Journal issue, I am thrilled to witness the convergence of innovative methodologies and cutting-edge technologies in these dynamic fields. Our journal serves as a catalyst for disseminating transformative research, novel algorithms, and pioneering applications that propel the realms of pattern recognition, soft computing, and machine learning to new heights.

Your expertise, relentless pursuit of knowledge, and scholarly contributions form the bedrock of advancements in these interconnected domains. Your work in developing robust algorithms, refining recognition techniques, and harnessing the power of soft computing and machine learning algorithms is instrumental in shaping the future of artificial intelligence and data-driven decision-making.

The interdisciplinary nature of this realm not only fosters innovation but also holds the promise of revolutionizing industries, healthcare, cybersecurity, and more. Your dedication to pushing the boundaries of these fields is invaluable, laying the groundwork for transformative breakthroughs with far-reaching implications.

I encourage each of you to share your pioneering insights, submit your groundbreaking research, and actively engage in the vibrant discussions within our journal. Let us collaboratively cultivate an environment where ideas flourish, collaborations thrive, and knowledge drives us toward unparalleled advancements.

Thank you for your unwavering commitment to advancing the frontiers of pattern recognition, soft computing, and machine learning. I eagerly anticipate the wealth of transformative insights and discoveries that will emanate from your contributions.

Warm regards,

*Prof. Steven Lawrence Fernandes
Editor-in-Chief*



TOUCH SCREEN CONTROLLED DEFENSE ROBOT: A COMPREHENSIVE REVIEW

Ramesh Nayak, Mithuna Shetty, Rakesh Ganapathi, Sushwitha Naik, Varsha Aithal*

Dept. of IS & E, Canara Engineering College, Benjanapadavu, Mangaluru, Karnataka, INDIA

ABSTRACT

Robots play a major role in many walks of life and are extensively used in the areas of defense, industries, medical and home appliances. They can carry out different risky jobs that cannot be done by human. The robot system can be built with the existing economic condition that can be used for different sophisticated robotic application. The control system consists of Touch screen and ZigBee modules, a microcontroller that collects and controls the robot. The system provides continuous visual monitoring through the wireless camera attached to the robot and sends continuous data to the control unit. The robotic arm fitted on the robot is employed for pick and place operations while the laser gun attached to the robot is utilized to hit the target object. The body of the robot consists of two wheels attached to geared motors. The robot is controlled through a Touch screen which is mounted on ARM9 via "ZIGBEE" device.

Received on: 09th-Dec-2015

Revised on: 27th-Jan-2015

Accepted on: 14th-Feb-2015

Published on: 04th-Apr -2016

KEY WORDS

Defense robot; ZigBee module; wireless camera; Touch screen; Laser gun

*Corresponding author: Email: varshaathal30@gmail.com; Tel: +91-8904094802; Fax: +40-9001010012

INTRODUCTION

The defence robot is fully controlled by the touch screen and the commands from the touchscreen via ZigBee transmitter were received by the microcontroller. So this defense robot can be used in military applications [1]. An automated defense robot building is planned, that has a laser gun attached, which is utilized for pointing laser rays to destroy the target object [1]. One of the most important things about these robots is that they have the capability to perform missions remotely in the field, without any actual danger to human lives [2]. In the proposed system, a robot is developed that is controlled through mini ARM9 (S3C2440) instead of PC, since ARM9 is portable [2]. This is specially designed defense robotic system to save human life and protect the country from enemies. This robot is attached with a robotic arm which is used to perform pick and place operations [3]. These defense robots used in military are usually employed with the integrated system including gripper, cameras and sensors [3, 4]. Robot is used to sense moving objects and metals hence this system is proposed with the help of low power ZigBee wireless sensor network to trace out the intruders and the robot will take the necessary action automatically [5]. This is specially designed defense robotic system to save human life and protect the country from enemies. In the existing systems, personal computer using ZigBee protocol is used to monitor the mobile robot. The robot has a camera attached, with the help of which, the robot can be driven to remote places [6]. The outcome of different activities can be monitored and displayed on ARM9 screen. A recent advancement in the technology has led everything in this world to go and connect to the Internet [7]. Using internet also the devices can be connected remotely. Either manually controlled or automatic controlled robots are developed in recent years [8]. Robots can also be used to sense bombs and fires and they can also be used to diffuse the bomb or cease the fire [9].

LITERATURE SURVEY

Application of radio frequency controlled intelligent military robot in defence

This robot can be used in defense and in real war field. It has a two barrel gun turret through which bullets can be fired. It has two cameras which are used to send the real time videos and audios and which can rotate up and down, left and right up for safety. The robot is radio operated; self-powered, has back tracking facility, in case of

loss of connection from the base station. For the aiming purpose and to view the road and the surroundings in which the robot is travelling, wireless cameras are installed. Radio frequency can be used to control the robot.

Table 1. The review report of the 10 latest papers

Refs	Mode of control	Robot using Android application	Technology used	Mode of vision	Interface used	Sensors and defense used	Robot with Pick and Place
[1]	Remote Control	Implemented	--	--	GUI	--	Implemented
[2]	Remote Controlled	--	Cloud Technology	Computer Vision	--	Light follow	--
[3]	--	--	Radio frequency	Camera	--	Backtrack Facility /Gun	--
[4]	--	--	Wireless	--	ZigBee	Fire & Humidity	--
[5]	--	Smart Phone	Wireless/RF	Camera	--	Bomb detection	--
[6]	--	Smart Phone	Image processing/ Wireless	--	ZigBee	--	--
[7]	Master/ Slave	--	Wireless	--	ZigBee	--	--
[8]	Automatic and Remote	--	--	--	--	Bomb Detector	--
[9]	--	--	Wireless	--	ZigBee	Non-Holonomic	--
[10]	Remote	--	--	Camera	--	Bomb Detector	--
Proposed System	Automatic	--	Wireless	Wireless Camera	ZigBee	Gun/ Obstacle	Implemented

7th sense: a multipurpose robot for military

Thus aim is to provide a robotic system that can combat in wars and other military purposes. This system is the first of several such programs that are looking at revamping the infantry soldier's gear. It basically has two modes. One mode is the automatic mode and the other mode is user control mode. The automatic mode uses face recognition technique to combat intruders. In certain unavoidable circumstances the control comes to user who can control the operations of the robot from remote location using a computer. One of the main advantages of our system is that the mode switching can be done very fast without any delay. It also helps to provide medical aid for needy.

Wireless control of pick and place robotic arm

In few places where humans cannot touch metallic objects or suspected objects (Bombs) this project can be used. The remote operations can be controlled using android application .It has a transmitting and receiving end. . The main advantage of this robot is to avoid extra pressure on the suspected objects. The android application device transmitter acts as a remote control that has the advantage of adequate range, while the receiver end Bluetooth device is connected to the microcontroller to drive DC motors via motor driver IC for necessary operation.

Development of a robotic arm for dangerous object disposal

This project is being carried out to detect the deadly act such as bomb and dangerous unsuspected objects this results in loss of number of lives. Hence this paper proposes the development of a robotic arm for dangerous

object disposal. Using integrated development environment, robotic arm was developed. Microcontroller programmed with integrated development environment software is used. This device has a camera which transmits the captured video to a television set. The system is activated by a remote control thereby providing a line of defence to human lives and preventing loss of proven and tested personnel.

Quality of connectivity guarantee of ZigBee based wireless mobile sensor network

Cases such as environmental monitoring exploration security service the sensor networks are being used. In this paper motion planning and connectivity of multiple robots is based on the sensor networks which are distributed in a ZigBee. In a rescue task it changes dynamically, where the robots need to keep connectivity between other robots. This method enables the mobile robot to be controlled under non holonomic constraint which is related to the quality of communication as a real time and real world application.

Mobile robotic system for search mission

Robots are being used increasingly since it has multiple features like it can be controlled through smart phones, avoid obstacles, diffuse bomb and perform critical tasks. This project is being used for rescue and search mission. This robot is controlled wirelessly using RF technology and it uses ultrasonic sensors to detect obstacles. It is equipped with a camera to provide multidirectional view can send video stream wirelessly to the device. The places which cannot be reached by the human can be accessed by this robot.

A study of IOT enabled smart store

It is usually found that the store owners find it difficult to refill the store periodically. To make the store smart the proposed system uses Internet of Things (IOT) technology. With the smart phone the store owner will get the notification about their stocks and the various requirements of the store. Hence it will be easy for the store owner to refill the store. Various options can be selected by the customer based on their need. The current status of the store and the products available can be known using the Smart Store App.

Eagle O: a semi-autonomous robot

Autonomous robots have many applications in manufacturing industry, space exploration, defence research, etc. A semi-autonomous robot can be build using this project. A key characteristics of this robot it follow light source for navigation purpose and captures physical data in real time mode. . The other goal behind this project is to develop a model for space exploration robots. It is very unlikely this robot can be operated in the space

Implementation of an in-campus fire alarm system using ZigBee

A centralized wireless fire control system using wireless sensor network technology is developed to protect huge area, like a college campus or an industrial park. The five danger prone zones of the campus is connected with a central control room through a ZigBee communication interface such that in case of any fire break in any of the building, a direct communication channel is developed that will send an immediate signal to the control room. Multi hopping technique is adopted for the effective transmitting of the signal in case if any of the emergency zone lies out of reach of the central node. The system developed is implemented in Atmega32 with temperature and fire and humidity sensors.

Real-time indoor surveillance based on smart phone and mobile robot

Image processing techniques, fuzzy theory, wireless communications, and Smartphone are integrated to a wheeled mobile robot (WMR) for the purpose such as real-time object recognition, tracking and indoor surveillance. Command signals are transmitted using ZigBee technology between web camera, wheeled mobile robot and the base computer [10]. The Webcam is used to capture its surroundings of WMR. Hue-Saturation-Value (HSV) colour space is used for classification of colours. Experiments show that the proposed control design and system integration of the wheeled mobile robot works well in indoor real-time surveillance. The WMR is applied to surveillance usage, it can be controlled remotely by a smart phone via WIFI and perform indoor patrol and monitor its surroundings

PROPOSED METHODOLOGY

Looking at the [Table-1](#) the proposed system methodology are asfollowing:

ARM7 LPC2148

The LPC2148 microcontroller is 32 bit, 64 pin operating at 3.3V, 12 MHz crystal for system clock and 32 KHz crystal for RTC. Internal MUC has 512 KB flash memory and 40KB static RAM. A 128-bit wide memory interface and unique accelerator architecture enable 32-bit code execution at the maximum clock rate.

ARM9 S3C2440

ARM9 S3C2440 is designed to provide hand- held devices for general application with low power and high performance. It has speed of 400 MHz with RAM of 64 MB. Flash memory capacity is 1 GB. It has special features like audio I/O, camera, USB and Ethernet. Its Operating supply is at 5V and it supports Windows and Linux.

Zigbee

ZigBee is a low-cost, low-power, wireless protocol defined in IEEE standard 802.15.4 (2003 version) for low-rate WPANs. It is highly secure, reliable and easy to install. Data transmission rates vary from 20 kilobits/second in the 868 MHz frequency band to 250 kilobits/second in the 2.4 GHz frequency band.

L293D driver

L293D driver is a 16 pin Motor Driver IC which allows DC motor to drive in either direction. It can supply a maximum current of 600mA per channel. In the proposed system two L293D are used.

PIR sensor

Passive Infra-Red Sensor is used for detecting moving objects. Its operation is based on infrared technology. It operates with high sensitivity, high reliability and ultra-low voltage operating mode. This sensor is used to detect presence of intruders in the secure zone.

Inductive proximity sensor

Inductive proximity sensor is used to detect metallic targets. The main components of the inductive proximity sensor are coil, oscillator, detector and the output circuit. Any metallic target in the coil's magnetic field absorbs some energy which affects the oscillator field. Once the oscillation amplitude of the disturbance reaches a threshold value, the sensor is triggered. This sensor is used to detect presence of explosives.

Wireless camera

Camera mounted on the robot section has linear transmission distance of 50 - 100M. The operating voltage level of transmitting unit is 9V DC and the current level is 300mA. It has resolution up to 1280 x 480 pixels. This is used for broadcasting live information to control unit for necessary action to be taken.

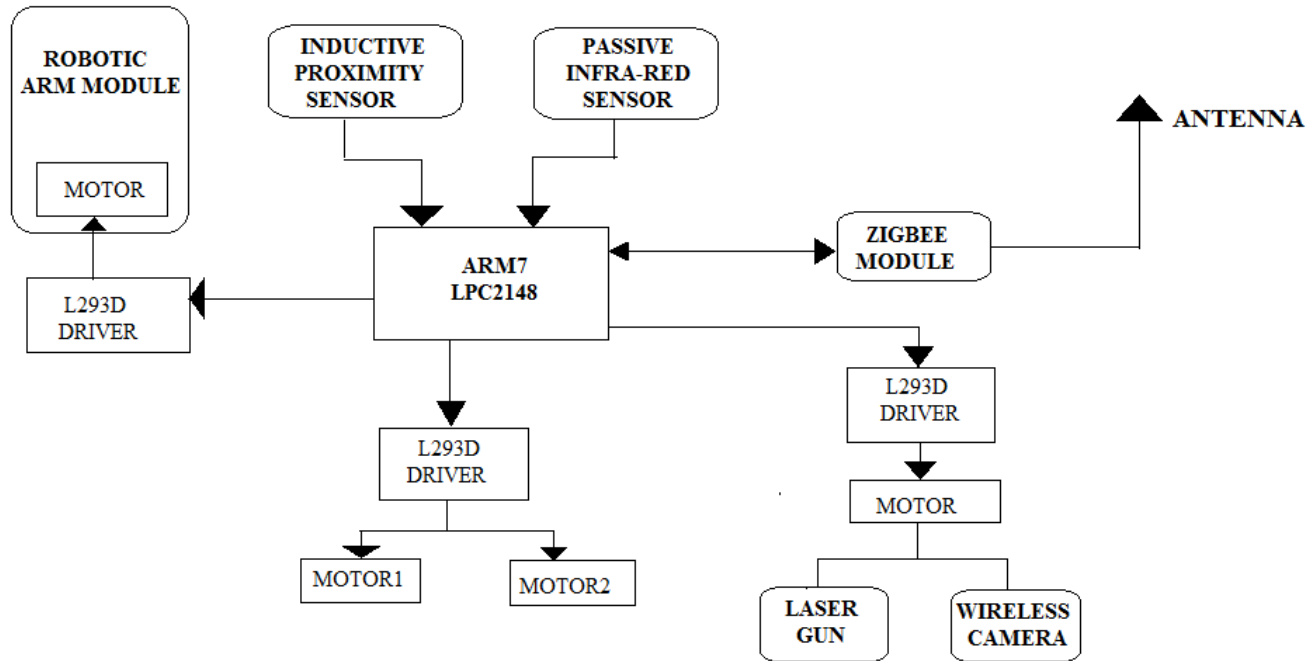


Fig: 1. Architecture of robot unit

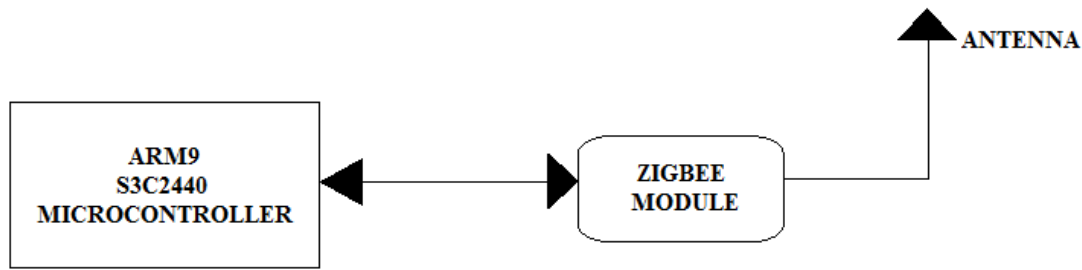


Fig: 2. Architecture of control unit

P1.24, P1.25, P1.26 is assigned to a variable SW1, SW2, SW3. P1.16 is assigned to COIL_A which is the stepper motor port. For the movement of the robot in forward and backward direction three functions are used which is delay (int), motor_cw() is a clockwise rotate function and motor_ccw() is anticlockwise rotate function.

This software is used to burn the hex file from the Keil software on to the microcontroller. There are 5 steps before which we can burn the hex file on to the microcontroller. The entire project phases are shown in figure one by one. **Figure- 1** will indicate the architecture of the robot unit. **Figure- 2** will show architecture of only control unit. **Figure- 3** will show the snapshot of the Keil Software. **Figure- 4** will indicate the snapshot of the Flash Magic. The final figure, that is, **Figure- 5** will show the snapshot of the robot. This is the hardware model of the Project.

```

C:\Keil\ARM\Examples\Measure\Measure.uvproj - uVision4
File Edit View Project Flash Debug Peripherals Tools SVCS Window Help
MCB2130
Abstract.txt STP.C*
026
027 #include <lpc21xx.h>
028 #include <stdio.h>
029 #define SW1 24 //SW1 (P1.24)
030 #define SW2 25 //SW2 (P1.25)
031 #define SW3 26 //SW3 (P1.26)
032 #define COIL_A 16
033 void motor_cw(void);
034 void motor_ccw(void);
035 void delay(int);
036 unsigned char STEP[] = {0x09, 0x0C, 0x06, 0x03};
037
038 void delay(int n)
039 {
040     int i,j;
041     for(i=0;i<n;i++)
042     {
043         for(j=0;j<0x3FF0;j++)
044             {};
045     }
046 }
047 void motor_cw(void)
048 {
049     unsigned int i=0;
050     while (STEP[i] != '\0')
051     {
052         IOSET1 = STEP[i] << COIL_A;
053         delay(5);
054         IOCLR1 = STEP[i] << COIL_A;
055         delay(5);
056         i++;
057     }
058 }
059 }
060
    
```

Fig. 3. Snapshot of Keil software

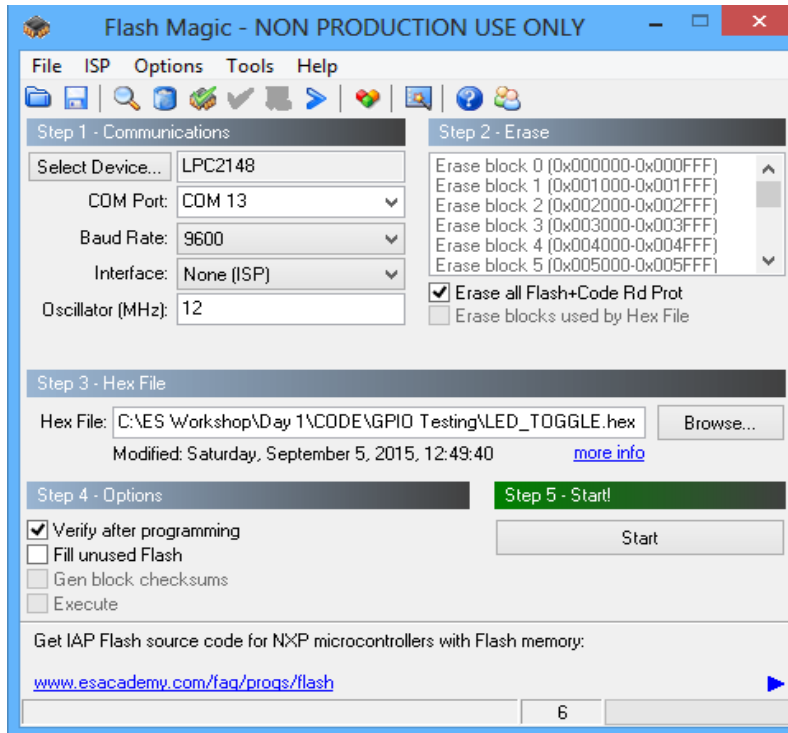


Fig. 4. Snapshot of flash magic

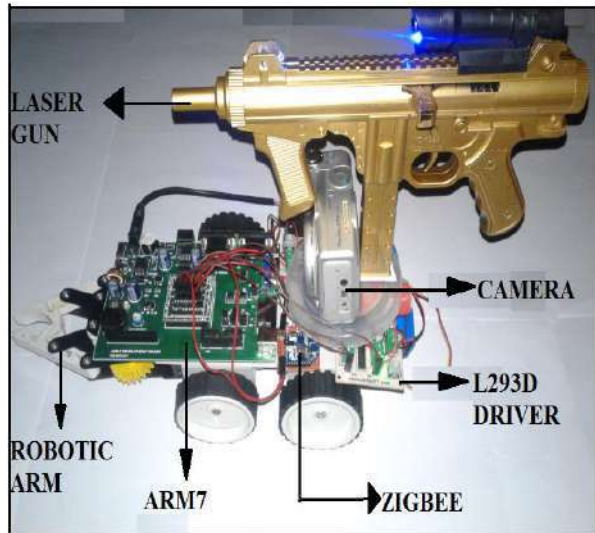


Fig: 5. Snapshot of robot

RESULTS

ARM9 is used as the control unit. Nine buttons are present on the screen of the control unit which is programmed to perform different events in the Robot section. Initially, "COM" button is selected to initialize the communication between robot and control unit. Various events can be triggered based on requirement. The user selects any command from the control unit. This signal is transmitted through the ZigBee module from the control unit. In the robot unit another ZigBee module is attached which acts as the receiver, it receives these signals and corresponding operations are carried out. When any moving object is detected by the PIR sensor, "Human motion Detected" message is displayed on the display screen. Similarly the messages "Obstacles Detected", "Pick and Place" and "Metallic objects Detected" message are found to be displayed. The target is aimed by using a Laser pointer gun. "SHOOT" function is activated by selecting the corresponding button in the display screen. Similar to the above activities, a number of other activities are possible like robot movement, laser triggering etc.

CONCLUSION

The proposed system gives an exposure to design a multifunctional defence robot. This robot has a widespread industrial, defense and home applications. The laser gun attached to the robot is an excellent substitute for the weapons carried by the soldiers. The Laser gun can be triggered with the help of wireless camera. It can be used in a hostage situation to pinpoint the exact location of terrorists with the help of wireless camera, saving many lives during rescue mission. Another application is home security system to sense movement of intruder through PIR sensor. In Industries, this robot can be used to pick and place objects that could be hazardous to human. The current range of operations is up to 100m and can be made more sophisticated. Laser gun found to be very accurate in pointing to the target.

CONFLICT OF INTEREST

Authors declare no conflict of interest.

ACKNOWLEDGEMENT

None.

FINANCIAL DISCLOSURE

No financial support was received to carry out this project.

REFERENCES

- [1] S Naskar, S Das, A K Seth, A Nath. [2011] Application of Radio Frequency Controlled Intelligent Military Robot in Defense,” *International Conference on Communication Systems and Network Technologies (CSNT)*, Katra, Jammu, 396–401.
- [2] L Srinivasavaradhan, G Chandramouli, AG Maniprashanna.[2009] 7th sense. A multipurpose robot for military, 5th International Conference on Perspective Technologies and Methods in MEMS Design, *MEMSTECH Zakarpattya*, 158–160.
- [3] Muhammed Jabir NK, Neetha John, Muhammed Fayas, Midhun Mohan, Mithun Sajeew, and Safwan CN.[2015] Wireless Control of Pick and Place Robotic Arm Using an Android Application,” *International Journal Of Advanced Research In Electrical, Electronics And Instrumentation Engineering*, 4(4).
- [4] A O Oke and A A folabi.[2014] “Development of a robotic arm for dangerous object disposal, *6th International Conference on Computer Science and Information Technology (CSIT)*,153–160.
- [5] A Oda, T Nakabe and H Nishi.[2009] Quality of connectivity guarantee of ZigBee based wireless mobile sensor network,” 7th *IEEE International Conference on Industrial Informatics, INDIN 2009*. Cardiff, Wales, 452–457.
- [6] A Sharma and Balamurgan MS. “Mobile robotic system for search mission, International Conference on Innovations in Information, *Embedded and Communication Systems (ICIECS)*, Coimbatore, 2015, 1–4.
- [7] Ramesh S Nayak, Shreenivas Pai N, Akshay Nayak, Akhil Simha N. [2016] A Study On IOT Enabled Smart Store,” *IIOABJ*, 7(2): 61–67.
- [8] Z Mughal, SK Garan and R Kamoua.[2011] Eagle O: A semi-autonomous robot,” *Systems, Applications and Technology Conference (LISAT), 2011 IEEE Long Island*, Farmingdale, NY, 1–5.
- [9] Sairam S Sunny, R Singh and R Singh.[2015] Implementation of an in campus fire alarm system using ZigBee, 2nd International Conference on Computing for Sustainable Global Development (INDIACom),New Delhi, 732–737.
- [10] SY Juang, JG Juang. [2012] Real-time indoor surveillance based on smartphone and mobile robot,” *10th IEEE International Conference on Industrial Informatics (INDIN)*, Beijing, 475–480.

ABOUT AUTHORS



Prof. Ramesh Nayak is currently working as associate professor in Canara Engineering College, Benjanapadavu, Mangaluru, Karnataka, INDIA. He is currently faculty in the department of Information Science and Engineering. He received his M.Tech degree from University of Mysore, Mysore, India. He is pursuing PhD in image processing. His research interest includes Image processing, Data Mining, Computer Networks. He has teaching experience of 14 years and research experience of 3 years. He has published research papers in national, International conferences and Journals.



Ms. Varsha Aithal is currently pursuing B.E degree in IS&E department, Canara Engineering College, Benjanapadavu, Mangaluru, Karnataka, INDIA.



Mr. Rakesh G, is currently pursuing B.E degree in IS&E department, Canara Engineering College, Benjanapadavu, Mangaluru, Karnataka, INDIA.



Ms. Mithuna Shetty, is currently pursuing B.E degree in IS&E department, Canara Engineering College, Benjanapadavu, Mangaluru, Karnataka, INDIA.



Ms. Sushwatha Naik, is currently pursuing B.E degree in IS&E department, Canara Engineering College, Benjanapadavu, Mangaluru, Karnataka, INDIA.

PERFORMANCE EVALUATION OF SPARSE BANDED FILTER MATRICES USING CONTENT BASED IMAGE RETRIEVAL

Hima T. Suseelan*, Sooraj Sudhakaran, V. Sowmya, K. P. Soman

Centre for Computational Engineering and Networking (CEN), Amrita School of Engineering, Coimbatore, Amrita Vishwa Vidyapeetham, Amrita University, INDIA

ABSTRACT

Content Based Image Retrieval (CBIR) is an extensively used application in the field of Image Processing. It is used to search through a massive database and retrieve the images that have similarity with the query image. In this paper, performance is evaluated for Sparse Banded Filter matrices (ABfilter) against the standard edge detection filters through Content Based Image Retrieval. Performance factor of ABfilter directly relates to its edge detection capabilities. Here, edge detection followed by the Singular Value Decomposition (SVD) is done for feature extraction for both the query and images in database. Query image feature and database image features are matched and those having similar values are retrieved. Similarity measurement is done by computing the distance between corresponding features. Experimental results indicate that retrieval results using ABfilter is much better than using standard edge detection filters for the same, which in turn establishes its superiority in edge detection.

Received on: 15th-Dec-2015

Revised on: 24th-Feb-2016

Accepted on: 06th-Mar-2016

Published on: 11th-Apr-2016

KEY WORDS

Content Based Image Retrieval;
Singular Value Decomposition;
Histograms; Edge Detection;
Sparse banded filter matrices;
Euclidean distance

*Corresponding author: Email: himathaivalappil@gmail.com Tel: +919585984782

INTRODUCTION

Vision is the most important of our senses and plays a vital role in human perception [1]. Electronic snapshots of real world scenarios such as photographs, scanned documents, printed texts, manuscripts, artwork can be termed as digital images. Digital images are stored as numerical values having fixed number of rows and columns [2]. Image processing is used for analyzing and manipulating digital images. It is a kind of signal processing where an image is given as an input and an enhanced version or the features/characteristics associated with the image is produced as an output. Image processing has been proved as a promising technology for analysis in various fields and applications. It is used in most instances including medical imaging, remote sensing, artificial intelligence, military, film industry, forensic studies, agriculture etc. [1]. Image retrieval system is used in agriculture for determining insect attack and growth [3]. It is also used for detecting weeds and for differentiating weeds from soil regions [4]. Identification of targets from satellite photographs, recognition of enemy aircraft from radar screens and provision of guidance systems for cruise missiles are some instances in military applications [5]. Identity of fingerprints, shoe prints and tire threads are done using image retrieval in digital forensics [5] [6]. Face recognition is also an advanced technology used in forensics [6]. MR brain imaging is one of the main application in medical imaging [7]. Also, image retrieval is used to display images relating to a named patient, and can be used to find similar past cases [5].

Traditionally, images were managed by annotating their contents and were retrieved using text based retrieval methods. But, the exponential increase in digital data made it almost impossible to prepare the databank for images. Two main challenges faced were massive labor required for manual annotation and different perception of same image by different people [8]. Limitation of text based method paved the way for Content Based Image Retrieval (CBIR). It is also known as Query by Image Content (QBIC). It aims at extracting and indexing images using its visual content such as shape, color, textures and other information that can be used for retrieval. Each image is described using its own features rather than metadata such as tags, descriptions or keywords [9]. Unlike in Text Based Image Retrieval (TBIR), characteristics are extracted automatically. Being the most recognizable feature, color is widely used in image retrieval. Color in a digital image is represented as RGB, HSV, YCbCr, CIElab etc. Color histograms are used to denote the pixel count of various colors stored in the image. Textural

features are also an effective method to represent an image. It produces a mathematical symbolization for representing the repeating patterns on the surface of the image. Remarkable texture analysis methods include directionality, coarseness, line-likeness, regularity, as well as roughness. Furthermore, Gabor features are also used in texture analysis task. Shape is another visual feature used in CBIR. Compared to others, image retrieval using shape features is one of the toughest task. An image is a 2D object when digitally represented, but is 3D in real world. Mapping from a 3D representation to 2D results in loss of one dimension. Thus, shape extracted represents only a partially projected object. Further researches are ongoing in this field [10].

Edges are also one of the major feature used in the fields of image retrieval. It denotes sudden change of intensities in an image. Edge detection is a process for detecting the boundaries of objects present in an image. There are several methods to implement edge detection. However, the most can be considered as two: gradient and Laplacian [11]. Gradient method is done by finding the minimum and maximum values belonging to the first derivative of the image. Zero crossings in the second derivative are used for Laplacian edge detection. Canny, Prewitt, Roberts, Sobel are types of filters used for edge detection. Performance of the application is conditional to the selected edge detection algorithm. Efficient edge detection techniques are required by applications such as data compression, object recognition and tracking, image segmentation and pattern recognition.

Latest trends in edge detection include quick edge detection with the help of structured forests. The edge mask so formulated helps in detecting the edges in the image by the method of mask processing. The main advantage is that; it can be used for real time applications since its edge detection capability is much faster than presently used modern approaches [12]. Another method includes the Roberts Edge Detection using CUDA and OpenGL, which makes use of the Pixel Buffer Object (PBO) for image creation using CUDA on pixel by pixel basis and displaying the so obtained by using OpenGL. This image so formed is edge detected using Roberts filter [13]. A method for image retrieval using shape features for similarity measurement is proposed [14]. A weighted bipartite graph matching algorithm and homogenous attribute is used to find the correspondence between features.

In this paper, performance evaluation of ABfilter is done using Content Based Image Retrieval. As per theory [15], ABfilter uses a new approach using sparse banded matrices to reduce the chance of appearance of unrelated images, which in turn suggests that its edge detection is advanced. We confirm this by experimental approaches. The rest of the paper is arranged as follows; IInd section describes the scheme used for evaluating the performance of the ABfilter along with the theory related to the ABfilter as well as Singular Value Decomposition. In Section III, experimental results are narrated. Section IV explains the experimental setup and conclusion of the paper is done in Section V.

MATERIALS AND METHODS

ABfilter

The main concept behind ABfilter [16] is the use of the sparse banded filter matrices proposed by Selesnick et.al. [15] for one dimensional signal processing. The concept is then applied to the two dimensional and used for edge detection of images [16]. The sparse banded high pass filter is applied for rows and columns to extract the vertical and horizontal edges of the images respectively. Due to the sparsity property associated with the filter, it presents much efficient computation when compared with the existing standard filters. The main advantage which makes this filter outperform other filters is that it is possible of capturing continuous edges without any kind of parameter tuning.

Singular Value Decomposition (SVD)

Canonical form or decomposition of matrix is one among the most valuable idea in the field of linear algebra. Singular value decomposition takes a special role in decomposition of matrices. Matrix A is factorized into product $U\Sigma V^T$; U and V^T are unitary matrices, Σ is diagonal matrix [17] [18].

$$A = U\Sigma V^T$$

where A is a real matrix of size $m \times n$,

$$\Sigma = \text{diagonal}(\sigma_1, \sigma_2, \dots, \sigma_n)$$

consists of diagonal elements which are non-negative in nature arranged in decreasing order,

$$V = (v_1, v_2, \dots, v_n) \text{ and } U = (u_1, u_2, \dots, u_n)$$

are orthogonal. Frobenius norm is denoted by $\| \cdot \|$ and is defined by,

$$\| A \|^2 = \sum_{p,q} a_{pq}^2 = \sum_q \sigma_p^2$$

PROPOSED WORK

The proposed work discusses the implementation of the ABfilter in the Content Based Image Retrieval application to evaluate its edge detection capabilities. The algorithm for the retrieval process used here is Line Edge Singular Value Pattern [19] which incorporates the notion of edge detection and Singular Value Decomposition [19]. The experiment compares the retrieval outputs obtained from ABfilter and standard edge detection filters (Sobel, Roberts, Prewitt and Canny) and accuracy is observed. The retrieval process is represented in [Figure-2].

ALGORITHM

- 1) The query image as well as the image database is loaded and then converted to grayscale as shown in [Figure-1 A]. Both query and database is first subjected to edge detection [20] using the ABfilter as well as standard set of edge detection filters like Canny, Prewitt, Sobel and Roberts. From this output, we select a 3x3 block as shown in [Figure-1 B].
- 2) The absolute values of the edge detected output is determined as in [Figure-1 C].
- 3) Singular Value Decomposition (SVD) is determined for the selected 3x3 block and the maximum value of Singular Value Matrix is computed. The center pixel is replaced by this maximum value as in [Figure-1 D]. In this way, the procedure is applied to all the pixels in the image and are replaced by their corresponding maximum values.

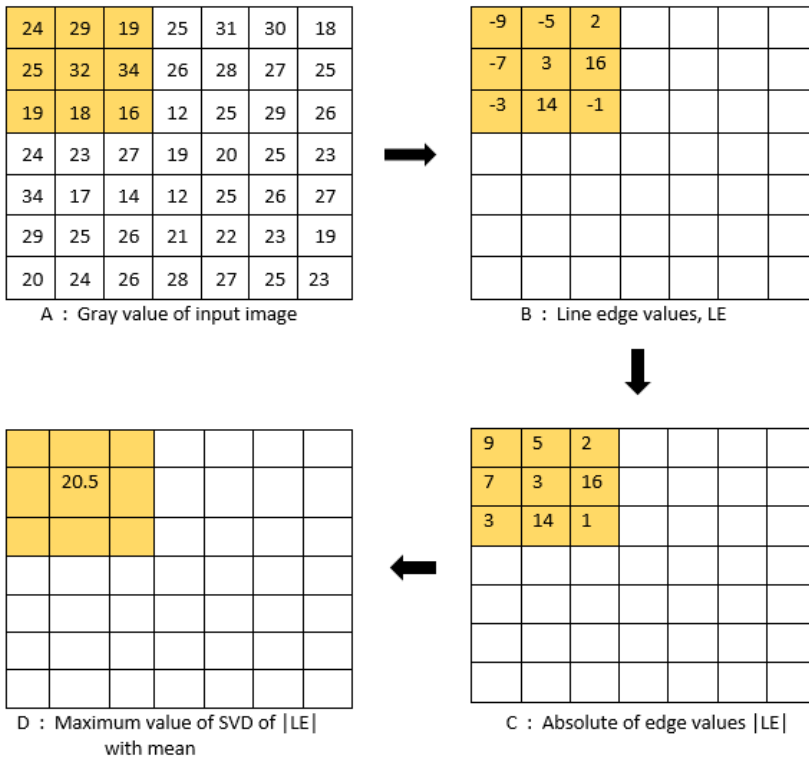


Fig: 1. Depiction of determining maximum singular value in 3x3 block

- 4) Histogram is computed for the previously obtained matrix.
- 5) The histogram so obtained is normalized. This step marks the end of the feature extraction process with features being the normalized histogram.

- 6) The above steps from 2 to 6 is repeated for all the images in the database as well as for query image for feature extraction process.
- 7) The next step followed by feature extraction is retrieval. Pairwise Euclidean distance for the query image feature is calculated followed by calculating the pairwise Euclidean distances for all the features in the database.
- 8) Difference between the query features and each of the database feature is calculated.
- 9) Then absolute value of the difference is computed followed by taking its summation.
- 10) The computed value is matched with a threshold value.
- 11) The threshold value is calculated by taking the mean of the all the above mentioned computed values.
- 12) Images that falls under threshold value are retrieved.

FLOWCHART

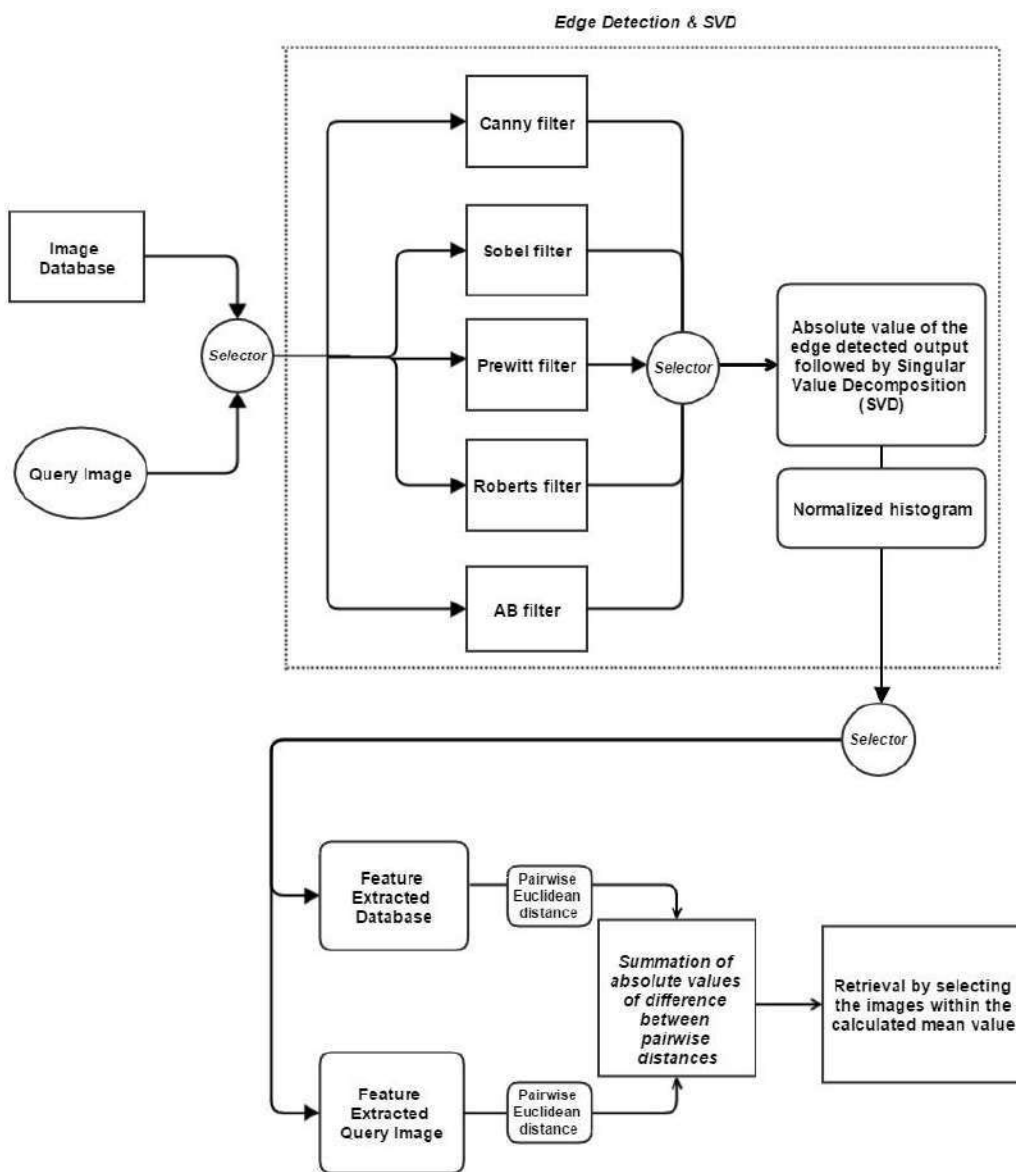


Fig: 2. CBIR retrieval process

RESULTS

The experimental results for the retrieval for class ‘Rose’ is shown in [Table-1]. It consists of 10 images with image numbered from 41 to 50. Each of this image is taken as query image and the algorithm is followed for feature extraction. Query image feature and database image features are matched for retrieval process. Retrieval for Canny, Sobel, Prewitt, Roberts and ABfilter is noted. In [Table-1], precision explains how much images are correctly retrieved. It is given by the formula [21],

$$\text{Precision \%} = \frac{\text{No. of images relevant to the content retrieved}}{\text{Total no. of images retrieved}} \times 100$$

When the query image numbered 41 is passed for retrieval, ABfilter retrieves all the 10 images in the class correctly among the 70 in the entire database taken for performance testing. This gives a precision of 24% as per the above formula. Both Sobel and Roberts retrieves 8 out of the 10 images while Canny and Prewitt retrieves only 6 images. So likewise, all the images in the class Rose are tested for retrieval and the average precision is calculated. In the end, ABfilter gives the best retrieval with 27.9 %. The experiment is repeated for all the 7 classes and it was determined that ABfilter correctly retrieves all the images in same class as that of query image.

The overall retrieval results so obtained is compared as shown in [Table-2]. Overall retrieval is computed by calculating the mean of precision of the filters applied to the entire database consisting of 70 images, 7 class with 10 images each. ABfilter has the best precision out of all of them with 23.69%. Corresponding graphical results are shown in [Figure-3].

Table: 1. Retrieval output for the image class “Rose” by different filters

Image No.	Canny Retrieval			Sobel Retrieval			Prewitt Retrieval			Roberts Retrieval			ABfilter Retrieval		
	Relevant	Total	Precision %	Relevant	Total	Precision %	Relevant	Total	Precision %	Relevant	Total	Precision %	Relevant	Total	Precision %
41	6	40	15	8	36	22	6	35	17	8	36	22	10	42	24
42	8	43	19	6	33	18	6	35	17	10	34	29	10	36	28
43	8	43	19	10	38	26	10	39	26	8	33	24	10	39	26
44	10	42	24	8	36	22	8	37	22	6	37	16	10	35	29
45	10	43	23	10	33	30	10	35	29	10	33	30	10	35	29
46	6	40	15	6	34	18	6	34	18	6	36	17	10	36	28
47	10	40	25	10	34	29	10	35	29	10	33	30	10	35	29
48	8	43	19	6	35	17	6	35	17	6	37	16	10	36	28
49	10	42	24	10	34	29	10	35	29	10	33	30	10	35	29
50	10	40	25	10	33	30	10	35	29	10	33	30	10	35	29
	Average precision %		20.8	Average precision %		24.1	Average precision %		23.3	Average precision %		24.4	Average precision %		27.9

Table: 2. Overall retrieval results (precision rate) for all the image classes using different filters

Categories	Canny	Sobel	Prewitt	Roberts	ABfilter
Bus	16	21.3	21.8	23.2	23.1
Dinosaur	23.7	22.4	21.7	17.2	26.1
Food	19.5	23.8	23.4	23.3	20.6
Horse	18.7	19.6	20	19.8	22
Monuments	20.6	25.3	25	23.8	24
Rose	20.8	24.1	23.3	24.4	27.9
Tribal	21.1	18.5	18.4	20.8	22.1
Average precision %	20.06	22.14	21.94	21.79	23.69

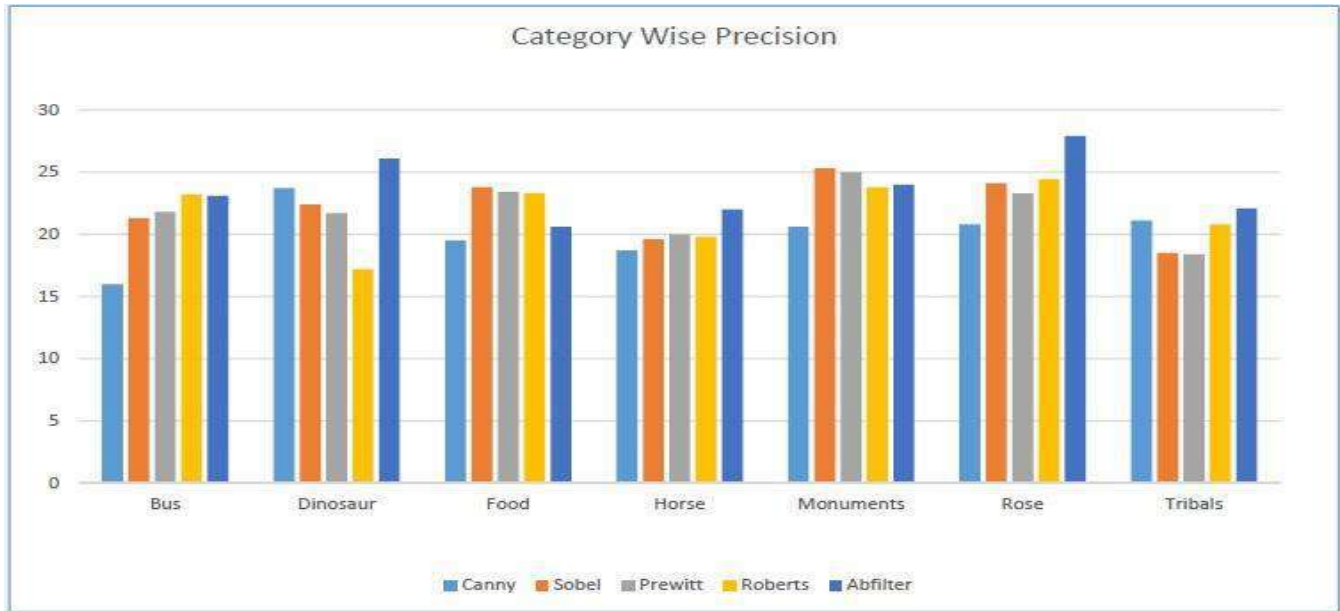


Fig 3: Category wise retrieval plot

The result confirms that the ABfilter has best content retrieval when compared to the filters like Roberts, Prewitt, Sobel and Canny.

[Figure-4] shows the sample edge detection of an image by all the filters. It is evident that the ABfilter captures all the horizontal and vertical variations perfectly. Moreover, it only detects the object of interest. While in Canny, it is seen that along with the object, it also detects the background. Rest Prewitt, Roberts and Sobel exhibits edge detection with discontinuities. This solidifies the fact that the ABfilter has better edge detection capabilities with respect to other filters.

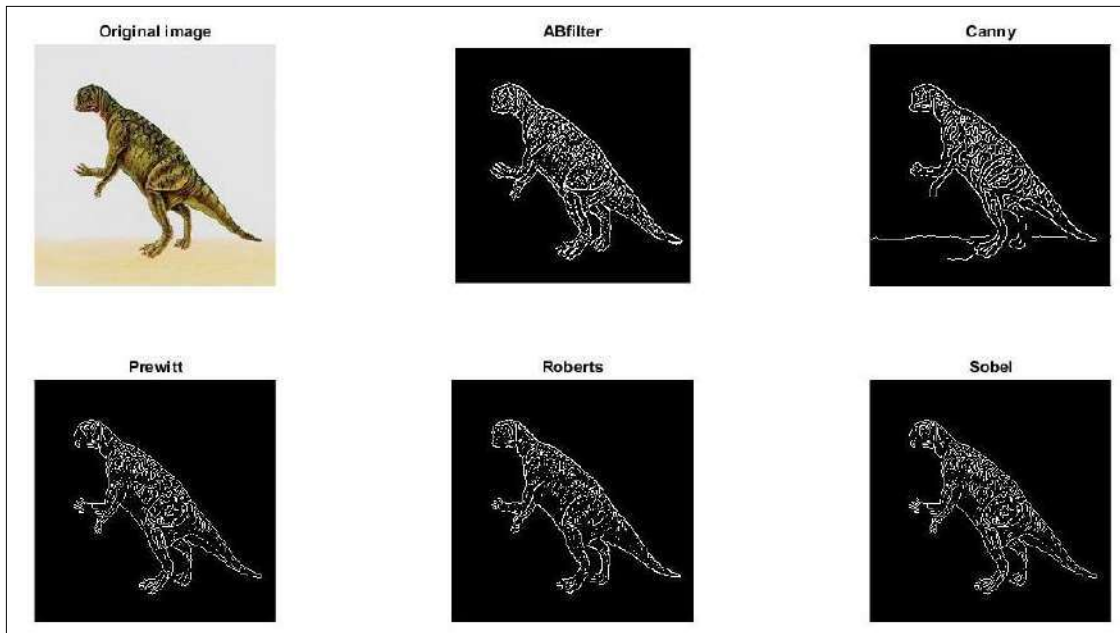


Fig 4: Edge Detected Outputs of filters

DISCUSSION

In order to perform this experiment, we have used Matlab and WANG database [19] for implementing the program. It is a subcategory of Corel stock database consisting of 10 classes of 100 images each, which are selected manually and thereby totaling up to 1,000 images. The image dimensions are 256 x 384 or 384 x 256 pixels. Assume that user is having an image pertaining to a particular class and searching for similar images in the database. Here, all the 99 images pertaining to same class as that of query image is considered relevant while the rest are deemed irrelevant. For our experiment, we took 7 classes (Bus, Dinosaur, Food, Horse, Monument, Tribals and Rose) out of the 10 classes and from each class having 100, we randomly selected 10 images for performance testing. So our database amounts to a total of 7 classes each are having 10 images. Then, images belonging to each class are individually passed as query image to the program for retrieval purposes. The ABfilter gives the good retrieval which is evident from the experimental results indicated by Table-1 and -2.

CONCLUSION

This paper highlights the edge detection capability of ABfilter which is practically evaluated by its application in Content Based Image Retrieval. Retrieval of the ABfilter is compared with the standard edge detection filters. During the observation, it has been determined that the ABfilter filter performs much better when compared with the others. By conducting the experiments throughout the different image classes, it has been established that the ABfilter retrieves only the content related to query image from the image database and thereby giving best retrieval rates among all. Hence, it is experimentally established that the edge detection property of the ABfilter is much superior to the standard edge detection filters. ABfilter can serve as a replacement to the standard edge detection filters in the image processing applications like medical imaging, autonomous car etc.

Advantages of ABFilter

- Has less discontinuity, when compared with the existing edge detection methods.
- Sparsity property of the banded filter leads to efficient computation of edge extraction without any parameter.

CONFLICT OF INTEREST

Authors declare no conflict of interest.

ACKNOWLEDGEMENT

None.

FINANCIAL DISCLOSURE

No financial support was received to carry out this project.

REFERENCES

- [1] Gonzalez Rafael C, RE Woods. [1992] Digital Image Processing. Addison-Wesely Publishing Company
- [2] Bara, Binamrata, Sandeep Gonnade, and Toran Verma. Image Segmentation and Various Techniques-A Review.[2014] International Journal of Soft Computing and Engineering (IJSCE) ISSN: 2231—2307.
- [3] Marwaha Sanjay, Satish Chand, and Ankita Saha. Disease diagnosis in crops using content based image retrieval.
- [4] Mandlik Mr Vinay S, and Sanjay B Dhaygude. Agricultural Plant Image Retrieval System Using CBIR.
- [5] Singh, Jagpal, Jashanbir Singh Kaleka, and Reecha Sharma. "Different approaches of CBIR techniques.[2012] Int. J Comput. Distributed Syst 1: 76—78.
- [6] Chen Yixin, et al.[2005] Content-based image retrieval for digital forensics. *Advances in Digital Forensics*. Springer US, 271—282
- [7] Fathabad Y Fanid, and M Balafar. [2012]Application of content based image retrieval in diagnosis brain disease. *Int. Journal on Technical and Physical Problems of Engineering* 4.4: 122—128.
- [8] Rajdeep Kaur, Kamaljit Kaur. [2015] Study of Different Techniques for Image Retrieval. *International Journal of Advanced Research in Computer Science and Software Engineering*
- [9] Chaudhari Reshma, and AM Patil.[2012] Content Based Image Retrieval Using Color and Shape Features.*International Journal of Advanced Research in Electrical, Electronics and Instrumentation Engineering* 1.5
- [10] Shrivakshan GT, and C Chandrasekar. [2012] A comparison of various edge detection techniques used in image processing. *IJCSI International Journal of Computer Science Issues* 9.5 :272—276.

- [11] KR Dinesh, and Shanmugasundaram Hariharan. [2014] Approaches and Trends in Content based Image Retrieval. *Proc. of Int. Conf. on Advances in Communication, Network, and Computing, CNC*
- [12] Dollár Piotr, C Lawrence Zitnick.[2014] Fast edge detection using structured forests. *Pattern Analysis and Machine Intelligence, IEEE Transactions on*37.8 (2015): 1558—1570.
- [13] Cali, Marco, and Valeria Di Mauro. [2016] Performance Analysis of Roberts Edge Detection Using CUDA and OpenGL
- [14] Patil Shweta R, and VS Patil.[2016] Similarity Measurement using Shape Feature for Image Retrieval. *International Conference on Global Trends in Engineering, Technology and Management (ICGTETM-2016)*
- [15] Ivan W Selesnick, Harry L Graber, Douglas S Pfeil and Randall L.[2014] Barbour: Simultaneous Low-Pass Filtering and Total Variation Denoising. *IEEE Transactions on Signal Processing, P.1109—1124*
- [16] Sowmya V, Neethu Mohan, and KP Soman.[2015] Edge Detection Using Sparse Banded Filter Matrices.*Procedia Computer Science* 58 :10—17.
- [17] Golub Gene, and William Kahan. [1965] Calculating the singular values and pseudo-inverse of a matrix. *Journal of the Society for Industrial and Applied Mathematics, Series B: Numerical Analysis* 2.2: 205—224.
- [18] Stewart, Gilbert W. [1993] On the early history of the singular value decomposition. *SIAM review* 35.4 :551—566
- [19] Swati Thakur, Megha Singh. [2015] Content Based Image Retrieval using Line Edge Singular Value Pattern. *International Journal of Advanced Research in Computer Science and Software Engineering* Marr,
- [20] David, Ellen Hildreth. [1980] Theory of edge detection. *Proceedings of the Royal Society of London B: Biological Sciences* 207.1167 :187—217.
- [21] Shiwani Gupta, Amitkumar Sandesara, Ashwini Singh and Jithesh Ranjak. [2014] Singular Value Decomposition for Image Classification”. *IJSRD International Journal for Scientific Research & Development*. 2(02): 2014. ISSN (online): 2321—0613

ABOUT AUTHORS

Hima T Suseelan received her B.Tech degree in Computer Science and Engineering in 2014. Currently she is pursuing her M.Tech degree in Computational Engineering and Networking (CEN) from Amrita School of Engineering, Coimbatore, India. Her research interests include Digital Image Processing and Software engineering.

Sooraj Sudhakaran received his B.Tech degree in Electronics and Communication in 2011. Currently he is pursuing M.Tech degree in Computational Engineering and Networking (CEN) from Amrita School of Engineering, Coimbatore, Amrita Vishwa Vidayapeetham, Amrita University, India. His research interests include Digital Image Processing and Embedded systems.

Sowmya V. currently serves as Assistant Professor at Amrita Centre for Computational Engineering and Networking (CEN), Coimbatore campus. Her research area includes Image processing, Hyperspectral Image Classification, Pattern Recognition and Machine Learning.

Dr. K. P Soman currently serves as Head and Professor at Amrita Centre for Computational Engineering and Networking (CEN), Coimbatore campus. His research interest includes Software Defined Radio, Wireless Sensor Networks (WSN), High Performance Computing, and Statistical Digital Signal Processing (DSP) on Field Programmable Gate Array (FPGA), Machine learning Support Vector Machines, Signal Processing and Wavelet & Fractals.

SPECIES GENERATION FOR PARALLEL CODE BY CLASSIFYING THE ALGORITHMS

Mustafa Basthikodi¹ and Waseem Ahmed²¹Research Scholar, Dept. Of CSE, BIT, Mangalore, INDIA²Dept. Of CSE, HKBKCE, Bangalore, INDIA

ABSTRACT

Many-core and multi-core systems are expected to be major trends for the future decades. In this way of parallel computing, it may become great difficult to choose on which target architecture to execute a certain algorithm or application. Many core machines along with GPUs increased the extensive amount of parallelism. Some compilers are updated to emerging issues with respect to the threading and synchronization. Proper classification of algorithms and programs will benefit largely to the community of programmers to get chances for efficient parallelization. In this work we have analyzed the existing species for algorithm classification, where we discuss the classification of related work and compare the amount of problems which are difficult for classification. We have selected set of algorithms which resemble in structure for various problems but perform given specific tasks. These algorithms are tested using existing tools such as Bones compiler and A-Darwin, an automatic species extraction tool. The access patterns are produced for various algorithmic kernels by running against A-Darwin and analysis is done for various code segments. We have identified that all the algorithms cannot be classified using only existing patterns and created new set of access patterns.

Received on: 24th-Dec-2015
 Revised on: 27th-Jan-2016
 Accepted on: 04th-Feb-2016
 Published on: 17th-Apr -2016

KEY WORDS

Index Terms— Algorithm Classification, Access Patterns, Bones, A-Darwin, Parallel Programming.

*Corresponding author: Email: mbasthik@gmail.com Tel: +919844535720 Fax: +91-8242235775

INTRODUCTION

In the past few decades, we have seen a tremendous growth of single-core processor performance. This growth has enabled technology to exist everywhere in the society. To overcome the limitations in the performance of the single-core processor parallelism is exploited. Enabled by the Moore's law, large number of processors per chip (i.e. multi-core) is already a major trend and expected to continue for the next decade [1].

When multi-core is expected to grow 100-core processors by 2020 [1], other trend already enables larger than 2000 cores. This trend (many-core) uses much smaller processing cores, making high throughput parallel processors. An example for such a many-core processor is GPU. Even though many-core processors are suitable for a certain types of applications, other applications may prefer multi-core processors. This creates a heterogeneous environment, with dual types of processors in single system or a single chip.

The multi core architectures enabled performance growth of processors by introducing the parallelism in programs. Because of the heterogeneous computing environment and parallelism, the parallel architectures face challenges in code development and in predicting the performance of the processor. Even though there is amount of research work carried on compilers, parallelization and automatic parallelization, programmers use programming languages such as OpenMP, OpenCL and MPI. Determination of the parallel program performance is needed to check whether the parallelization is required and which part of the program to be parallelized. All the available auto parallelization solutions are not fully automatic. Because of the revolutions in the hardware technologies, such diversified platforms and the need of programming the hardware efficiently has increased the programming models accordingly. The programming models such as Intel TBB [2], OpenACC [3], OpenMP [4], OpenCL [5], Nvidia CUDA [6] and OpenHMPP [7] are some of the models presently available for parallel programmers for writing the applications.

Present trends in the parallel architectures are largely towards the bigger number of processing devices on the chip. This led to the parallel architectures growing as mainstream, with the growth of many specialized multi-core architectures and accelerators. The problem of programming with these architectures effectively using several processing elements [8] is a biggest challenge. There are many approaches [9] to address this issue. The one that

is very challenging is the automatic parallelization. Many difficult applications often spend most of their run time in the nested loops. This is most common in many of the engineering and scientific applications.

The idea of auto parallelization is to free programmers from the error-prone and the time consuming manual parallelization process. Even though the automatic parallelization process has improved its quality in the last few decades, completely auto parallelization of the serial programs by translators remains a biggest challenge because of its need for the complicated program analysis and unknown facts during compilation process. The focus of the automatic parallelization is on programming control structures such as loops, because, maximum of the run times of a program is taken inside some of the loops. For example, an algorithm for the parallel loop identification may be integrated in the parallelization platform as shown in the diagram below which converts automatically serial code in to parallel code.

The front end view of the classification of the algorithm is shown in **Figure- 1**. The figure indicates how classified source code can be parallelized automatically to parallel source code. The figure also shows how the serial code can be compiled in to a parallel code, how to predict the performance. Our focus is on Algorithm Classification part in **Figure- 1**. The overall system will be given with serial code as a input and produces output as parallel program.

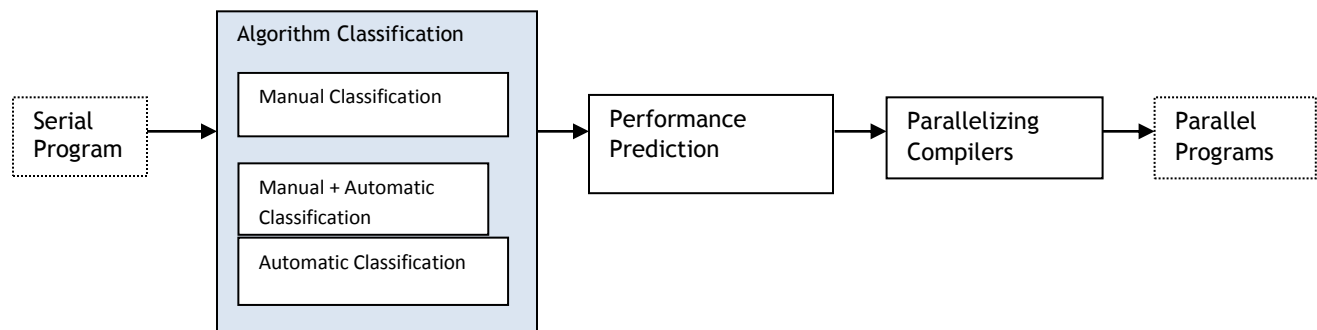


Fig: 1. Front end view of the Algorithm Classification.

In this work, the existing classification of algorithms [10], ‘Algorithmic species’ that summarizes significant data for parallelizing the algorithm based on classes is studied in depth by compiling various code segments in BONES[11] compiler. The access patterns are generated using ADARWIN and analyzed for different algorithmic kernels.

We retake ‘algorithmic species’ a access pattern based classification of algorithms [12], and created a increased set of patterns, that summarizes significant data for parallelizing the algorithm based on classes.

The theory behind algorithmic species is subject to the polyhedral model, requiring code to be represented as a set of static affine loop nests. Characterization of array references is introduced with respect to loop nests. Transformations are defined to merge characterizations referring to the same array and to translate them into algorithmic species, allowing classification of non static affine loop nests. The classification is subject to the more detailed abstractions that retain additional performance-relevant information and that take the loop nest structure into account. A tool is modified based on the presented theories to automatically classify program code.

MOTIVATION

The change towards diverse and parallel computing conditions has made programming the challenging tasks. Making complete use of multi-threading and using efficiently memory hierarchy of a processor are the best examples of issues faced by programmers and compilers where programmers looking for a manual solution and compilers looking for an automated solution. We recommend that the classification of algorithms can largely reduce those tasks for compilers and programmers.

We encourage programmers to use an classification of algorithms as a tool to make parallel programming easier. This can help the programmers in identification of problems similar to same class of algorithms and identify available parallelism by applying known parallel patterns.

We visualize classification of algorithms as way that facilitates communication between programmers to describe computational issues. This also facilitates design and improves compiler's quality, for example, automatic parallel compilers, source code to- source code compilers, and automatically tuning compilers.

The classification of algorithms that describes the characteristics of algorithm in destination framework shortens many of the architecture related issues. The decisions taken by the underlying compiler for parallelizing the code will be on the data attached in algorithm classes. These will largely solve the problem of compiler designs.

The categorization does not change around time and new feature code may be created when the tools lodge to the changes in the feature hardware. We shun an algorithm categorization as a suitable tool to meet face to clash the futuristic and infinity challenges in parallel computing.

More ever, the algorithm classes may contain in a superior way the algorithm information than is presently available to a compiler that may cause to increase the quality of code. We devise the classification of algorithm to adopt a mean compiler study technique, by bringing the pedigree of algorithm plan into a common place.

Below given are the requirements that to be considered for the goals to be achieved.

- (i) Algorithm classes must be automatically extracted from the source code. If not, the program code may have to be extracted manually by the compilers. Ultimately, this is not capable of, considering the concern of classes that may be fault prone and may place a big burden on programmer's head.
- (ii) A categorization intend be innate and ethereal to understand. Although we demand classes to be automatically extracted, we contemplate algorithm to be manually used, as a appliance for programmers.
- (iii) The algorithm classes must be defined formally. This will guarantee the compilers correctness, and also allows programmers to understand completely the class properties and facilitates automatically extract the classes from source code.
- (iv) There should be set boundaries for defining the completeness of algorithm classification, i.e. a single algorithm must belong to one of the predefined classes.

The classes must involve in it, amount of parallelism, the structure, the data reuse information to produce the code efficiently. Also provide circumstances to travel through caching and locality.

Keeping in mind the goals and algorithm classification requirements, we glance at the existing classification of algorithms and check whether our requirements are met.

RELATED WORK

Many algorithmic classifications have been referred before designing the new species. Few of them, with the similar work are highlighted here. Several algorithms have been discussed by many people, such as the ones presented by Allen, Kennedy, Darte and Vivien, Wolf, Lam, and Feautrier [13][14][15]. These algorithms uses of various mathematical notations and tools. Additionally, these do not depend on common representation of the data dependences. The schemes of transformations for common loops in which dependence vectors express precedence constraints on the iterations of loops are presented [16][17]. As per the Wolf and Lam presentation, the dependences extracted from the loop nests must be positive lexicographically. This gives us a simple test for the legality of compound transformations such as, It is legal to have any code transformation that ignores the dependences which are lexicographically positive. The theory of loop transformation is applied to the issue of increasing the degree of coarse-grain or fine-grain parallelism in the loop nests.

Pierre Boulet and Alain Darte surveyed many algorithms on loop parallelization[18], analyzed their dependence representations, generated loop transformations, the required code generation methods, and capability to incorporate different optimization techniques such as the maximal detection of parallelism, the permutable loop detection, the minimization of synchronizations, the code generation easiness, and so on[19][20]. They ended the study by presenting results which are related to the code generation and loop fusion for the specific class of the shifted linear schedules.

Most of the existing automatic parallelization techniques are not fully automatic. The parallel computing introduces challenges in programming and compilation both. The work in [21] introduced the challenges in parallel computing and algorithm classification. It explains the algorithmic species that captures algorithm details from single loop or nested loops and loop bodies. Five access patterns that combine to an algorithmic species are illustrated along with the examples. One of the five access patterns is assigned to each array, accessed in the loop nest. The access patterns combination, of input and output data of the nested loop, forms the species. This

approach enables to form an unlimited number of species with the use of only five access patterns. The limitations of the approach are highlighted below.

First, the paper uses the polyhedral model, which imposes limits to the program code, which are classified. According to the paper, for loops to be classified must have static and affine loop bounds and the loop bounds must remain constant throughout the scope of the loop. Second, the array accesses are affine and explicit, the pointer arithmetic is not supported in the approach. This also requires that the multidimensional arrays are explicitly addressed per dimension instead of a flat array with an index calculation. Third, the extraction tool ASET used by the author works only for C code, although the species is program language independent. Fourth, The tool ASET considers fully filled iteration space polyhedra in classifying loops and no gaps in the iteration space are supported, which means loops must have stride 1. Fifth, all the program structures (e.g. multiple initializations in loop nest, conditional statements within loops, programs with statements in between algorithmic species, etc) are not supported in ASET which limits the number of statements of various types to be addressed.

PARALLEL ACCESS PATTERNS

The array access patterns element, chunk, neighborhood, full and shared, where, the input arrays are assigned either one of the five patterns whereas the output arrays are assigned either one of the patterns, excluding neighborhood. If an array is accessed from element 0 to 127 it might be that some of the elements in this range are not accessed at all. The same holds for neighborhoods and chunks, partial neighborhoods or partial chunks are still classified as neighborhood or chunk. In addition to these five patterns, We introduce species variant, constant, compare and update to deal with the programming statements such as variable and constant initialization, comparison statements, increment and decrement statements.

```

for (i=0; i<=256; i++) {
    for (j=0; j<=256; j++) {
        p[i][j]=999;
    }
}

```

Listing 1: An example for constant initialization in doubly nested loop

We show an example algorithm, in Listing 1, where all loop iterations are independent and these may be executed parallelly. The amount of parallelism is equal to the number of loop iterations and is denoted as `parallel(256,256)`. The loop body consists of initialization statement which assigns constant to array variable `p[i][j]`. The constant number is input and the two dimensional array `p` is output in this algorithm. The array is accessed at index 0 to 256 in both the dimensions. When we combine the input and output, their access range and their array access pattern, we find the algorithmic species as:

`parallel(256,256) constant --> p[0:256,0:256] | element`

Here, output array is accessed element-wise and that the combination of array names, ranges and access type defines the algorithmic species of this algorithm.

```

for (k=0; k<=128; k++) {
    for (i=0; i<=128; i++) {
        for (j=0; j<=128; j++) {
            p[i][j]=max(p[i][j],
                p[i][k] && p[k][j]);
        }
    }
}

```

Listing 2: An example for comparison in triple nested loop

The Listing 2 shows an example of a triple nested loop with comparison and assignment operations. The matrix `p` elements are compared and the maximum of compared elements is assigned to `p[i][j]`. The algorithm produces each element of result `p` by comparing with two elements of same matrix every time. Finding the maximum of two

elements of the matrix is classified as compare and the result produced as element. The resulting species is given below:

parallel(128,128,128) (p[0:128,0:128], p[0:128,0:128]) | compare → p[0:128,0:128]|element

The species can be understood as: in order to create an element of p in the range from 0 to 128 we need to compare two elements of matrix p with row and column length 128 each. This pattern-combination of 'compare and producing element' can be performed in parallel a total of 128 times each. Consider the following example algorithm for illustrating the access pattern variant.

```
for (i=0; i<=64; i++) {
    for (j=0; j<=64; j++) {
        if ((i==0) || (j==0))
            V[i][j]=0;
        else V[i][j]=-1 ;
    }
}
```

Listing 3: An example for comparison and initialization in doubly nested loop

In order to initialize the matrix element V[i][j], the variables i and j are compared with zero. The variable initialization, comparison and constant initializations are classified as the patterns variant, compare and constant. The variables i and j are accessed from 0 to 64 and accordingly the output elements can be produced in parallel. The algorithmic species is constructed as shown below:

parallel(65,65) variant[0:64],constant | compare → V[0:64,0:64] | constant

Here, to produce every element of V, which is constant, is compared with the constant value. Where, V is variable with index ranging from 0 to 65 and is classified as variant.

```
for (i=0; i<8; i++) {
    res+=A[i]+B[i+2];
}
```

Listing 4: An example for reduction to scalar element

In listing 4, illustrated the example of reducing sum of two vectors in to a scalar quantity. Here, the index of vector A ranges from 0 to 7 and B ranges from 2 to 9. In every iteration, the element of A and B are added and the output variable res is updated. This operation of incrementing the value for every iteration of the loop is classified as the pattern update. The algorithmic species for the listing 4 is constructed as below:

parallel(8) A[0:7] | element ^ B[2:9] | element → res| update

IMPLEMENTATION AND RESULTS

This Bones and A-Darwin along with required gems are installed in quad core system for experimentation. Bones is the source-to-source compiler that is designed based on algorithmic skeletons and the algorithmic species. This compiler takes as input C-code and generates parallel code as output. Target processors include NVIDIA GPUs for CUDA, AMD GPUs for OpenCL and CPUs for OpenCL and OpenMP [22][23]. The Bones compiler is based on CAST C-parser, which is used to parse input source code into the AST (Abstract Syntax Tree) and to generate desired code from the transformed abstract syntax tree.

A-Darwin (short for 'automatic Darwin') is automatic extraction tool, which is based on CAST, a C99 parser which allows analysis on AST. From the AST, the tool extracts the array references and constructs a 5 or 6-tuple for each loop nest. Following, merging is applied and the species are extracted. Finally, the species are inserted as pragmas in the original program code.

The code segments of various algorithm classes are executed to analyse the output of A-Darwin.

We have executed and analyzed 50 kernels of 15 algorithmic classes using Bones Compiler and A-Darwin tool. We have found that there are few kernels of various algorithmic classes for which A-Darwin is not considering all the possibilities of code.

Table: 1. Hit Ratio for Algorithm Classed considering multiple kernels of each class

Algorithmic Class	Kernels	Hit Ratio
Arithmetic and Logic	4	75%
1 D Convolution	2	100%
Computer vision	4	75%
MinMax Computation	3	67%
Floyds	2	50%
Warshals	2	50%
Horspool	2	50%
Kruskals	3	67%
Bankers	4	75%
Knapsack	3	67%
K-Means	4	75%
Jacobi	4	100%
2mm	3	100%
3mm	3	100%
Sorting	7	72%

The evaluation of the algorithms listed in **Table- 1** is done by running the specified number of kernels in each algorithmic class mentioned. The third column Hit Ratio is the amount of kernels executed successfully, i.e. the percentage of kernels for which patterns are generated accurately. We have executed 4 kernels of the Arithmetic and Logic algorithmic class, out of which 3 kernels successfully executed resulting 75% of the hit ratio. Similarly two kernels each from 1 D convolution, Floyd algorithm, Warshals algorithm, Horspool algorithm are considered for execution, resulting the hit ratio of 100%, 50%, 50%, 50% respectively. The three kernels each from MinMax Computation, Kruskals algorithm, knapsack algorithm, 2mm and 3mm algorithmic classes are executed resulting the hit ratio of 67%, 67%, 67%, 100% and 100% respectively. The four kernels each from computer vision, Bankers, K-means and Jacobi algorithmic classes are executed resulting the hit ratio of 75%, 75%, 75% and 100% respectively. The seven kernels from sorting algorithmic classes are executed to achieve the 72% of hit ratio.

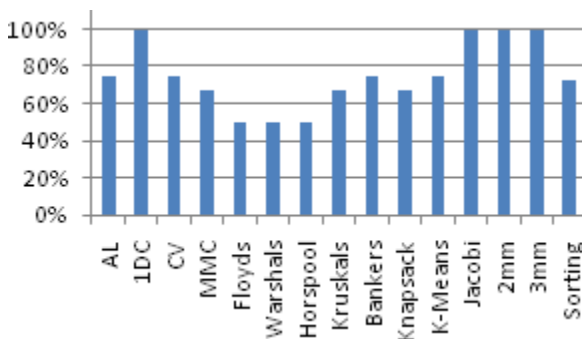


Fig: 5. Graph illustrating the Hit Ratio of kernels for algorithmic classes

The chart in **Figure-5** illustrates the Hit Ratio of the kernels for 15 different algorithmic classes. There are few kernels having statement like comparisons, conditional statements, mathematical functions comes under miss ratio.

CONCLUSION AND FUTURE WORK

The Automatic parallelization is needed to make manual programmer to write the programs without errors and save the time comparatively. In this work, we have analyzed the existing access patterns thoroughly and listed out many of the kernels those cannot be classified based on these patterns. The new access patterns are designed in order to improve the classification ratio.

The A-Darwin source code is modified to incorporate the changes to tool by adding the new functionalities. Currently the tool is working for the additional access patterns. The work is carried to include more number of mathematical functions which maximize the hit ratio for algorithmic classification. The present work is also based on the array references. So, the final work will be to classify the algorithms based on pointer references.

CONFLICT OF INTEREST

Authors declare that there is no conflict of interest.

ACKNOWLEDGEMENT

None.

FINANCIAL DISCLOSURE

No financial assistance received during my research work.

REFERENCES

- [1] B Catanzaro, A Fox, K Keutzer, et al. [2010], Ubiquitous Parallel Computing, *IEEE Micro*, 30:41–55.
- [2] C Pheatt. [2008] Intel threading building blocks, *J. Comput. Sci. Colleges*, 23(4):298–298.
- [3] S Wienke, P Springer, C Terboven, D an Mey.[2010] OpenACC:First experiences with real-world applications, in Proc. 18th Int. Conf. Parallel Process., 859–870.
- [4] L Dagum and R Menon. [1998] OpenMP: An industry standard API for shared-memory programming, *IEEE Comput. Sci. Eng.*, 5(1): 46–55.
- [5] JE Stone, D Gohara, and G Shi. [2010] OpenCL: A parallel programming standard for heterogeneous computing systems, *Comput.Sci. Eng.*,12(3): 66.
- [6] J Nickolls, I Buck, M Garland, and K Skadron.[2008] Scalable parallel programming with CUDA, *ACM Queue*, 6(2): 40–53.
- [7] R Dolbeau, S Bihan, and F Bodin.[2007] HMPP: A hybrid multicore parallel programming environment, in Proc. Workshop General Purpose Process. Graph. Process. Units.
- [8] Wolf ME.[1998] A loop transformation theory and an algorithm to maximize parallelism, Computer System Lab, Stanford University., CA, USA Lam, M.S.
- [9] Pierre Boulet, Alain Darté. [1997] The parallelization Algorithms for loops: parallelism extraction to code generation. *Technical Report 97–17*, LIP,ENS-Lyon, France.
- [10] PJJM Custers. [2013] Algorithmic Species: Classifying Program Code for Parallel Computing, Electronic Systems group, Eindhoven University of Technology.
- [11] H Corporaal, C Nugteren. [2012] Introducing ‘Bones’: A Paralleliz-ing Source-to-Source Compiler Based on Algorithmic Skeletons, GPGPU-5: The Workshop on General Purpose Processing on Graphics Processing Units. ACM.
- [12] Kathryn S McKinley, Ken Kennedy.[1994] Improving data locality and maximizing loop parallelism via loop fusion and distribution”,Springer.
- [13] M Wolfe. [2010] Implementing the PGI Accelerator Model, in GPGPU-3: Workshop on the General Purpose Processing on Graphics Processing Units. ACM.
- [14] Paul Feautrier.[1992] Some of the efficient solutions to the affine scheduling problem, *International Journal on Parallel Programming* :313–348.
- [15] Paul F.[1992] Some of efficient solutions to the affine scheduling problem, Part II: multi dimensional time, *International Journal on Parallel Programming*:389–420.
- [16] Frederic Viven, Alain Darté. [1996] A Optional line and medium grain parallelism detection for polyhedral reduced dependence graphs, PACT’96, Boston, *IEEE*.
- [17] Johnson R, Beck K. [1994] Patterns generating architectures, The European Conference on Object- Oriented Programming: 821. Springer, 139–149.
- [18] K Kennedy, R. Allen. [2002] Optimization of Compilers for Modern Architectures, Morgan- Kaufman.
- [19] Thomas Holl, Dirk Heuzerot, Gustav Hogstrom. [2003] Automatic design pattern detection: IWPC-03:IEEE , International Workshop, page 94, Washington, DC, USA.
- [20] Monica S Lam, Micheal E Wolf. [1991] Loop transformation theory and an algorithm to maximize parallelism. *IEEE, Parallel Distributed Systems* :452–471.
- [21] CW Kessler, J Enmyren. [2010] SkePU: A Multi-backend Skeleton Programming Library for Multi-GPU Systems,in HLPP ’10: 4th International Workshop on the High-level Parallel Programming and Applications. ACM.
- [22] Mustafa B, Waseem Ahmed. [2014] Parallelization Approaches using OpenMP for Strassens Matrix Multiplication and Canny Edge Detector, *International Journal of Information Processing(IJIP)*,8(4):89–97,ISSN: 0973–8215.
- [23] Mustafa B, Waseem Ahmed. [2015] Parallel Algorithm Performance Analysis using OpenMP for Multicore Machines, *International Journal of Advanced Computer Technology(IJACT)*, 4 (5):ISSN: 2319–7900.

ABOUT AUTHORS



Mustafa Basthikodi was born in Mangalore, India, in 1979. He received the B.E. degree in Computer Science and Engineering from the Mysore University, Mysore, India, in 2001, and the M.E. degree in Computer Science and Engineering from the Bangalore University, Bangalore in 2008. Currently Pursuing PhD in High Performance Computing and Embedded Systems from Visvesvaraya Technological University (VTU), Belgaum. In 2001, he joined the Department of Computer Science & Engineering, PACE, Mangalore, as a Lecturer, and worked till 2006. From 2006 to 2008, He worked as Senior Lecturer in Department of Computer Science & Engineering in SJBIT, Bangalore. In 2008, He joined IBM as Senior Software Engineer and worked till 2010. Since 2010, He is working as Associate Professor and Head, Department of Computer Science & Engineering, in BIT, Mangalore. He has published in various National and International Conferences. He has received few best technical paper awards and also Best performer award in industry. He has also worked as Technical Programme committee member for the various conferences. He is a Life Member and resource person for Computer Society of India. His subjects of Interest include High Performance Computing & Embedded Systems, Green & Cloud Computing, Compiler construction tools & technologies.

Dr.Waseem Ahmed is currently a Professor in the Department of CSE at HKBK College of Engineering, Bangalore. Prior to this he has been served at different capacities in academic/work environments in the USA, UAE, Malaysia, Australia and India. He obtained his BE from RVCE, Bangalore, MS from the University of Houston, USA and PhD from the Curtin University of Technology, Perth, Western Australia. He has published extensively in various reputed International Journals and Conferences. He is a reviewer for various IEEE/ACM Transactions and magazines. His current research interests include heterogeneous computing in HPC and embedded Systems. He is a member of the IEEE.

A COMPREHENSIVE EVALUATION OF WASTE MANAGEMENT SYSTEMS

Ramesh Sunder Nayak*, Deepthi, Deepthi Rai, Prathiksha, Sriram K. Bhat

IS&E Department, Canara Engineering College, Mangaluru, Karnataka, INDIA

ABSTRACT

Managing the waste has become the integral part of our day to day life. It is very essential to dispose the day to day wastes in an efficient and easy manner. Lack of waste management can result in disturbance of the environmental balance and in turn lead to the degradation of the health and hygiene of society. The main problem that has arisen deals with the detection, monitoring and management of wastes. The existing method of monitoring the waste system is a complex and tiring process that requires a lot of human effort, cost and hence will not be compatible with the development in the technologies. Hence there is a need to automate the whole process of waste management. This paper proposes the same. ZigBee is one of the most anticipated and promising technology catching up pace in the recent years. This work presented here provides a new way of approaching the problem of waste management. The system consists of four main subsystems namely Smart Trash System (STS), Local Base Station (LBS), Vehicle System and Main Station. The proposed system will be able to automate the entire process of solid waste monitoring and manage the collection of the waste efficiently. The technologies that have been proposed for the automatic waste management are practical and can be used in order to promote the concept of Green Environment.

Received on: 25th-Dec-2015

Revised on: 29th-Feb-2016

Accepted on: 16th- Mar-2016

Published on: 15th-Apr-2016

KEY WORDS

Smart Bin; Local Base Station;
Main Station; Vehicle System.

*Corresponding author: Email: ramesh.nayak.spi@gmail.com Tel: +9001010010; Fax: +40-9001010012

INTRODUCTION

Due to the advancement in science and technology there is always a tendency to automate all the manually controlled things. As the tendency increases there is an increase in the risk of exploitation. Automating all the manually done things reduces the human effort. Manually controlled products involve a higher cost and effort when compared to automated systems. There is a need to address the problem of waste management and this has to be done immediately [1]. The purpose of addressing the problem of waste management is done by keeping in mind the health and hygiene of the society and the world as a whole. Solid waste which is the main cause of environmental pollution has been defined under Resource Conservation and Recovery Act as any solid, semi-solid, liquid or contained gaseous material from agricultural, commercial, mining or industrial operations and from community activities [2]. Be it locally or globally waste management is a continuously increasing problem. Solid wastes arise mainly from the activities of humans and animals. In general terminology, solid wastes can be defined as the organic and inorganic waste materials produced by various activities of the society and which have lost their value to the first user [3]. The day to day domestic waste is collected as a whole, by placing a dustbin at a particular place for a lane or street. The process of checking the status of the bin is the toughest part. In the existing method, the municipal worker has to look through all the different areas where the bins are placed in order to collect the waste. This is a tiring and a time consuming task. The existing method of the waste management system is considerably inefficient, when the current development in technology is taken into consideration [4]. There is no guarantee that the worker will arrive to the right place, at the right time to collect the waste. In order to overcome the problems faced due to the existing method, a new way of approaching the waste management system automatically is proposed. It is the leap taken in the direction of automating the waste management to make it more efficient [5]. A Recent advancement in the technology has led everything in this world to go and connect to the Internet [6]. Using internet, it is possible to build an intranet and coordinate all the bins there by having a centralized system.

LITERATURE SURVEY

For literature survey recent papers are considered. The summary of each of them is presented below

Overview for solid waste bin monitoring and collection system

This paper is based on finding solutions for solid waste management [7]. The technologies being used in this paper are Radio Frequency Identification (RFID), Global Position System (GPS), General Packet Radio Service (GPRS), Geographic Information System (GIS) and web camera. The collection trucks are embedded with RFID reader which helps in retrieving all the customer as well as bin information from the FRID tags placed in each bin. The location of the bins is given by GPS. Authentication by the use of driver id is needed to start the collection session. The waste disposal trucks with the help of RFID readers pick up the RFID tagged bins. The RFID tags are keys for retrieving the information stored in back end databases.

Automated waste clearance

This paper is based on the Automation concept which is under the domain of Public Cleanliness and Hygiene [8]. The entire trash bins will be embedded by specific sensors so as to notify the departments whether it is full or not. The bin status will be sent to the server. The server is directly connected to the worker's profile. In this manner the worker gets alerted about the bin being full. A certain mathematic calculation is implemented so as to determine the time gap between the sensors. Based on the results, the workers will be notified about the time left for the bin to be full before he arrives to the location. After the worker clears the waste, the server is updated automatically and the sensors are reset to their original state.

RFID and integrated technologies for solid waste bin monitoring system

This paper is based on a system which consists of a trash bin which is embedded by a RFID tag, a truck which is fitted with a RFID reader, a server based on GPRS/GSM, a map server based on GIS, a database server and a control server [9]. The RFID readers mounted in the trucks retrieve the bin location via GPS. This information is regularly transferred in real time through GPRS to a database which is centrally located. A web application is designed so that the users can view the current location of the trucks individually during collection. A map server stores a digital map which displays the positions of the trucks as well as trash bin information. The RFID tag notes the data of the bins. This data is transmitted to the RFID reader present in the truck. By using this technique, the system can come to know whether the truck has arrived to the bin location or not. The amount of waste can be determined by the intensity of grey image (0 to 255). The data collected is dependent upon the camera position. Thus the amount of waste can be calculated and the graphical user interface can be used to show the result.

Smart garbage collection system in residential area

This paper is based on a concept that includes a camera being mounted on each garbage collection marker as well as a load sensor fitted at the bottom of the trash bin. The camera is used to take regular snapshots of the trash bin. The camera and the load sensors are set with a threshold value so that they can be compared. A microcontroller is used to perform the comparison. An idea about the garbage level can be conceived by performing image analysis and the weight of garbage can be evaluated by using the load sensor. The threshold level of the trash bin is checked by the controller. The controller, with the help of GSM module, sends a message to the local central office of the garbage collection unit so that it can notify that the garbage needs to be collected [10]. Due to this, the authorities send the garbage collecting vehicle to dispose the wastes, which is performed by implementing a robot mechanism.

A smart waste management with self-describing objects

This paper is based on the concept of associating smart waste management with digital information. The digital information which is associated to a waste can be stored within a QR code or a RFID tag memory. If the QR codes are used, the objects are needed to be in the line of sight [11]. In the case of RFID technology, the information in the RFID tags can be retrieved without requiring the object to be in a particular position during the operation. Nowadays, the UHF tags are being used in the area of supply chain management since the data can be read easily within a distance of five meters from the antenna of the reader. This UHF tag based concept uses the memory of the tags to store the information in data banks memory. This tag memory is used to store the digital information of the associated waste. The smart waste system requires only RFID reader to read the data. The paper also proposes a classification system of the wastes. According to this proposal, a particular type of waste is

allocated to an unique identification number. The classification is used to store the reference number which represents the waste type in the memory of each tag connected to each type of waste.

Real time bin status monitoring for solid waste collection route optimization

This paper is based on the reduction of solid waste management cost by optimization of the waste collection route, the location and number of bins used as well as their collection frequency [12]. The proposed system is implemented and started from throwing of waste inside the bin which results in updating the database in the control station for that trash bin. The trash bin is installed with a sensor which will be in sleep mode. The accelerometer sensor identifies the event when the bin cover is opened. The Hall Effect sensor measures the bin overload status by evaluating a time threshold. The data transmission from the bin is done by using ZigBee. The data is received at a remote monitoring point by with the help of GPRS coordinator. Due to this, the data sent by the GPRS coordinator is received by the Control Station and the data is stored for further processing. This technique is further optimized by using integer linear programming.

Smart recycle bin- a conceptual approach of smart waste management with integrated web based system

This paper is based on a concept of a Smart Recycle Bin [13]. This Smart Recycle Bin can be used for recycling glass, paper; aluminium can as well as plastic products. The bin automatically evaluates the value of the wastes and provides 3R card. The points collected on the 3R card can be used to rebate any item or can be cashed out in the bank account depending on the type or number of recycle waste. The aim of this system is collecting points according to the disposal activities done into specific bins. A calculator module is configured within an application algorithm which controls and coordinates the points system of the recycle bins. This concept increases the effectiveness of waste management of items which can be recycled.

An approach for monitoring and smart planning of urban solid waste management using smart-M3 platform

This paper is based on a waste management system which has a bin in which there are two types of sensors: a proximity sensor located on the upper part of the bin and a weight sensor located in the bottom of the bin [14]. The proximity sensor is used to measure the level of the wastes in the bin and the weight sensor is used to find the weight of the wastes present in the bin. Every bin has a ZigBee module installed which will be able to measure the physical quantities to the nearest light pole. The gateway of the system is implemented by a Raspberry PI which is used to collect process and transmit the data measured by the two sensors to the central control center. The control center uses the data retrieved by the sensors to implement efficient and effective optimization strategies as well as to find solutions for problems based on organization of resources on solid waste management. The control center is also responsible to inform any vehicle whether and when the bin is empty or full.

Waste bin monitoring system using integrated technologies

This paper is based on a system which implements waste management by using ARM 7 controller and ZigBee technology. The waste bins inserted with various sensors are placed at different localities. If the threshold values at the bins are exceeded, then the sensor will detect that and the data is transmitted to the ARM 7 controller using ZigBee technology. When a smart bin is detected as full by the ultrasonic sensor, the data is sent in the form of a command through ZigBee. The command is retrieved by a ZigBee receiver and the condition of the garbage bin is shown in a Liquid Crystal Display as well as on the computer. Simultaneously, the same message is sent to a driver's mobile through Short Message Service. The message consists of the entire bin information including the location of the garbage bin [15].

RFID-based real-time smart waste management system

This paper is based on a system which is proposed a RFID based waste management system [16]. This proposed system consists of a smart waste RFID tag, a RFID Reader as well as a Waste Management IT System (WMITS). A passive unique RFID tag is used in this system since passive tags do not require battery. These tags are powered by the RFID Reader and have a read range of about 10 meters. The antenna in the RFID Reader picks up the radio

waves. The RFID Reader is attached to the Personal Digital Assistant (PDA) and the unique identification number of the bin is displayed. The PDA is installed in the garbage collecting vehicle. The waste collector truck consists of a robotic arm and the weighing system is present in the arm. The weight of the bin can be determined by the help of load sensors present in the weighing system. The Bin ID is used in the calculation of waste disposal charges of individual houses and the result is stored in a temporary storage in the PDA. At the end of the work shift, all the data is stored in a SQL back end server for storage and processing of information. This data transfer is implemented by using Wi-Fi connection and the internet.

The literature review summary [Table-1] as follows:

Table: 1. Summary of the literature review

References	Interface used	Sensors Used	Technology Used	Mode of Control	Result Analysis	Usage	Provision of new features
[1]	RFID reader	UHF tag, RF tag	RFID	Semi-Automatic	Available	Smart Bin Application based on tags	NO
[2]	Smart Space	Proximity Sensor, Load sensor	Smart M3-platform	Automatic	Available	Better management of resources	YES
[3]	ARDIUNO board	Simple transmitter and receiver	ARDIUNO SIM module	Semi-Automatic	Not Available	In time and proper disposal of waste	NO
[4]	RFID reader	RFID transmitter and receiver	RFID, GIS, GPRS	Semi-Automatic	Available	Improved database for waste collection	NO
[5]	Wireless sensor network	Accelerometer, load sensor, temperature sensor	GSM, GPRS	Automatic	Available	Reduces the operation cost	YES
[6]	RFID reader, camera	RFID transmitter and receiver	RFID, GPS, GPRS, GIS, Image processing	Semi-Automatic	Available	Monitoring and management of status of the bin	NO
[7]	Mobile Wi-Fi network	RFID tags, HBM SSC load cells	RFID and load self-sensor technology	Automatic	Available	Tracking customer identity, weight and missing, stolen bins	YES
[8]	Micro-controller	Web camera, load sensor	Robotic Mechanism	Automatic	Not Available	Avoid the overflowing of garbage from the container	NO
[9]	RFID reader	RFID tags	Wireless Internet	Semi-Automatic	Not Available	Improved collection of recyclable waste	NO
[10]	ARM Micro-controller	IR sensors	ZigBee and GSM technology	Semi-Automatic	Not Available	Monitor the solid waste collection	YES
Proposed	Serial Communication	Ultrasonic sensor, load sensor	ZigBee, Ad-hoc networks	Automatic	Available	Least expensive, reduced amount of human effort and efficient	YES

The Table shows that the proposed system is far better compared to the one already available.

PROPOSED MEHTODOLOGY

The architecture of the proposed system is shown in the [Figure– 1](#).

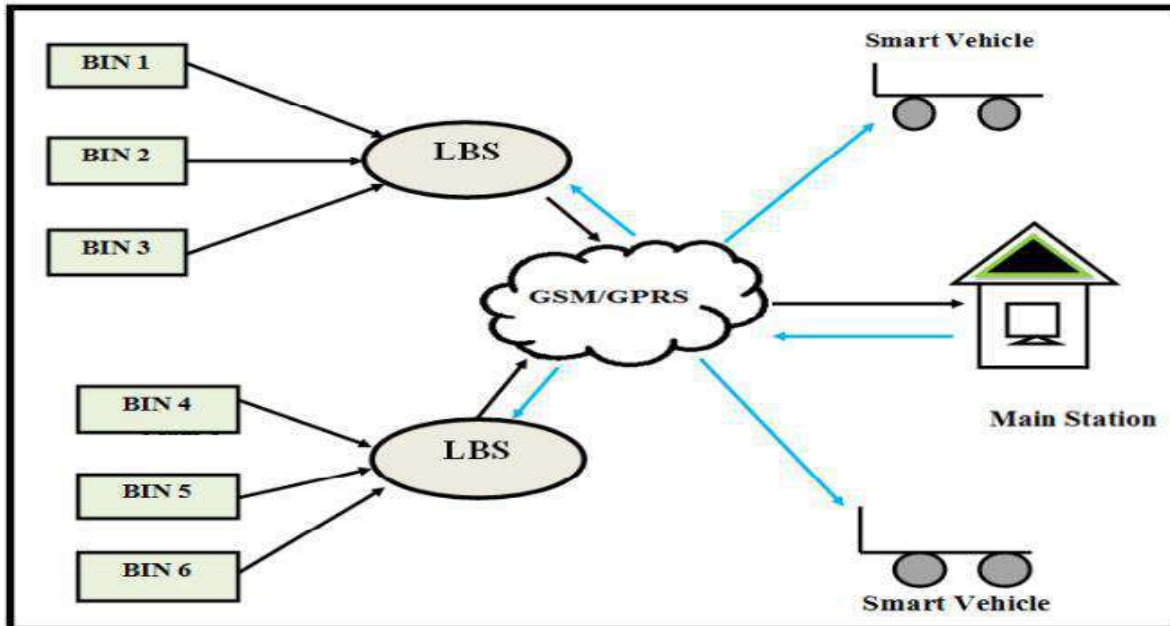


Fig: 1. Architecture of AWMS

Virtualization Smart Bin System consists of electronic device known as “Smart Trash Bin”, which includes sensors and a ZigBee transmitter. Two types of sensors which are used in Smart Trash Bin are Ultrasonic Sensor and Load Sensors. The Ultrasonic sensor is used to detect the level of wastes in the Smart Trash Bin. The Load sensor is used to detect the weight of the waste present in the Smart Trash Bin. Whenever the threshold value any one of the sensors is reached, it gets activated and generates a high signal. This signal is transmitted by the ZigBee transmitter present in the bin and is received by the ZigBee receiver situated at the local base station. After receiving the signal, the local base station identifies the unique bin ID, decodes the trash bin location and then sends a signal to the main station about the location of the trash bin. The Main station will send the Bin information to the Smart Vehicle through GSM/GPRS. The Smart Vehicle consists of a Liquid Crystal Display (LCD) in which the bin location is displayed. Thus the workers approach to the location of the bin and collect the wastes.

RESULTS AND DISCUSSION

The [Figure– 2](#) depicts the webpage for managing the wastes in the Automatic Waste Management System. This portal is controlled by the Main Station. Using this webpage, the status of the Smart Trash Bins placed at many locations in the city can be efficiently and effectively monitored. The webpage consists of the areas of the Local Base Stations and the status of the Smart Trash Bins located within these areas.

The main problems of the existing solid waste collection process and management system are as follows:

- Lack of the information about the collecting time and area.
- Lack of the proper system for monitoring, tracking the trucks and trash bin that have been collected in real time.
- There is no estimation to the amount of solid waste inside the bin and the surrounding area due to the scattering of waste.
- There is no quick response to urgent cases like truck accident, breakdown, longtime idling.
- There is no quick way to response to client's complaints about uncollected waste.

- Consumption of manpower to collect the trash.
- Time consuming

Automatic Waste Management System



Fig: 2. Web portal for automatic waste management system

Compared to this, the proposed automated, efficient waste management system will do the following

- Saves time, human efforts.
- Makes the entire process traceable to see cleanliness is maintained in the city there by preventing spreading of diseases.

In the currently employed method concerned municipal employee has to look for the filled waste bins manually across different places in the different geographic area/street for checking regularly. He needs to analyze data manually. The proposed system is successfully employed in dust beans and found that it has solved a lot of problem related to solid waste collection, monitoring, minimizing cost and accelerate the handling management.

The outcome of the proposed system is found to be:

- Efficient handling of wastage.
- As soon as the Smart Trash Bin gets filled by the trashes or wastes, the signal is sent to the local base station.
- Once the base station receives signal from the smart trash bin signal, separate signal is sent to the Main Station.
- The Main Station sends signal to Smart Vehicle along with dumping yard details

CONCLUSION

The automatic waste management process is a step that is taken in order to reduce the hardship of manual collection and detection of wastes in an automatic manner. The developed system is a combination of four main subsystems. Those are Smart Trash System (STS), Local Base Station (LBS), Main Station (MS) and Smart Vehicle. The system makes use of the ZigBee technology which is a low cost, low power, wireless mesh network. The purpose of proposing the automatic management process is in terms of its efficiency and time saving nature when compared to the already existing one. In the currently employed method the concerned municipal worker has to locate the bins manually and check the status of the trash bin. This is a very complex and a time consuming process. Hence, there is an immediate need to automate the process of waste management to reduce the human effort and therefore reduces the cost of the whole process. This system can be implemented anywhere and is feasible. The reduced cost of the entire process makes it affordable. Hence the entire method used for the detection and management of waste makes the system efficient and intelligent. The system solves a considerable

amount of problems related to the waste collection, monitoring, reducing the cost and therefore accelerate the process of management.

CONFLICT OF INTEREST

Authors declare no conflict of interest.

ACKNOWLEDGEMENT

None.

FINANCIAL DISCLOSURE

No financial support was received to carry out this project.

REFERENCES

- [1] Filipowicz W, Bhattacharyya SN, and Sonenberg N. [2008] Mechanisms of post-transcriptional regulation by microRNAs: are the answers in sight?, *Nat Rev Genet* 9: 102–114.
- [2] Ivey KN, Muth A, Arnold J, King F W, Yeh RF, Fish JE, Hsiao EC, Schwartz RJ, Conklin BR, Bernstein HS, and Srivastava D. [2008] Microrna regulation of cell lineages in mouse and human embryonic stem cells, *Cell Stem Cell* 2: 219–229.
- [3] Chen JF, Mandel EM, Thomson M, Wu Q, Callis TE, Hammond SM, Conlon FL, and Wang DZ. [2006] The role of microrna-1 and microrna-133 in skeletal muscle proliferation and differentiation. *Nat Genet* 38:228–233.
- [4] The EUs approach to waste management, April 2012. [Online]. Available: <http://ec.europa.eu/environment/waste/index.html>
- [5] H Boileau and H Bjork. [2006] Comparing household waste treatment policies between two medium size cities: Borås (sweden) and chambéry (france),” in Proceedings of the 7th World Congress on Recovery, Recycling and Re-integration, June 2006. [Online]. Available: <http://csp.eworlding.com/3r/congress/manu.pdf/420.pdf>
- [6] Ramesh S Nayak, Shreenivas Pai N, Akshay Nayak, and Akhil Simha N. [2016] A STUDY ON IOT ENABLED SMART STORE, *IIOABJ*, 7 (2): 61–67.
- [7] SV Srikanth, P Pramod, K Dileep, S Tapas, M Patil, and C Sarat. [2009] Design and implementation of a prototype smart parking (spark) system using wireless sensor networks. *International Conference on Advanced Information Networking and Applications Workshops*, 2009, WAINA 09. May pp. 401–406.
- [8] A Verma, R Singh, RS Yadav, N Kumar and P Srivastava. [2012] Investigations on potentials of energy from sewage gas and their use as standalone system, International Conference on Advances in Engineering, Science and Management (*ICAESM*), 2012, Nagapattinam, Tamil Nadu, , 715–717.
- [9] Development of robotic sewerage blockage detector controlled by embedded systems - 2012 Shrivastava, AK.; Verma, A. Singh, SP.
- [10] RFID for the Business of Waste Management, www.falkensecurenetworks.com. Retrieved on November 22, 2011.
- [11] M Faccio, A Persona, and G Zanin. [2011] Waste collection multi objective model with real time traceability data”, science direct, *Waste Management*, 31(12):2391–2405.
- [12] Bin W, Qingchao A, Qulin WT, Shonglin Y. [2004] Integration of GIS, GPS and GSM for the Qinghai-Tibet railway information management planning. Proceedings of the Youth Forum on ISPRS Congress, Istanbul, pp. 71–74.
- [13] Claire Swedberg, [2007] NEC Works on RFID Tags, Readers for Bottle Caps, *RFID Journal*, <http://www.rfidjournal.com/article/articleview/3150/1/1/>, accessed on 10 October 2007.
- [14] Y Kai, Z Junmei, L Wenbin, Y Liu, G Lin and X Huixia. [2011] Weighing System of Fruit-Transportation Gyrocar Based on ARM,” *Third International Conference on Measuring Technology and Mechatronics Automation (ICMTMA)*, 2011, Shangshai, 2011, 1146–1149.
- [15] Tarmudi Z, Abdullah ML, Tap AOM. [2009] An overview of municipal solid waste generation in Malaysia, *Jurnal Teknologi* 51(F):1–15.
- [16] Mohd Nasir Hassan, Theng , Lee Chong and Mizanur Rahman, Mohd Nazeri Salleh, Zulina Zakaria , and Muhamad Awang. Solid waste management – what’s the Malaysian position, *Malaysian Journal of Environmental Management*, 2 : 25-43. ISSN 1511–7855.

ABOUT AUTHORS



Prof. Ramesh Nayak is currently working as associate professor in Canara Engineering College, Benjanapadavu, Mangaluru, Karnataka, INDIA. He is currently faculty in the department of Information Science and Engineering. He received his M.Tech degree from University of Mysore, Mysore, India. He is pursuing PhD in image processing. His research interest includes Image processing, Data Mining, Computer Networks. He has teaching experience of 14 years and research experience of 3 years. He has published research papers in national International conferences and Journals.



Ms. Deepthi is currently pursuing B.E degree in IS&E department, Canara Engineering College, Benjanapadavu, Mangaluru, Karnataka, INDIA.



Ms. Deepthi Rai is currently pursuing B.E degree in IS&E department, Canara Engineering College, Benjanapadavu, Mangaluru, Karnataka, INDIA.



Ms. Prathiksha P. is currently pursuing B.E degree in IS&E department, Canara Engineering College, Benjanapadavu, Mangaluru, Karnataka, INDIA



Mr. Sriram K Bhat is currently pursuing B.E degree in IS&E department, Canara Engineering College, Benjanapadavu, Mangaluru, Karnataka, INDIA.

DIGIT RECOGNITION USING MULTIPLE FEATURE EXTRACTION

Deepthi Praveenal Kuttichira*, V. Sowmya, K.P. Soman

Centre for Computational Engineering and Networking (CEN), Amrita School of Engineering, Coimbatore, Amrita Vishwa Vidyapeetham, Amrita University, INDIA

ABSTRACT

Digit Recognition is one of the classic problems in pattern classification. It has ten labels which are digits from 0-9 and each prototypes in the test set has to be classified under these labels. In this paper, we have used MNIST data for training and testing. MNIST database is a standard database for digit classification. A number of neural network algorithms have been used on MNIST to get high accuracy outputs. These algorithms are computationally costly. Here, we have used multiple feature extraction based on SVD and histogram to create testing and training matrix. To the feature vector formed by SVD, histogram values along x-axis and y-axis of an image is appended. These vectors are mapped to hyperplane using polynomial and Gaussian kernel. For classification open source software like GURLS and LIBSVM is used to obtain a fairly good accuracy.

Received on: 1st-April-2016

Revised on: 5th-April-2016

Accepted on: 10th -April-2016

Published on: 16th -April-2016

KEY WORDS

Support Vector Machine (SVM);
Single Value Decomposition (SVD); Overall accuracy (OA);
Class wise Accuracy (CA);
Regularized Least Squares (RLS), digit recognition

*Corresponding author: Email: deepthikuttichira93@gmail.com Tel: +40-9001010010; Fax: +40-9001010012

INTRODUCTION

Recognition of handwritten digit is a typical character recognition problem with ten labels, each corresponding to a digit from 0-9. Many classification methods like K-nearest neighbors, linear classifiers, SVMs, neural networks, convolutional neural networks etc. has been used on MNIST database. A comparison between these algorithms are given [1]. Our approach for solving digit recognition problem, requires less computational cost and has considerable accuracy.

In machine learning, there are two types of learning approaches called supervised and unsupervised learning [2]. Class labels are a priori knowledge for supervised learning. Whereas, in unsupervised learning class labels are not a priori knowledge. In our proposed method, we have used multiple feature extraction to create vectors for each prototypes for classification [3]. The learning method proposed here, uses SVM as a supervised learning method. In any classification, the objective is to find a curve that separates two classes of data points. If that curve is a straight line, then the data is said linearly separable. To find this curve or plane of separation, the data points are plotted in a space and then we try to find a curve that separates them into separate classes. If such a curve cannot be found in the plane on which data points were originally projected, then the data points are projected on to a higher dimensional plane and a curve or a hyperplane that separates these data points is found. For this the data points have to be mapped from lower dimensional plane to higher dimensional plane. This mapping of data points from lower dimension to higher dimension is done using kernel functions.

Several neural networks have been trained to give good accuracy for MNIST dataset [4]. Algorithm that gives the best accuracy is that of convolutional neural networks. Neural networks and most of these best performing algorithms require large dataset and heavy computation. The algorithm proposed in this paper uses a subset of MNIST dataset and is computationally less costly. The proposed algorithm can be run on an ordinary desktop PC with a fairly good accuracy of 85.5%. For classification, we have used two tools LIBSVM and GURLS. A comparative analysis of these two tools, based on the classification result given by them is presented in section 3 of this paper. The tools, LIBSVM and GURLS are two open source software that offer several libraries based on kernel function for SVM. LIBSVM was developed by C.-C. Chang and C.-J. Lin. [6]. GURLS was introduced by Tacchetti, Mallapragada et al. [8]. GURLS can be efficiently applied for multiclass problems [5]. LIBSVM has packages for various kernel methods for SVM [5]. GURLS uses Regularized Least Squares for

classification and regression [5]. We observed that GURLS gave better results for digit classification than LIBSVM. Section 2 of this paper describes the dataset, preprocessing techniques and algorithm used in this paper. Once the feature extraction was done we have used both GURLS and LIBSVM for classification. A comparison study of these two algorithms is presented in the section 3 of this paper.

MATERIALS AND METHODS

LIBSVM

LIBSVM provides several inbuilt kernel functions for SVM [5]. SVM maximizes the margin of line of separation between classes. Support Vectors are the data points that fall on the margin [2]. If data points can be classified to two classes, SVM can be visualized as follows. Let (a_i, b_i) be two sets of data point belonging to the respective classes where $i = 1, 2, \dots, n$. Let a_i of class 1 be labeled as +1 and b_i of class 2 be labeled as -1. Let A be the set that contains both a_i and b_i . The hyperplane that separates these two classes is given by the equation

$$w^T A - \gamma = 0 \quad (1)$$

Where $w = (w_1, w_2, w_3, \dots, w_n)$ and $A = (a_1, a_2, \dots, a_n, b_1, b_2, \dots, b_n)$. w is the weight matrix that is learned. A is the feature vector. γ is the bias term. Depending on the sign of the function the class is chosen. The decision function is given below

$$f(x) = \text{sgn}(w^T x - \gamma) \quad (2)$$

If the data points cannot be linearly separated, they have to be projected into a plane with higher dimension, where it can be partitioned linearly by a hyperplane [2]. The projection into higher dimensional plane is done using a mapping function called kernel function. A mapping function is:

$$\phi: \mathbb{R}^n \longrightarrow \mathbb{R}^k$$

Here $k \gg n$. The mapping is given as

$$K(a_i, a_j) = \langle \phi(a_i), \phi(a_j) \rangle \quad (3)$$

Few kernels provided by LIBSVM are listed below.

- LINEAR KERNEL

$$K(a_i, a_j) = a_i^T a_j \quad (4)$$

- POLYNOMIAL KERNEL

$$K(a_i, a_j) = (\gamma a_i^T a_j + r)^d, \gamma > 0 \quad (5)$$

- RADIAL BASIS FUNCTION KERNEL

$$k(a_i, a_j) = \exp(-\gamma \|a_i - a_j\|^2), \gamma > 0 \quad (6)$$

- SIGMOID KERNEL

$$k(a_i, a_j) = \tanh(\gamma a_i^T a_j + r) \quad (7)$$

Here γ , r and d are kernel parameters.

GURLS

GURLS is an open source software that uses RLS for classification [5]. In RLS say there are N data points $A = [a_1, a_2, \dots, a_n]$ belonging to \mathbb{R}^n and let $Y = [y_1, y_2, \dots, y_n]$ where Y is the label vector such that $y_i \in \mathbb{R}^p$. In RLS for a p -class problem every data point x_i will have a corresponding y_i which belongs uniquely to a particular class in p . So the goal is to learn the weight matrix W , which maps the data vectors to the unique label vector. Learning of weights is a minimization problem of the form:

$$\min_w \sum_i \|w a_i - y_i\|_2^2 \quad (8)$$

GURLS is a very efficient multiclass classifier [5]. One of the biggest advantages of GURLS is its automatic parameter tuning. GURLS models the problem faster too. The kernel used from GURLS library for this paper is Gaussian kernel with RBF type. Its mathematical formulation is

$$K(a_i, a_j) = \exp(-\gamma \|a_i - a_j\|^2), \gamma > 0 \quad (9)$$

MATHEMATICAL BACKGROUND

For feature extraction, we have used the concept of Singular Value Decomposition (SVD). SVD is a decomposition method in Linear Algebra which decompose a matrix into three sub matrices U, S, V. If A is a $m \times n$ matrix then U is a $m \times m$ matrix that contains the Eigen vectors of $A^T A$ and V is a $n \times n$ matrix containing Eigen vectors of AA^T . S is a $m \times n$ diagonal matrix that contains square roots of non-zero Eigen values of AA^T and $A^T A$

$$A = USV^T \quad (10)$$

DATASET

The dataset used for our paper is a subset of MNIST database. MNIST contains 60,000 images for training and 10,000 images for testing. We have used 1,200 images for training and 200 images for testing. The testing image set for each class is set to 20. The number of training images is decided by keeping the ratio of test and train of MNIST database. MNIST dataset was created from NIST dataset in which training data was collected from US Census Bureau employees and testing data taken from American High School students. MNIST dataset contains 28×28 pixel grayscale images for each prototypes. **Figure- 1** shows some sample images from MNIST dataset. The images shown are rather the well written ones in the dataset.

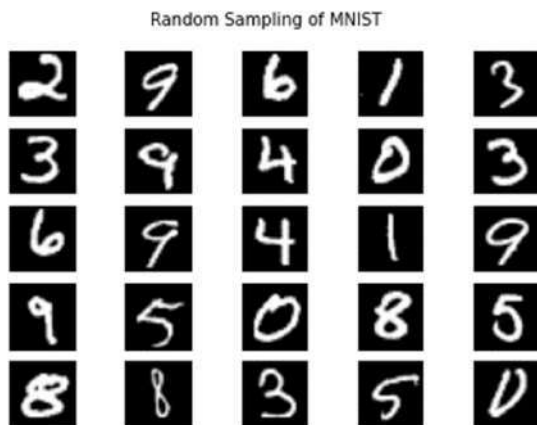


Fig. 1. Sample images of MNIST Dataset

PREPROCESSING

The prototypes for testing as well as training were cropped closely to the digits and then resized to 28×28 pixels. This was done to center align the digits. Blurring helps in digit recognition as specified in ref [7] [4]. The blurring technique that we have used in this paper is Gaussian. Gaussian blur blurs the digits along its gradient. It helps to blur the sharp outlines and enhance digit recognition [2]. The mathematical formulation of Gaussian blur is

$$g(r, s) = e^{-(r^2 + s^2)/(2\sigma^2)} \quad (11)$$

The fast decay offered by this Gaussian blur helps in reducing the computational time [4]. The standard deviation σ controls the blur. A value of 0.9 is used as standard deviation. This is the same value specified in the [7]. **Figure- 2** shows Gaussian blurred corresponding to the digit 5. As decay factor increases, blurring also increases. The decay factor is chosen in such a way that, the blurring does not result in loss of structural information of the digit but does blur the fine outlines of the digit. Choice of the decay factor plays an important role in decreasing computational time [7].

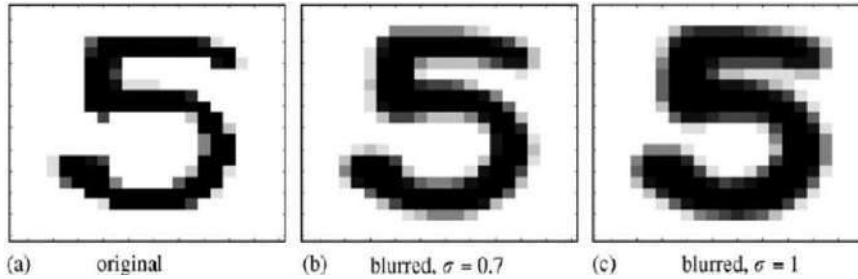


Fig: 2. Gaussian blurred image

FEATURE EXTRACTION

We have used two feature extraction techniques in this paper. For each prototype SVD is done and U^*S matrix is converted to a column vector. This gives a feature vector of size 784. To this feature vector we append the structural information of the prototype. As structural information we have taken "histogram of the prototype along x-axis as well as y-axis." It is the count of black pixels corresponding to each line and column of the prototype" [3]. So our final feature vector for each prototype has a length of 840 [784+28+28]. These feature vectors are extracted for all training data. Features of the same data type are labelled accordingly. The training matrix consists of these feature vectors and corresponding labels. This training matrix is given as input to LIBSVM and GURLS.

ALGORITHM

The algorithm used in this paper is briefly described below:

- Step 1: The prototype images of training data are cropped and then resized to 28×28 pixels. This is done to center align the digits.
- Step 2: Gaussian blur is added to the images with a decay factor of 0.9.
- Step 3: SVD of the prototype and histogram along x-axis and y-axis are taken.
- Step 4: The U^*S matrix is made into a column vector and the histogram values are appended together to form a feature vector of size 840.
- Step 5: The feature vectors along with labels form the training matrix.
- Step 6: Steps 1 to 4 are repeated for test prototype.
- Step 7: The training matrix and testing matrix are passed to GURLS and LIBSVM.
- Step 8: Classification result is obtained.

RESULTS AND DISCUSSION

ACCURACY COMPARISON

Here we have discussed the results obtained from LIBSVM and GURLS. The best results was given by GURLS using Gaussian kernel. Overall accuracy and class wise accuracy given by LIBSVM and GURLS are discussed here. First, the formulas used for calculating Overall accuracy (OA) and class wise accuracy (CA) are listed below [5].

$$CA = \frac{\text{Total no : of correctly classified digits of each class}}{\text{Total no : of digits in each class}} \quad (12)$$

$$OA = \frac{\text{Total No. of correctly classified digits}}{\text{Total no. of digits}} \quad (13)$$

The confusion matrix obtained from LIBSVM using polynomial function is shown in [Table- 1]. From confusion matrix, we can infer the number of test data that are correctly classified as well as misclassified. The elements along the diagonal of a confusion matrix shows the count of prototypes that are correctly classified according to the respective classes. The non-diagonal elements are the misclassified prototypes. From the confusion matrix of

[Table– 1] we can see that the digit 9 is highly misclassified as 1. This is because if the loop of digit 9 is too small, it can be easily mistaken as digit 1. Such similarities between digits that incur error rate can be easily observed using confusion matrix.

Overall accuracy and Class wise accuracies are 2 common accuracy measures for pattern classification [3]. These both measures for LIBSVM and GURLS are enlisted in [Table– 2]. Only for digit 6 and digit 9 LIBSVM shows a better accuracy. For rest all classes GURLS shows better accuracy. Digit 6 and digit 9 can be easily misplaced as 6 rotated would look like 9 and vice versa. GURLS also shows better overall accuracy than LIBSVM. GURLS parameter tuning is very efficient. The Gaussian kernel that we have used from GURLS library appears to be an apt mapping function for SVM based digit classification.

Table: 1. Confusion Matrix for Polynomial Function in LIBSVM

	Digit One	Digit Two	Digit Three	Digit Four	Digit Five	Digit Six	Digit Seven	Digit Eight	Digit Nine	Digit Zero
Digit One	15	0	2	0	0	0	0	1	0	2
Digit Two	0	14	0	3	0	1	0	1	0	1
Digit Three	1	0	14	0	1	0	1	0	0	3
Digit Four	0	0	0	12	0	1	1	0	3	3
Digit Five	0	1	3	0	13	0	0	3	0	0
Digit Six	0	1	0	0	1	19	0	0	0	0
Digit Seven	1	0	0	0	0	0	15	1	3	0
Digit Eight	1	0	1	0	0	0	1	13	1	3
Digit Nine	3	0	0	0	0	0	1	1	15	0
Digit Zero	0	0	0	0	0	0	0	0	0	20

Class wise accuracy of GURLS and LIBSVM is plotted in Figure–3. Except for digit 6 and digit 9 GURLS gives better results for all other digits than LIBSVM. Overall accuracy obtained by LIBSVM when using polynomial function for classification is 75% and that of GURLS is 85.5% when using Gaussian kernel. The overall accuracy plot between LIBSVM and GURLS is shown in Figure–4. Overall accuracy of GURLS is also higher than that of LIBSVM.

Table: 2. Class wise accuracy for Gaussian Kernel in GURLS and polynomial function in LIBSVM

	Digit One	Digit Two	Digit Three	Digit Four	Digit Five	Digit Six	Digit Seven	Digit Eight	Digit Nine	Digit Ten	OA
CA GURLS	95%	75%	90%	90%	65%	85%	90%	80%	65%	95%	85.5%
CA LIBSVM	75%	70%	70%	60%	65%	95%	75%	65%	75%	100%	75%

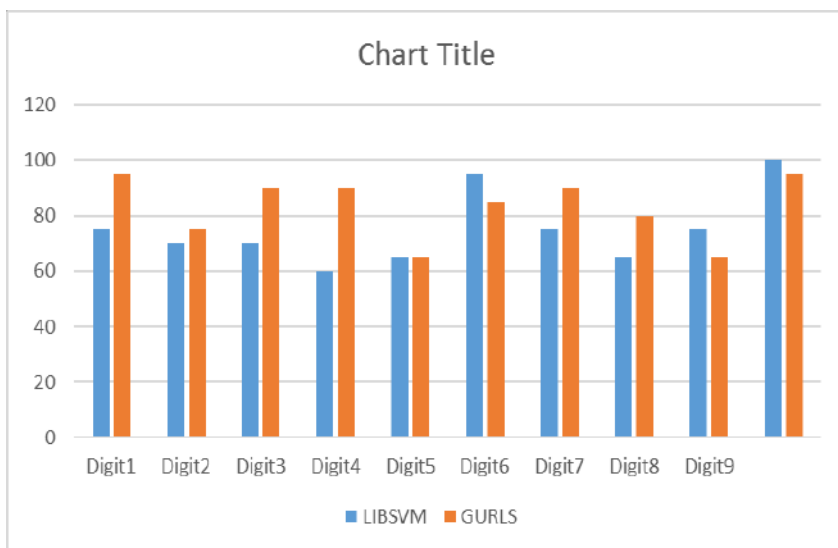


Fig: 3. Class wise accuracy of LIBSVM and GURL

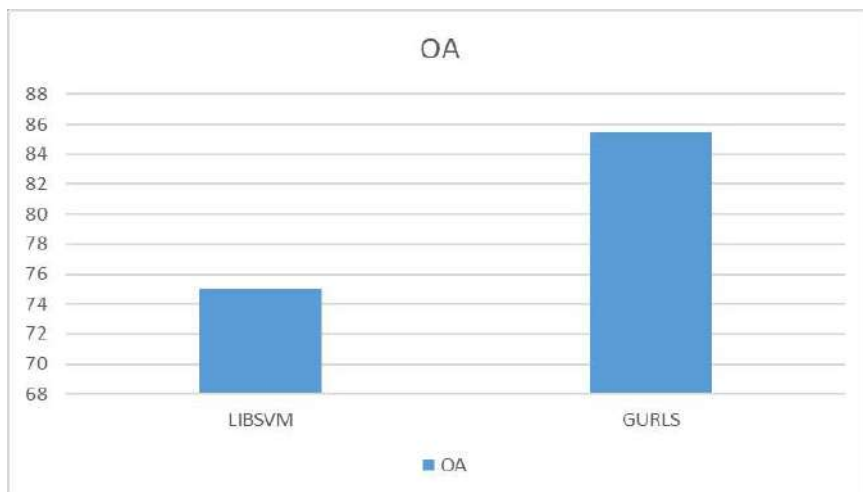


Fig: 4. Overall accuracy of LIBSVM and GURLS

CONCLUSION AND FUTURE WORK

We observed that for digit classification, using MNIST dataset, LIBSVM with polynomial classification function gave good classification with overall accuracy of 75%. But, a way better classification is provided by GURLS when used Gaussian kernel, which gave an accuracy of 85.5%. From this, we can infer that for digit classification using SVM, Gaussian kernel is ideal. Also, if handwritten data has minimum rotation based error then the accuracy of the proposed algorithm will be far better. Decay factor would vary according to different datasets. Tuning to a good decay factor enhances computational speed. Error rate can be further reduced by selectively increasing the sampling of structurally similar prototypes such as digit 1 and digit 9. Supervised learning for handwritten digit is good in computational perspective. Without any iteration the accuracy obtained is 85.5%. Including more scaled and rotated prototypes in the training set could improve the accuracy. Ideally if all such scaled and rotated prototypes are included, we should be able to obtain highly accurate classification for train any test data prototypes.

CONFLICT OF INTEREST

Authors declare no conflict of interest.

ACKNOWLEDGEMENT

None.

FINANCIAL DISCLOSURE

No financial support was received to carry out this project.

REFERENCES

- [1] Y LeCun, L Jackel, L Bottou, et al. [1995] Learning algorithms for classification: a comparison on handwritten digit recognition, *Neural Network: The Statistical Mechanics Perspective* 261–276.
- [2] KP Soman, R Loganathan, and V Ajay. [2009] Machine Learning with SVM and other Kernel methods. PHI Learning Pvt. Ltd.
- [3] Rafael M O Cruz, George DC Cavalcanti, Tsang Ing Ren. [2010] Handwritten Digit Recognition Using Multiple Feature Extraction Techniques and Classifier Ensemble. 17th International Conference on Systems, Signals and Image Processing.
- [4] Berkant Sawas, Lars Elden. [2007] Handwritten digit classification using higher order singular value decomposition. *Pattern recognition* 40: 993–1003.
- [5] Nikhila Haridas, V Sowmya, K P Soman. [2015] GURLS vs LIBSVM: Performance Comparison of Kernel Methods for Hyperspectral Image Classification. *Indian Journal of Science and Technology*, 8(24).
- [6] C.-C. Chang, C.-J. Lin. [2011] Libsvm: A library for support vector machines. *ACM Transactions on Intelligent Systems and Technology (TIST)*, 2(3): 27.
- [7] Patrice Y Simard, Yann A Le Cun, John S Denker, Bernard Victorri. [2000] Transformation Invariance in Pattern Recognition-Tangent Distance and Tangent Propagation. *Internat J Imag Systems Technol* 11 (3): 181–197.
- [8] A Tacchetti, PK Mallapragada, M Santoro, L Rosasco. [2013] Gurls: a least squares library for supervised learning. *The Journal of Machine Learning Research*, 14(1): 3201–320.

ABOUT AUTHORS

Deepthi Praveenlal Kuttichira received her B.Tech degree in Computer Science in 2015. Currently she is pursuing her M.Tech degree in Computational Engineering and Networking (CEN) from Amrita School of Engineering, Coimbatore, Amrita Vishwa Vidyapeetham, Amrita University, India. Her research interests include Machine Learning, Pattern Recognition and Big Data analysis.

Sowmya V currently serves as Assistant Professor at Amrita Centre for Computational Engineering and Networking (CEN), Coimbatore campus. Her research area include Image processing, Hyperspectral Image Classification, Pattern Recognition and Machine Learning.

Dr. K P Soman currently serves as Head and Professor at Amrita Centre for Computational Engineering and Networking (CEN), Coimbatore campus. His research interest include Software Defined Radio, Wireless Sensor Networks (WSN), High Performance Computing, Statistical Digital Signal Processing (DSP) on Field Programmable Gate Array (FPGA), Machine learning Support Vector Machines, Signal Processing and Wavelet & Fractals.

LEAST SQUARE BASED APPROACH FOR IMAGE INPAINTING

Aiswarya M. *, Deepika N., V. Sowmya, Neethu Mohan, K. P. Soman

Centre for Computational Engineering and Networking (CEN), Amrita School of Engineering, Coimbatore, Amrita Vishwa Vidyapeetham, Amrita University, INDIA

ABSTRACT

Images are widely used over various applications under the aegis of various domains like Computer vision, Biomedical, etc. The problem of missing data identification is of great concern in various fields involving image processing. Least square can be used for missing sample estimation for 1-D signals. The proposed system extends the missing sample estimation in 1-D using least square to 2-D, applied for image inpainting. The paper also draws a comparison between the Total Variation (TV) algorithm and the proposed method. The experiments were conducted on standard images and the standard metrics namely PSNR and SSIM are used to compare the image quality obtained using the proposed method (least square based) and TV algorithm.

Received on: 1st-April-2016

Revised on: 15th-April-2016

Accepted on: 20th -April-2016

Published on: 26th -April-2016

KEY WORDS

least square; inpainting;
missing sample estimation;
mask

*Corresponding author: Email: aishmadhu.92@gmail.com Tel: +91-8547633589

INTRODUCTION

Images play the most important role in human perception. In this digital world, we deal with a huge number of images every day. Today, almost all areas of technical endeavor is in some way or the other impacted by digital image processing. An image is a two-dimensional function with two spatial coordinates and a corresponding amplitude level. A digital image is a representation of an image as a set of digital values, called pixels [1].

In real world, the images may be corrupted with letters or scratches. There are also chances for loss of information due to noise or during transmission. In some other cases, we need to remove undesirable objects from the image, say for the case, in which we need to remove an object that destroys the beauty of the image. In order to reconstruct the image free from letters and scratch, or remove an unwanted object, we use image inpainting techniques. Image inpainting is one of the image restoration techniques in which, any lost information is restored using the nearby pixel information. It is considered as the safest way of restoring a degraded image. Digital inpainting has wider applications in image processing, vision analysis and film industry. It can be also be used for old film restoration and red eye correction [2]. The recent applications of image inpainting includes scratch removal from images, text erasing, object removal, disocclusion etc. Generally, the region of the image to be removed, known as mask is defined by the user, while in certain applications, the mask itself need to be detected from the image [3]. Inpainting is known by many names based on their applications, like 'error concealment' in telecommunication [4]. Variational inpainting, texture synthesis, Bayesian inpainting etc. are the most popular inpainting methods. The method is chosen based on the content and location of sampling [5]. In image enhancement problems, the pixel locations contain information regarding the real data as well as noise. Whereas, in case of inpainting, there will be no information related to the real data in the region to be restored [6].

The existing inpainting techniques can be broadly classified into diffusion based approaches and exemplar-based. In diffusion based approaches, linear structures or level lines (isophotes) propagate through diffusion. It is based on the Partial Differential Equations (PDE) and variational methods. The main drawback of the diffusion based method is that, when the region to be filled in is large, the output becomes blurred and is a time consuming process. In exemplar-based method, the best matching texture patches from the surrounding pixels is copied [7]. It works well for larger region restoration. It preserves both the structure and texture of the image [8]. Another inpainting technique that solely relies on PDE is an iterative algorithm. In this method, the information propagates in the direction of minimal change using level sets. Like the diffusion based algorithm, this also doesn't work well for

large missed regions and is highly time consuming. However, the efficient Total Variation (TV) inpainting method was inspired by this method, which uses anisotropic diffusion and Euler-Lagrange equation, and is based on the strength of isophotes [2]. It was first proposed by Fatemi, Rudin and Osher for image denoising [9]. In TV method, the sharp edges are recovered under some conditions [7]. The computationally expensive and time intensive nature of TV inpainting inhibits its wide spread usage in practical applications [10] [11].

In this paper, the 1-D least square missing sample estimation algorithm is mapped to 2-D images for image inpainting. The image to be inpainted and the mask to be removed are defined by the user. The proposed method uses least square approach for inpainting which not only produce a desired result, but also takes lesser time when compared to the conventional TV algorithm.

Section II is divided into three sub sections, in which the least square method, the mathematical background for the proposed method and missing sample estimation algorithm are discussed. Section III comprises the results which includes the calculated metrics and image outputs. Section IV discusses the importance of proposed method by drawing up an inference out of the results obtained. Section V concludes this paper.

MATERIALS AND METHODS

Least Square Method

The least square method is used to find the best fitting curve solution for a given set of points, mathematically. The basic least square problem is to find the best fitting straight line

$$y = Ax + b, \text{ where } x, y \in \mathbb{R}^n;$$

A is an $n \times n$ matrix; and
 x, y and b are $n \times 1$ vectors

It requires y to be equal to the sum of the linear combination of columns of A and an error vector b . The best fitting curve is estimated by minimizing the sum of squares of the offsets of points from the curve. The sum of squares are used instead of the absolute value so as to take the residuals as a continuous differentiable quantity.

Missing sample estimation

In some cases, the original signal may have missing parts or may be corrupted to the extent where the signal at hand may not even remotely resemble the original signal. This can be due to noise, interference or transmission error. In such problems, the missing samples are to be estimated from the available samples, irrespective of whether the missing sample are random or not. The method can be used independent of whether the missing samples follows a particular structure pattern.

Formulating the problem as a least square problem: [12]

Consider a signal x of length N . Let y be the signal with K number of known samples, where $K < N$.

$$y = Lx, \text{ where } L \text{ is a } K \times N \text{ selection matrix or sampling matrix}$$

For example, consider a signal of length 5. If only the second, third and last location information is known, then the matrix L can be written as

$$L = \begin{bmatrix} 0 & 1 & 0 & 0 & 0 \\ 0 & 0 & 1 & 0 & 0 \\ 0 & 0 & 0 & 0 & 1 \end{bmatrix}$$

The problem stated is, given the signal y and the matrix L , find x such that $y = Lx$. Also, the sum of squares of the second derivative of the whole signal should be minimum.

$$Lx = \begin{bmatrix} 0 & 1 & 0 & 0 & 0 \\ 0 & 0 & 1 & 0 & 0 \\ 0 & 0 & 0 & 0 & 1 \end{bmatrix} \begin{bmatrix} x(0) \\ x(1) \\ x(2) \\ x(3) \\ x(4) \end{bmatrix} = \begin{bmatrix} x(1) \\ x(2) \\ x(4) \end{bmatrix} = y$$

Vector y has the known samples of x .

$L^T y$ sets the missing samples of x to zero.

$$L^T y = \begin{bmatrix} 0 & 0 & 0 \\ 1 & 0 & 0 \\ 0 & 1 & 0 \\ 0 & 0 & 0 \\ 0 & 0 & 1 \end{bmatrix} \begin{bmatrix} y(0) \\ y(1) \\ y(2) \end{bmatrix} = \begin{bmatrix} 0 \\ y(0) \\ y(1) \\ 0 \\ y(2) \end{bmatrix}$$

L_c , which is the complement of L is given by taking those rows in the identity matrix that does not appear in L .

$$L_c = \begin{bmatrix} 1 & 0 & 0 & 0 & 0 \\ 0 & 0 & 0 & 1 & 0 \end{bmatrix}$$

An estimate vector \hat{x} can be represented as

$$\hat{x} = L^T y + L_c^T v \tag{1}$$

where v contains the values of the missing samples.

For example,

$$L^T y + L_c^T v = \begin{bmatrix} 0 & 0 & 0 \\ 1 & 0 & 0 \\ 0 & 1 & 0 \\ 0 & 0 & 0 \\ 0 & 0 & 1 \end{bmatrix} \begin{bmatrix} y(0) \\ y(1) \\ y(2) \end{bmatrix} + \begin{bmatrix} 1 & 0 \\ 0 & 0 \\ 0 & 0 \\ 0 & 1 \\ 0 & 0 \end{bmatrix} \begin{bmatrix} v(0) \\ v(1) \end{bmatrix} = \begin{bmatrix} v(0) \\ y(0) \\ y(1) \\ v(1) \\ y(2) \end{bmatrix}$$

where v is of length N-K and we have to estimate v .

By minimizing $\|F\hat{x}\|_2^2$ we can obtain v , where F is the second order difference matrix given by

$$F = \begin{bmatrix} 1 & -2 & 1 & & & \\ & 1 & -2 & 1 & & \\ & & \cdot & \cdot & & \\ & & & \cdot & \cdot & \\ & & & & 1 & -2 & 1 \end{bmatrix}$$

Using (1), we can find v by solving the problem

$$\min_v \|F(L^T y + L_c^T v)\|_2^2$$

$$\text{i.e. } \min_v \|FL^T y + FL_c^T v\|_2^2$$

$$\text{We have, } \min_q \|p - Hq\|_2^2 \Rightarrow q = (H^T H)^{-1} H^T p$$

Let $p = FL^T y$, $H = -FL_c^T$ and $q = v$, then the solution is obtained as

$$v = -(L_c F^T FL_c^T)^{-1} L_c F^T FL^T y \quad (2)$$

After getting v , the estimate \hat{x} can be constructed by using the equation (1).

Proposed Method

The proposed method uses the least square missing sample estimation technique for inpainting. In the proposed system, the missing data estimation which is applicable to 1-D signal is being extended to 2-D images. In the image to be inpainted I ($m \times n$) the pixels corresponding to zero value is replaced by Not a Number (NaN). These are the regions to be inpainted by neighborhood interpolation and are replaced using missing sample estimation using least square algorithm. The missing data estimation method is mapped on to 2-D by taking the image row vectors $I(i, :)$ which is of size $1 \times n$ and then implementing the 1-D algorithm is applied to select rows. Similarly, the algorithm is repeated for select column vectors $I(:, j)^T$ of size $1 \times m$ of the image matrix. Estimate the number of missing samples. Formulate the selection matrix, a $K \times N$ matrix where K is the number of available sample. The selection matrix is basically an identity matrix devoid of the rows corresponding to the missing samples in the signal x . L_c consists of rows of identity matrix not in L . Using equation (2) we obtain the result for both row wise and column wise iterations. The average of the results give the required inpainted image as the result. The flow chart for the algorithm is given in [Figure-1].

Algorithm:

1. Read the image and mask to the variables I ($m \times n$) and M respectively.
2. Resize the mask to the size of the image M ($m \times n$) and convert the mask to gray scale.
3. Convert the mask to binary image.
4. If the mask is white letters in black background, obtain the negative of the image.

$$M = 1 - M$$
5. If I is a color image, extract each plane and embed it with mask to create the image to be inpainted.
6. Else if it is a gray image embed the mask directly.
7. Replace all zeros with NaN which are the locations to be inpainted.
8. Do the row wise least square missing sample estimation of the image.
9. If at least one pixel value in that row is NaN, then consider that row.
10. Obtain the number of missing samples, k .
11. Create the sampling matrix, L by choosing the locations where the data is available and take its complement, L_c .
12. Obtain the solution 'x1' using least square algorithm.

$$x1 = -(L_c F^T FL_c^T)^{-1} L_c F^T FL^T y$$
13. Similarly, do column wise least square missing sample estimation to obtain 'x2'.
14. Take the average of the outputs of step 12 and 13 to get the inpainted image.

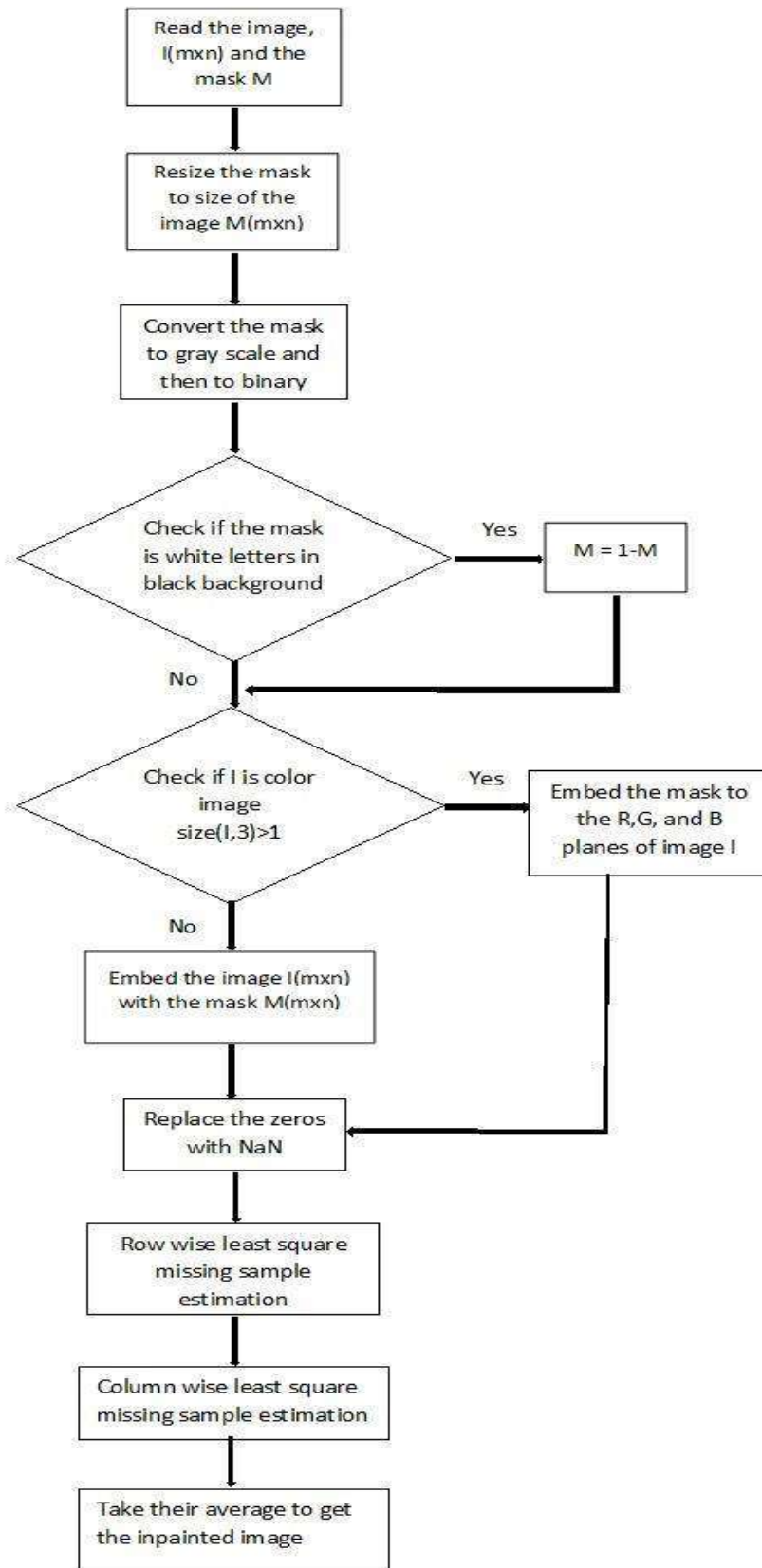


Fig: 1. Flowchart for Algorithm

DATA SET

The test images were taken from [13]. The dataset used for the experiment consists of four color images [Figure - 2(i)] and five gray scale images [Figure-2(ii)] with letter mask. Two kinds of letter masks, one with black letters on white background and the other with white letters on black background are used [Figure-2(iii)]. We also experimented on another seven images with scratches on them [Figure -2(iv)].

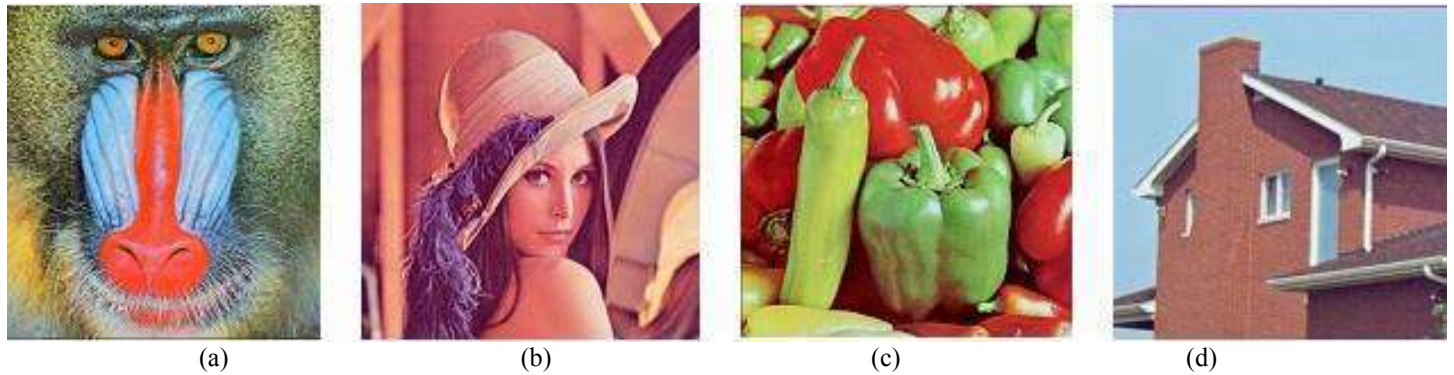


Fig: 2(i). Input Images Color: (a) Baboon, (b) Lena, (c) Pepper, (d) House



Fig: 2 (ii). Gray Scale Images: (a) Pirate, (b) Golden bridge, (c) Barbara, (d) Zelda Gifts, (e) Bob cat

Lorem ipsum dolor sit amet, consetetur sadip
diam nonumy eirmod tempor Invidunt ut la
magna aliquyam erat, sed diam voluptua. At
accusam et justo duo dolores et ea rebum. S
gubergren, no sea takimata sanctus est Lorer
sit amet. Lorem ipsum dolor sit amet, conse
elit, sed diam nonumy eirmod tempor Invid
dolore magna aliquyam erat, sed diam volup
et accusam et justo duo dolores et ea rebum
gubergren, no sea takimata sanctus est Lorer
sit amet. Lorem ipsum dolor sit amet, conse
elit, sed diam nonumy eirmod tempor Invid
dolore magna aliquyam erat, sed diam volup
et accusam et justo duo dolores et ea rebum

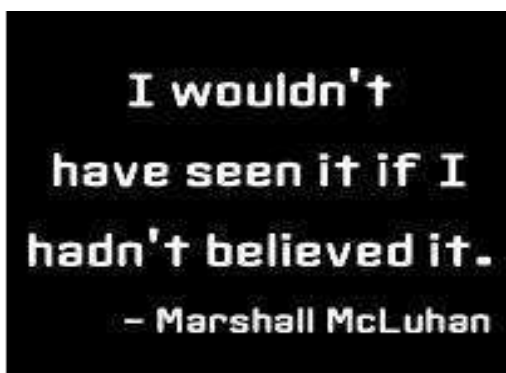
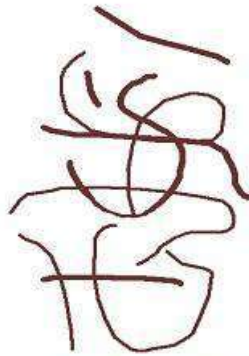


Fig: 2 (iii). Masks: (a) black letters with white background and (b) white letters in black background



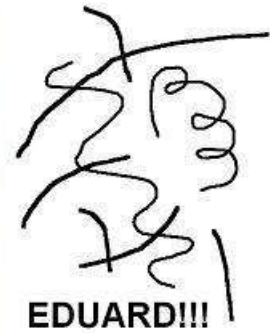
Astro



Astro scratch



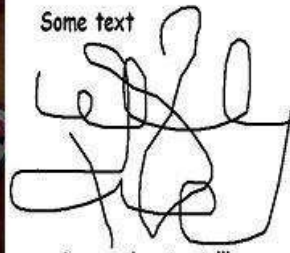
Eduard



Eduard scratch



Fruit



Fruit scratch



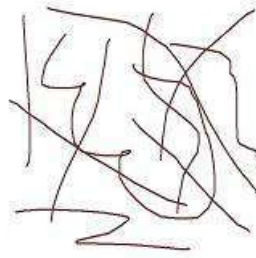
Linc



Linc Scratch



Ocean



Ocean scratch



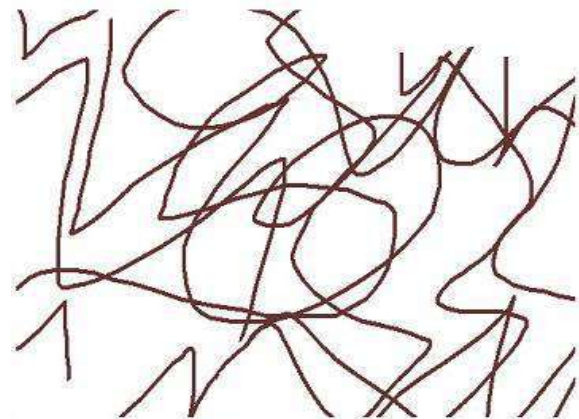
Portrait



Portrait scratch



Sig



Sig scratch

Fig: 2 (iv). Original Images and Masks (Scratch)

RESULTS

The following are the results of the experiments conducted. [Fig- 3(i)] shows the results obtained on color images using the proposed least square based approach. [Fig- 3(ii)] are the outputs obtained for inpainting for gray scale images. In both the cases the images are embedded with text masks (black letters in white background). [Fig-3(iii)] shows the result of the inpainting for images with scratch. Later the algorithm was compared with TV algorithm. The result obtained for inpainting of gray scale image (Bobcat) embedded with white letter mask, using proposed approach and TV algorithm are given in [Fig- 3(v)] and [Fig- 3(iv)] respectively. For the performance evaluation the standard quality matrices PSNR and SSIM are taken. [Table-1] compares the metrics calculated for the color and gray images with letter mask using the proposed least square method. [Table-2] compares the metrics evaluated for the set of seven images for scratch mask and [Table-3] shows the comparison between the proposed least square method and the classical TV method, using the calculated metrics and computation time.

Inpainting using proposed least square approach

Inpainting for color images

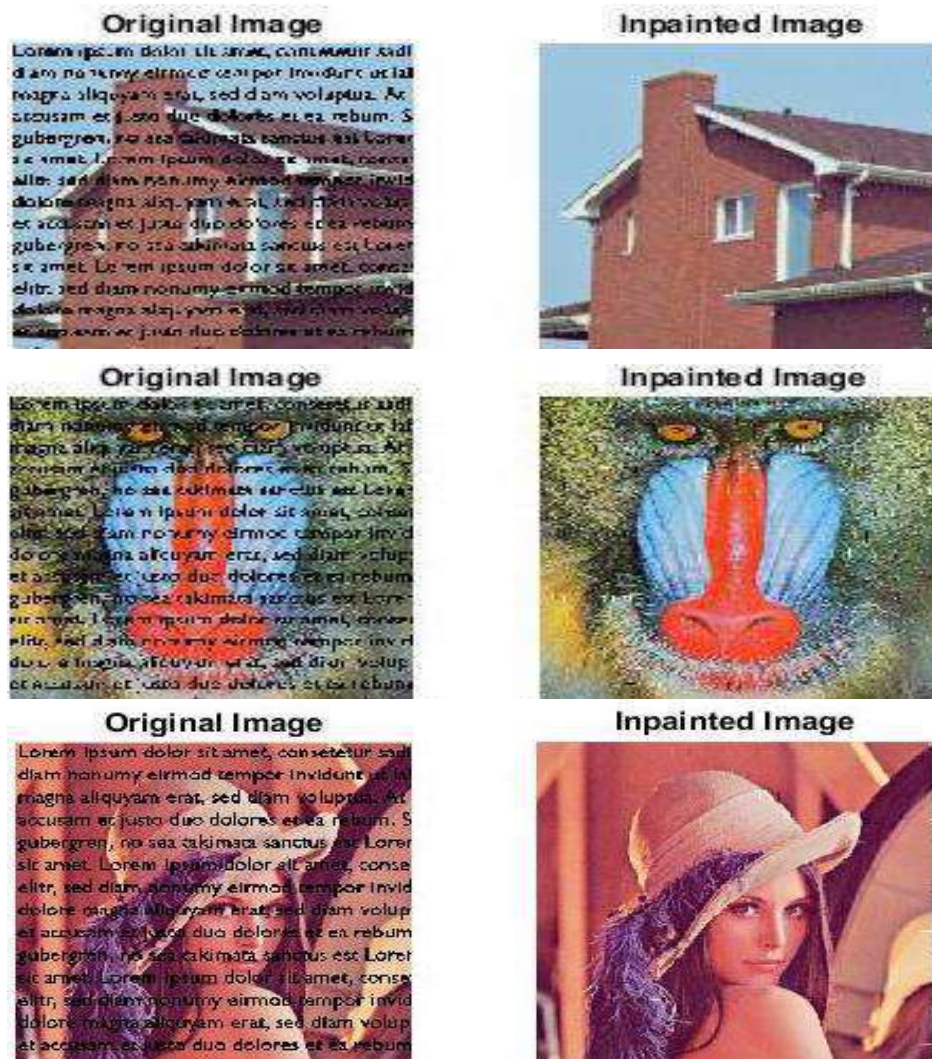
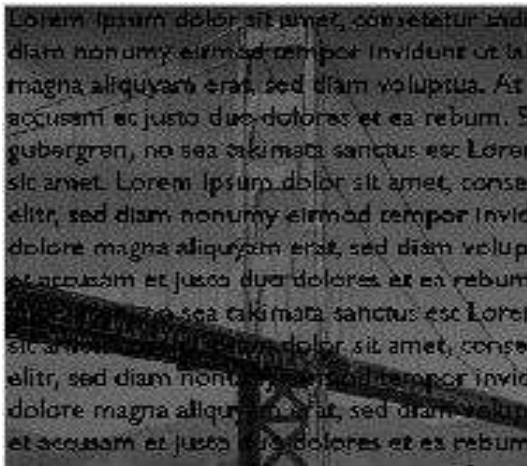


Fig: 3(i). Output of proposed method - Left: Color images with letters to be inpainted; Right: Inpainted output

Inpainting for gray scale images

Original Image



Inpainted Image



Original Image



Inpainted Image



Original Image



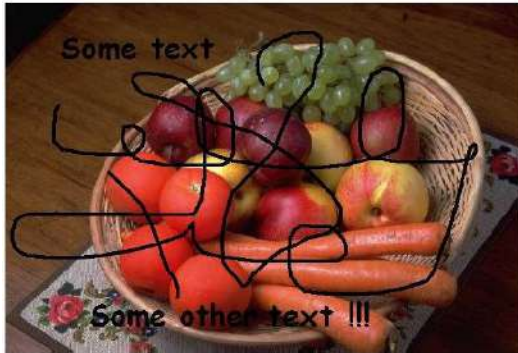
Inpainted Image



Fig: 3(ii). Output of proposed method - Left: Gray scale images with letters to be inpainted; Right: Inpainted output

Inpainting for color images with scratch

Original Image



Inpainted Image



Original Image



Inpainted Image



Original Image



Inpainted Image



Fig: 3(iii). Output of proposed method - Left: Images with scratch to be inpainted; Right: Inpainted output

Inpainting using TV method

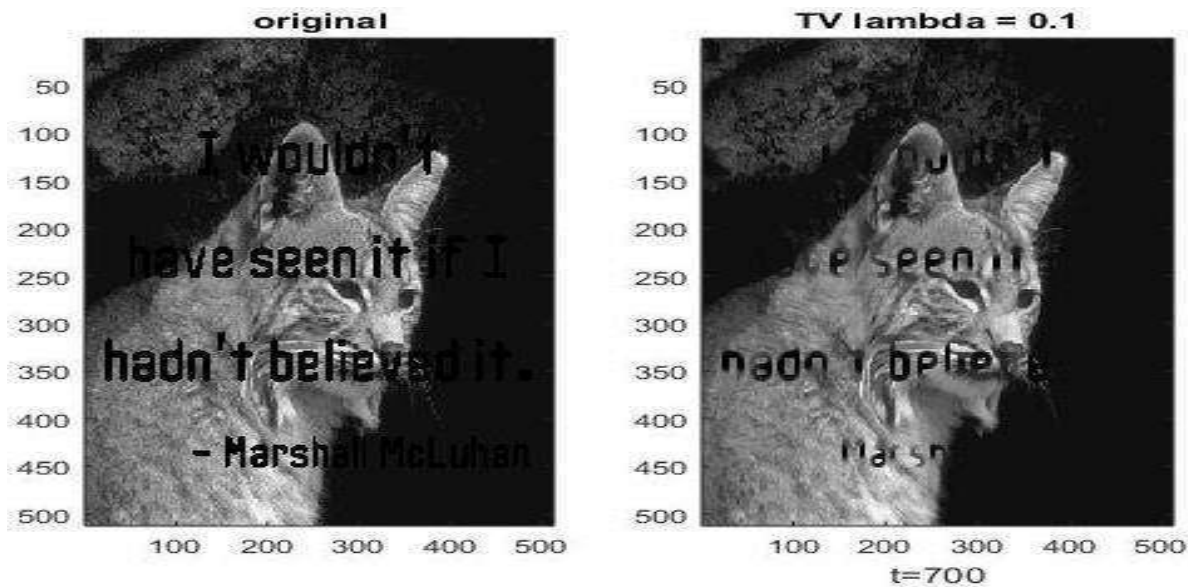
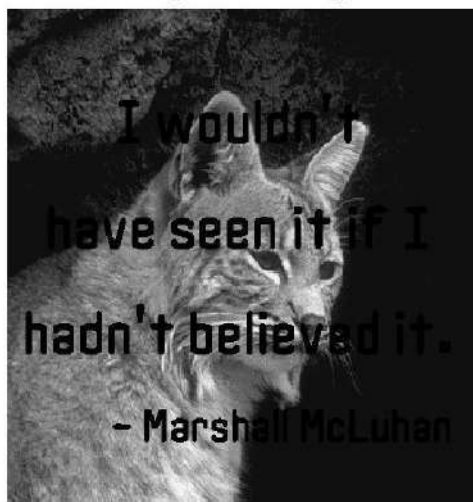


Fig: 3(iv): Output of TV method - Left: Images with letters to be inpainted; Right: Inpainted output

Original Image



Inpainted Image



Fig: 3(v). Output of proposed method - Left: Images with white letters to be inpainted; Right: Inpainted output

Table: 1. Computation of PSNR and SSIM for the inpainted color and gray scale images (with letters as mask) obtained using the proposed method

GRAY SCALE IMAGES					COLOUR IMAGES				
IMAGES	PSNR (dB)		SSIM		IMAGES	PSNR (dB)		SSIM	
	ORIGINAL	INPAINTED IMAGE (PROPOSED METHOD)	ORIGINAL	INPAINTED IMAGE (PROPOSED METHOD)		ORIGINAL	INPAINTED IMAGE (PROPOSED METHOD)	ORIGINAL	INPAINTED IMAGE (PROPOSED METHOD)
Golden Gate Bridge	7.3575	23.2524	0.4849	0.8327	House	7.1201	27.7246	0.4923	0.9805
Zelda Gifs	7.2768	28.0292	0.4953	0.8864	Baboon	7.3047	18.0012	0.6621	0.9004
Barbara	7.2491	19.7616	0.5364	0.8513	Lena	7.3373	26.2778	0.6725	0.9859
Bobcat (Black text mask)	7.3458	21.9375	0.5103	0.8678	Pepper	7.3232	18.0611	0.7094	0.9568
Bobcat (White text mask)	9.4269	18.8585	0.8286	0.9204					
Pirate	7.4524	19.7506	0.6228	0.8283					

Table: 2. Computation of PSNR and SSIM for the inpainted color and gray scale images (with scratch as mask) obtained using the proposed method

SCRATCH				
IMAGES	PSNR (dB)		SSIM	
	ORIGINAL	INPAINTED IMAGE (PROPOSED METHOD)	ORIGINAL	INPAINTED IMAGE (PROPOSED METHOD)
Astro	10.3396	16.7556	0.8539	0.9441
Eduard	10.7427	36.4272	0.8501	0.9879
Fruit	10.1785	19.0196	0.8921	0.9837
Linc	18.0899	29.4684	0.9781	0.9952
Ocean	12.5589	21.8784	0.8936	0.9806
Portrait	12.2981	22.4735	0.8663	0.943
Sig	9.2693	19.2938	0.7791	0.9188

DISCUSSION

The main objective of this paper is to show that the least square missing sample estimation method mapped for inpainting gives better result in no time when compared to the traditional total variation method. [Fig-4] shows that the elapsed time for the proposed method is much less than that for TV method. The TV method was experimented only on the gray scale images, which itself took a considerable amount of time to obtain the result. The maximum time taken for inpainting on gray scale images with letter mask, using the proposed method was 4.392885s whereas, the minimum time for the TV method was 380.051024s. Apart from having less computational time, the proposed

model gives an output of good visual quality when compared to the outputs obtained for the TV inpainting as shown in [Figure -3(v)]. The output of the TV inpainting is blurred. Also from [Figure-5] and [Figure -6], we can infer that the PSNR and SSIM values are impressive for the proposed method. The PSNR computed for the ‘Bob cat’ image using the TV and proposed method are 20.7637dB and 21.9375dB respectively. Also SSIM for the image using the two methods are 0.4715 (TV) and 0.8678 (proposed method) [Table-3]. We can see that there is an improvement of 1.1738dB in PSNR and 0.3963 in SSIM. This improvement can be verified visually by the output images shown in [Figure-3(iv)] and [Figure-3(v)]. From this comparison, we can conclude that the proposed least square based approach is more appropriate for image inpainting

Table: 3. Performance comparison of the proposed technique for image inpainting against the TV algorithm based on PSNR, SSIM and the computational time

GRAY SCALE IMAGES						
IMAGES	PSNR (dB)		SSIM		TIME (s)	
	TV	PROPOSED METHOD	TV	PROPOSED METHOD	TV	PROPOSED METHOD
Golden gate bridge	20.718	23.2524	0.3863	0.8327	392.083227	1.316435
Zelda gifs	21.6133	28.0292	0.7602	0.8864	406.260955	1.020285
Barbara	17.1117	19.7616	0.3508	0.8513	420.562651	4.392885
Bobcat	20.7637	21.9375	0.4715	0.8678	380.051024	4.18181
Pirate	16.5703	19.7506	0.2519	0.8283	397.130245	1.408976

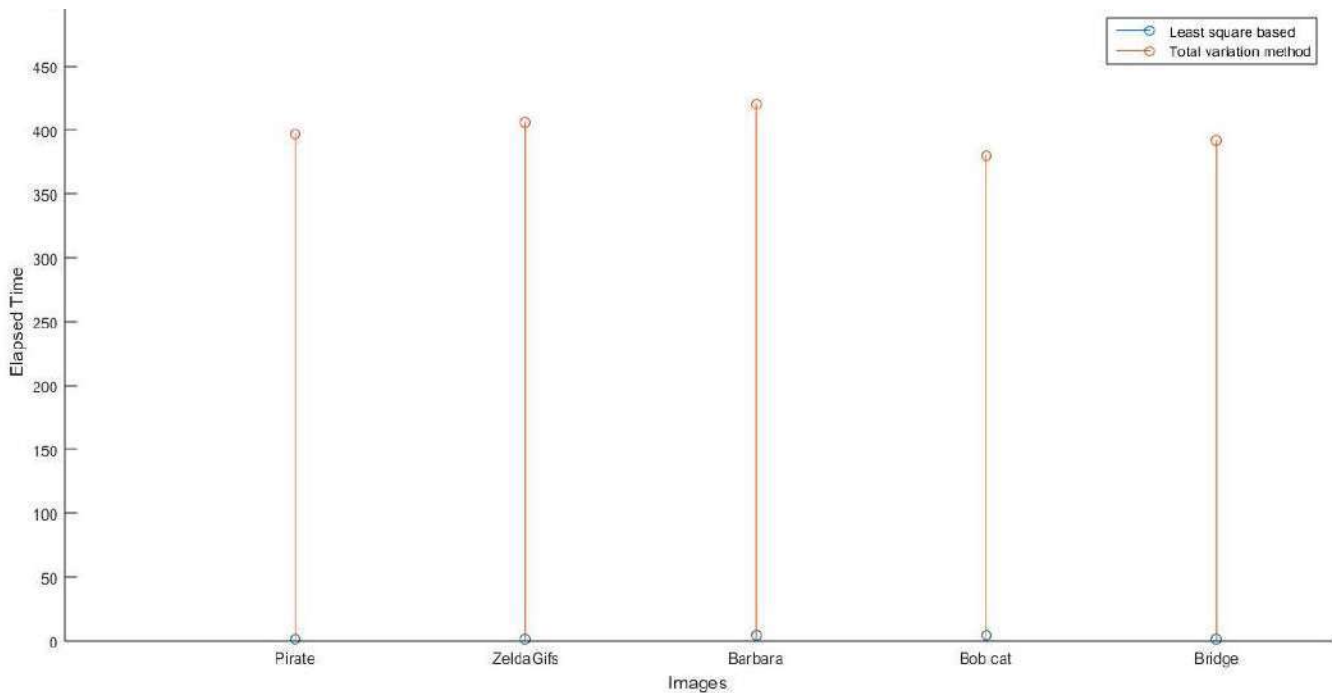


Fig: 4: Comparison of the elapsed time for TV method and the proposed method

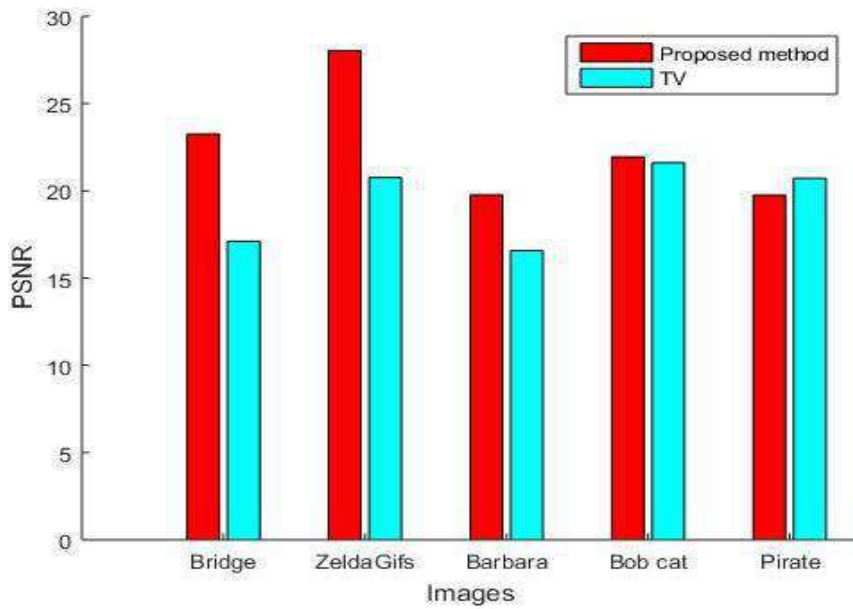


Fig: 5. Comparison of the PSNR values for the proposed method and TV based on [Table-3]

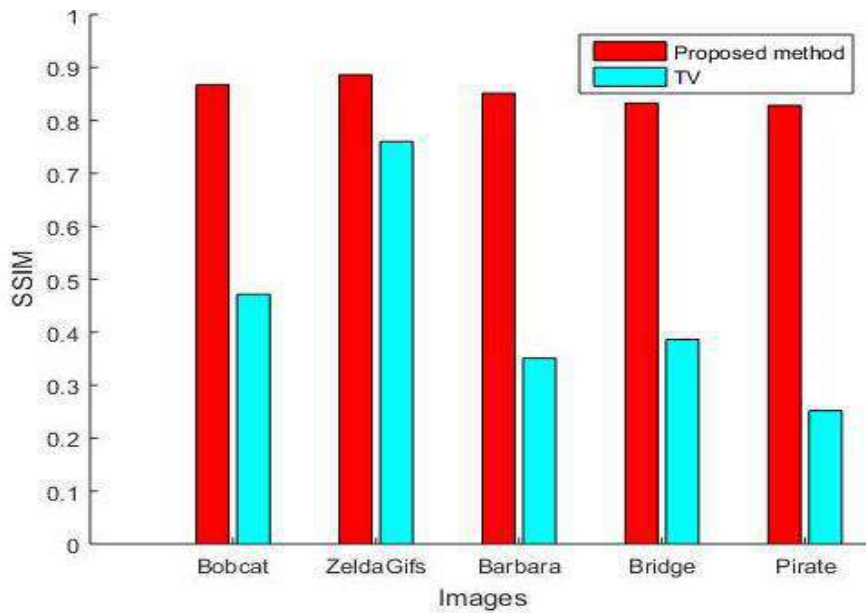


Fig: 6. Comparison of the SSIM values for the proposed method and TV based on [Table-3]

The comparison between the PSNR values of the original image and the inpainted image is shown in [Fig-7]. It can be seen from the graph that there is a considerable increase in the PSNR value. The SSIM value comparison is shown in [Fig-8]. It can be seen that the SSIM values of all the inpainted images are nearly equal to 1. Using the proposed approach the PSNR and SSIM has been improved, on an average to 13.429dB and 0.214 respectively.

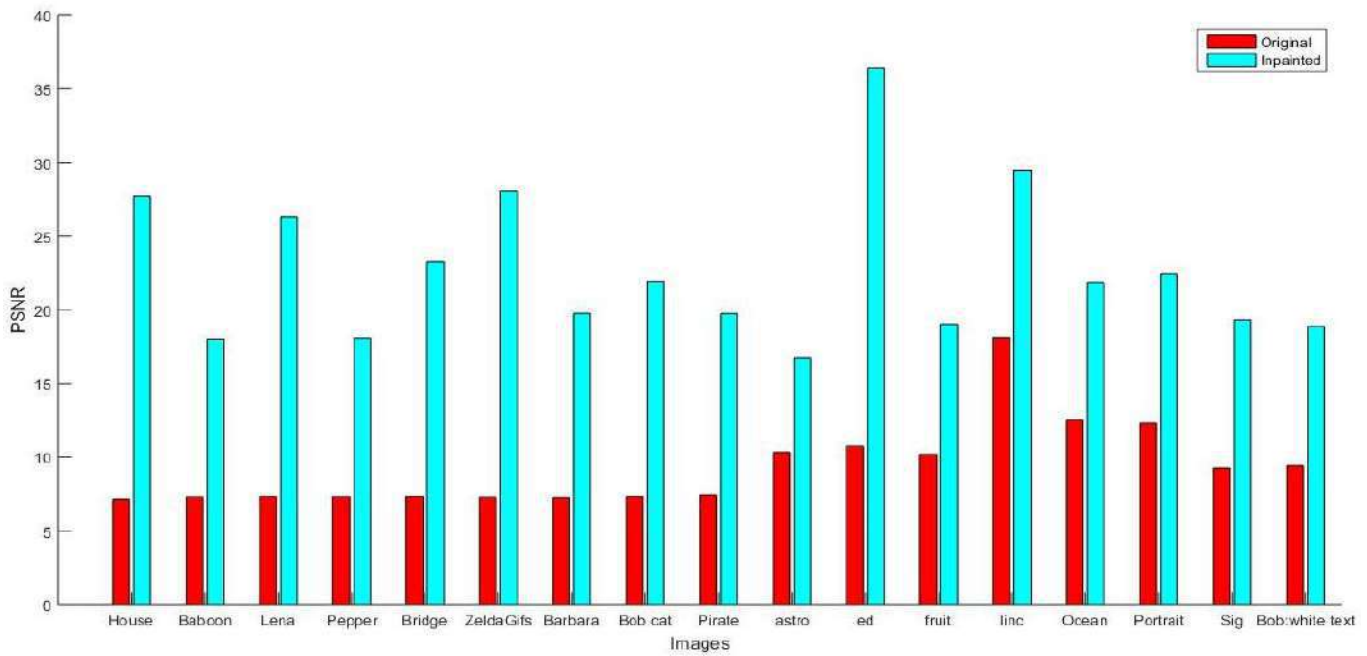


Fig. 7. Comparison the PSNR values of the original and the inpainted image based on [Table-1] and [Table-2]

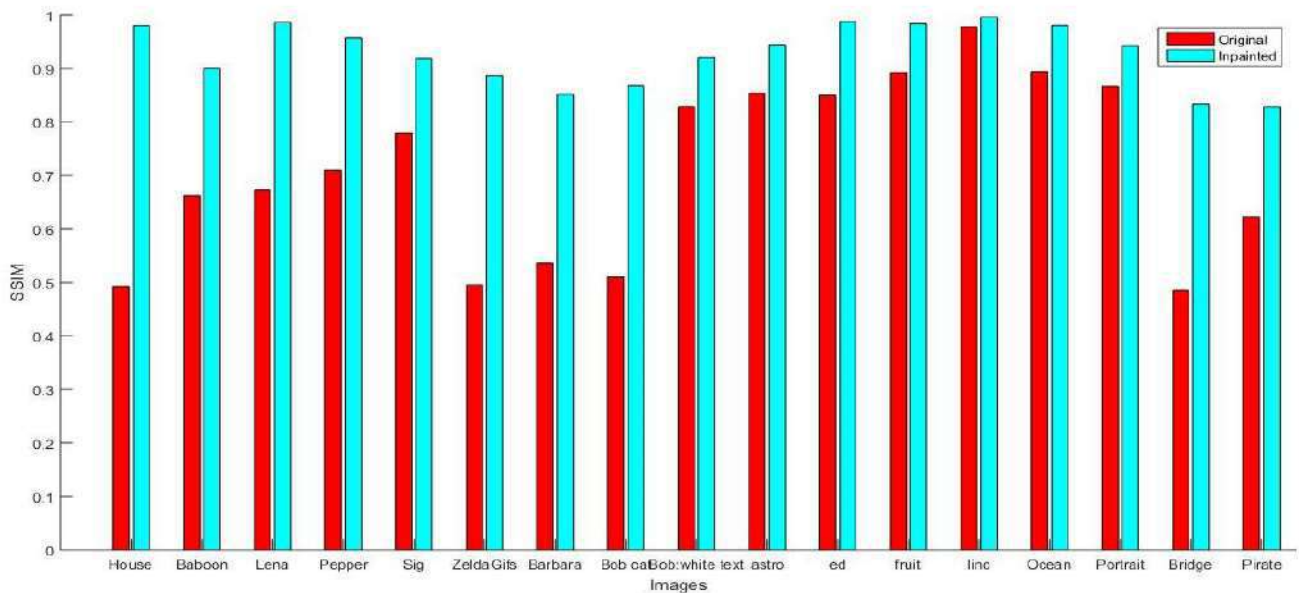


Fig. 8. Comparison of the SSIM values of the original and the inpainted image based on [Table-1] and [Table-2]

CONCLUSION

This paper presents a least square based approach for image inpainting. The least square based missing sample estimation method for 1-D signal is being extended to 2-D images for inpainting. The proposed approach is experimented on standard test images embedded with letter and scratch masks and the results are compared with TV

method. The efficiency of the proposed approach is assessed by computing standard quality metrics such as PSNR and SSIM. It shows that our approach performs well for images covered with letter and scratch masks. Also the time complexity of our approach is much less compared to the classical TV method. The drawback of the proposed approach is that, it fails for patch based inpainting. In future direction, we can extend this method for patch based image inpainting.

CONFLICT OF INTEREST

Authors declare no conflict of interest.

ACKNOWLEDGEMENT

None.

FINANCIAL DISCLOSURE

No financial support was received to carry out this project.

REFERENCES

- [1] Gonzalez, Rafael C. RE woods, Digital Image Processing. Addison-Wesely Publishing Company (1992)
- [2] Khedikar, Sanket S., and P. N. Chatur. A Review of Literature On Image Inpainting And Super Resolution.
- [3] Wagh, Priyanka Deelip, and D. R. Patil. Text detection and removal from image using inpainting with smoothing. *Pervasive Computing (ICPC), 2015 International Conference on*. IEEE, 2015.
- [4] K P Soman and R Ramanathan. [2012] Digital signal and image processing -The sparse way, Elsevier.
- [5] Rudin, Leonid I., Stanley Osher, and Emad Fatemi. Nonlinear total variation based noise removal algorithms. *Physica D: Nonlinear Phenomena* 60.1 (1992): 259-268.
- [6] Bertalmio, Marcelo, et al. Image inpainting. *Proceedings of the 27th annual conference on Computer graphics and interactive techniques*. ACM Press/Addison-Wesley Publishing Co., 2000.
- [7] Getreuer, Pascal. Total variation inpainting using split Bregman. *Image Processing On Line* 2 (2012): 147-157.
- [8] Goyal, S. R. Digital Inpainting Based Image Restoration.
- [9] Selesnick, Least squares with examples in signal processing, [Online], March, 2013.
- [10] Li, Fang, et al. A fast implementation algorithm of TV inpainting model based on operator splitting method. *Computers & Electrical Engineering* 37.5 (2011): 782-788.
- [11] Li, Fang, and Tiejong Zeng. A Universal Variational Framework for Sparsity-Based Image Inpainting. *Image Processing, IEEE Transactions on* 23.10 (2014): 4242-4254.
- [12] L.I. Rudin, S. Osher, E. Fatemi, Nonlinear total variation based noise removal algorithms, *Physica D*, vol. 60, pp. 259-268, 1992. [http://dx.doi.org/10.1016/0167-2789\(92\)90242-F](http://dx.doi.org/10.1016/0167-2789(92)90242-F)
- [13] <http://sipi.usc.edu/database/database.php?volume=misc&image=25#top>

ABOUT AUTHORS

Aiswarya M received her B.Tech degree in Applied Electronics and Instrumentation in 2014. Currently she is pursuing her M.Tech degree in Computational Engineering and Networking (CEN) from Amrita School of Engineering, Coimbatore, Amrita Vishwa Vidyapeetham, Amrita University, India. Her research interests include Digital Image Processing and Embedded Systems.

Deepika N received her B.Tech degree in Electronics and Communication Engineering in 2014. Currently she is pursuing M.Tech degree in Computational Engineering and Networking (CEN) from Amrita School of Engineering, Coimbatore, Amrita Vishwa Vidyapeetham, Amrita University, India. Her research interests include Digital Image Processing and Embedded Systems.

Sowmya V currently serves as Assistant Professor at Amrita Centre for Computational Engineering and Networking (CEN), Coimbatore campus. Her research area include Image processing, Hyperspectral Image Classification, Pattern Recognition and Machine Learning.

Neethu Mohan completed her M.Tech degree in Remote Sensing and Wireless Sensor Networks (CEN) from Amrita School of Engineering, Coimbatore, Amrita Vishwa Vidyapeetham, Amrita University, India. She is currently a research scholar in the field of Signal Analysis. Her research interest includes signal and image analysis.

Dr. K P Soman currently serves as Head and Professor at Amrita Centre for Computational Engineering and Networking (CEN), Coimbatore campus. His research interest include Software Defined Radio, Wireless Sensor Networks (WSN), High Performance Computing, Statistical Digital Signal Processing (DSP) on Field Programmable Gate Array (FPGA), Machine learning Support Vector Machines, Signal Processing and Wavelet & Fractals.

NOVEL IMPLEMENTATION OF MULTIMODAL BIOMETRIC APPROACHES TO HANDLE PRIVACY AND SECURITY ISSUES OF RFID TAG

J. V. Gorabal*, Manjaiah D. H., and S. N. Bharath Bhushan

Department of Computer Science & Engineering SCEM, Mangalore, KA, INDIA

Department of Computer Science, Mangalore University, Mangalore, KA, INDIA

ABSTRACT

In the present scenario there is huge technology revolution in all dimension of life, in this context one such promising technology is Radio frequency Identification technology which is a very strong substitute for Barcode in automatic identification systems. As the technology is growing in the same speed issues like eavesdropping, cloning, spoofing etc are becoming nig threat for the development of this smart technology. Since research is ongoing process, it is the constructive process to contribute some novel approaches in the field of automatic identification technology. Since in coming days RFID tag based applications may make big revolutions to make the life of the people more smart. In this direction as a part of my research work this article contributes in designing a security system to handle critical issues in RFID enabled applications. At present Biometric security is gaining lot of importance in providing security for many applications. Since Biometric traits are unique in its nature obviously this technology stands most promising in place password or token based mechanism. Here we proposed a multimodal biometric based security systems to handle critical issues. The proposed work uses feature level fusion approach, the same is experimented with F-Measure, Precision and Recall. The results are very comprehensive, robust and promising in its nature.

Received on: 10th -Apr-2016

Revised on: 29th-Apr-2016

Accepted on: 5th-May-2016

Published on: 10th-May-2016

KEY WORDS

Radio frequency, Privacy, Security, Multimodal, Biometric.

*Corresponding author: Email: jvgorabal@gmail.com

INTRODUCTION

Radio frequency recognizable proof (RFID) empowers the ID of various RFID tags. The distinguishing proof procedure is performed over a remote system without the assistance of observable pathway or physical touch between the RFID tags and the RFID reader [1]. These better optimal properties like low installation costs, convenient to use, easy to manage and less computational hassles, etc., are making the RFID technology to be most suitable to replace conventional strategies. It is the most suitable candidate to replace technology like Barcode systems. In the present situation many RFID systems are massively installed across the globe, which are useful for object tracking, manufacturing, supply chain management, tiny goods management, retailing and for different applications, for example in defense and admission management. The RFID research has the enormous force of gathering data about an object and variables [1, 2]. There are so many issues in RFID management system, since it is cutting edge technology, the term confidentiality, competence, heterogeneity, dependability have lots of roles to play in the coming days.

Since RFID technology is gaining lot importance in the market [3], intruders are also hyperactive in killing the technology by disclosing confidential information, denial of service attack, data corruption, which are the biggest threat to the growth of the technology, but as we know no technology is free from issues and hurdles. Being researchers, engineers, it is an opportunity to handle the hurdles to make this technology a promising technology for the mankind of this modern digital world.

The present research focuses on handling privacy and security issues and proposed many solutions to protect the system and make the technology as popular as possible, but still there are some issues left unanswered. Many researchers in their proposed solutions like hazing, cryptographic approaches, pseudo names, secret-words etc, but these are not enough to withstand the attacks. Hence it made us to focus on a typical and unique methodology to deploy.

As we know biometric traits are the one gaining lot of importance in providing security to the stakeholders. Biometric features are permanent and unique which are concrete during pregnancy, even twins will have different biometric print, may be retina, finger and face. Taking this into consideration RFID enabled applications like E-Passport, where stakeholder data is very precious, challenge to protect from intruders. This situation made us to think to act upon privacy and security issues and a made us to design a solution to enable the technology for the intended functionality which certainly will make the RFID system trustworthy and dependable [4].

RELATED WORK

At present there is lot of research is in progress to protect the privacy of consumer. In this process there are several techniques and approaches are contributed by many researchers to handle the various issues associated with RF ID technology. Following are the techniques which will be considered for handling above mentioned critical issues. Those techniques includes blocker tag, password approach, hashing approach, tag killing approach and encryption approach. But non of these approaches can handle the issues effectively. As a solution to this issue, in this article we proposed a novel and effective yet efficient methodology which incorporate multimodal biometric approach to handle privacy and security issues associated with RFID technology.

PROPOSED MODEL

Picture encryption for privacy and security issues of RFID

This section exhibits a picture encryption based model to handle protection and security issue of RFID innovation. The goal of this work is to build up a solid and ideal calculation for giving the security to the RFID labels [5]. This specific methodology guarantees to give a superior security to the framework. This model capacities two stages, for example, information encryption stage and the contrasting of the encoded information.

Information encryption stage

Since the indispensable target of the proposed procedure is to give security to the RFID systems, biometric properties like face and knuckle are considered. Precisely when this information are put away by using honest to goodness biometric information by electronic devices, they are subjected for pre-planning computations. Once the information is preprocessed, the RGB biometric information is changed over into double information. Right when, the information is changed over to parallel, i.e., blend of 0's and 1's are given as data RLE data encryption computations an immediate and persuading figuring for encoding the information. RLE computation counts perceive the two fold information and make the relating encoded yield.

Coordinating data at encrypted level

Once the information is produced, they are put away in the knowledge base for next computation. The following diagram of the calculation is to think about this information at scrambled level [6].

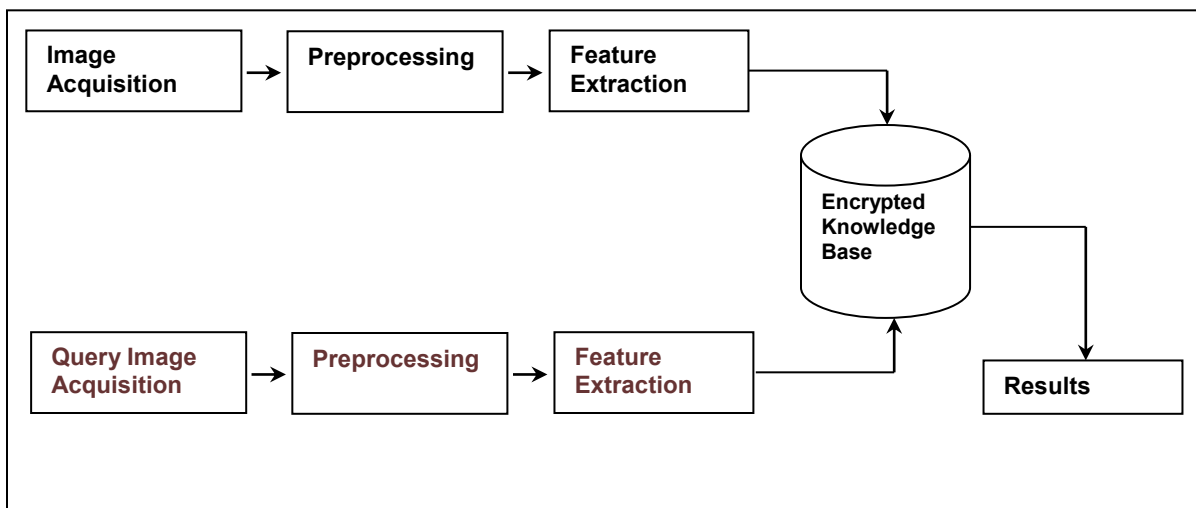


Fig. 1. Block Diagram of the Anticipated Model

ALGORITHM

Algorithm: Image Data Encryption Mechanism
Start:
 I_{data} (Input collection of Training Data)
 $I_{PreProcess}$ (Pre processing (I_{data}))
 $Twofold \leftarrow Twofold(I_{PreProcess})$
 $I_{encoded}$ (RLEncoding ($I_{twofold}$))
 $KB \leftarrow I_{encoded}$
 $I_{Testing_Data}$ (Input collection of Testing Data)
 $I_{PreProcess_Testing_Data}$ (Pre processing ($I_{Testing_Data}$))
 $I_{Test_twofold} \leftarrow Twofold(I_{PreProcess_Testing_Data})$
 $I_{Test_encoded}$ (RLEncoding ($I_{Test_twofold}$))
 For me (1: Num_Classes
 Result ($I_{Testing_Data}$) (Compareing ($I_{Test_encoded}$, $KB(i_Class)$))
End

Multimodal biometrics for privacy and security issues of RFID

This strategy addresses the privacy and security issues in RFID technology. With the help of multimodal biometric traits like “face and knuckle by using a fusion of the biometric trait features [7, 8]. The proposed model can be categorized into three various levels. First level discusses the data acquisition and feature extraction. Second level discuss about the encrypted knowledge base construction. Third level discusses processing of encrypted data for addressing privacy and security issues of RFID [9].

Data acquisition and feature extraction stage

Since the essential target of this work is to address the security and privacy issues of RFID systems, we are considering the multimodal biometric information i.e., face, and knuckle[10]. At the point when this information is captured in a given unit of time by using proper biometric information securing gadgets, they are subjected for pre-processing computations. Once the information is stored, the RGB biometric information is changed over into twofold information. When, the information is changed over to twofold, i.e., combination of 0's and 1's are given as data to run length encoding algorithm.

Construction of encrypted knowledge base

Once the data acquisition and feature extraction is accomplished, construction of encrypted knowledge base is the next step. Run Length Encoding (RLE) is the lucid and impressive encoding technique which accepts the twofold data and generates the corresponding encoded output. After the encryption of the biometric traits are completed, all the individual traits encrypted information are fused and then stored in the knowledge base for further computation. Working principle of Run Length Encoding is as shown in the following.

Input: 1111001110
 Encoded Output: 41203110.

Data compression at the encrypted level

“Once the encrypted knowledge base is constructed, supervised learning algorithms like” nearest neighbor, k nearest neighbor, support vector machine and artificial neural network classifiers are designed for identification of the authorized stakeholders.” Once the all the training is completed with biometric traits like face, knuckle next phase is the recognition phase. During the recognition time, the same biometric traits like face knuckle information of the new user is considered. Then the newly obtained data are subjected for preprocessing and encrypted using run-length encoding scheme. After the successful completion of data encryption, the data compared with knowledge base. The proposed model of the above discussed method is graphically presented in the following figure.”

Algorithmic model

Algorithm:
 Input: Two biometric traits like face and, knuckle
 Output: Authenticated user or unauthenticated user.
 Method:
CreateNode()

```

// Node a new data structure used to store all three biometric traits.
For me (1 to n // n = number of biometric traits.
for j ← 1 : m // m=database size.
Node(i,j)←Three biometric trait like face, knuckle.
    end
end
Node_Preprocessing(i,j)←Pre processing (Node(i,j))
Node_Binary(i,j)←Binary(Node_Preprocessing(i,j))
Node_Encoded(i,j)← RLEncoding ("Node_Binary"(i,j))
KB ← Node_Encoded
Testing Phase:
TestNode(1,1)←First Biometric Trait (Face)
TestNode(1,1)←Seond Biometric Trait (Knuckle)
PreProcess_TestNode←Pre processing (TestNode)
PreProcess_TestNode_twofold ←Twofold (PreProcess_TestNode)
PreProcess_TestNode_encoded← RLEncoding (PreProcess_TestNode_twofold )
for i ← 1 : Num_Biometric_Traits
    for j ← 1 : Dataset Size
        Result = Compareing (PreProcess_TestNode_encoded , KB(i,j))
    end
end
end
Algorithm Ends
    
```

RESULTS AND DISCUSSION

This section shows the sufficiency of the proposed framework on two arrangements of biometric qualities data and knuckle dataset [11]. With the deciding objective of evaluation of the results, three most basic measures like precision, recall and f-measures are considered for each trial. The results of the experiments are presented in Table-1.

Table: 1. Result of Data matching at encrypted level

	"ORL Face Dataset "		"UmistFace Dataset"		"Knuckle Dataset "	
	40 / 60	60/ 40	40 / 60	60/40	40/ 60	60/40"
Precision	.88500	.88833	.88400	.98000	.88050	.88333
Recall	.88600	.88949	.88564	.99089	.88000	.88596
F- Measure	.88549	.88890	.88481	.99044	.88024	.88462
CA	.88500	.88830	.88400	.90000	.88000	.88333

Table: 2. Result Multimodal Biometric Approach

	40/ 60			60/40		
	Precision	Recall	F- Measure	Precision	Recal I	F- Measure
Nearest Neighbor	0.7712	0.7955	0.78335	0.7833	0.8199	0.8016
k Nearest Neighbor	0.7856	0.7922	0.7889	0.7966	0.8201	0.80835
Support Vector Machine	0.8296	0.8347	0.83215	0.8712	0.8566	0.8639
Artificial Neural Network	0.8895	0.8911	0.8903	0.9012	0.9515	0.92635

How proposed model works in RFID applications

With RFID technology enabled applications like passport stakeholders E-Passport (RFID Tag) is uniquely identified by UID unique identification No which is scanned by an RFID scanner with proper database and middleware. To check the authenticity of the user, the user has to submit his biometric traits, these biometric traits are used to compute and generate UID. If this UID and scanned UID are same then scanned the RFID tag belongs to legitimate user is fake. Like this our proposed methodology protects the users' information and validates the same for further press [12].

Here we proposed multimodal approaches and conceived calculations for feature extraction and the development of knowledge base with the assistance of more than three distinctive biometric characteristics like face and knuckle databases are viewed as Accuracy can be seen as a measure of exactness or consistency, however the audit is a measure of zenith. Four unique classifiers were considered for the assessment of the proposed strategy. At the end we have figured accuracy, review and f-measure. The results of the tests are mentioned in the **Table-2**.

CONCLUSION AND FUTURE WORK

The proposed mechanism comprises of two stages like information encryption and coordinating of encoded information. The algorithm is fundamentally broke down on two biometric information viz face and knuckle. In the proposed approach we used RLE encryption for the biometric attributes and with the help of the encoded knowledge base is developed. During authentication process user has to submit the above mentioned two traits to validate. Our experiments proved that this method can be deployed to protect the user's private information in RFID technology based applications. In future the same technology may be used for more than four to five biometric traits to provide a robust security measures for RFID enabled applications.

ACKNOWLEDGEMENT

None

CONFLICT OF INTEREST

Authors declare no conflict of interest.

FINANCIAL DISCLOSURE

No financial support was received to carry out this project

REFERENCES

- [1] A Juels. [2006] RFID security and privacy: a research survey. *Journal of Selected Areas in Communication (J-SAC)* 24(2): 381–394.
- [2] V Daniel Hunt Albert, Puglia, Mike Puglia.[2007] RFID a Guide to Radio frequency Identification Technology.
- [3] Yanjun and Zuo.[2010] Survivable RFID Systems: Issues, Challenges, and Techniques, *IEEE Transactions* 40(4):406–418.
- [4] Ari Juels.[2010] RFID Security and Privacy A Research Survey: *IEEE Journal on selected areas in communications.* 24 (2).
- [5] JV Gorabal, Manjaiah DH,[2014] Image data encryption approach for security issues International, *Journal of Information Technology Management Information System (IJITMIS)*, 5(2):59–64.
- [6] A Ross and A.K Jain. [2003] Information Fusion in Biometrics, *Pattern Recognition Letters*, 24(13),2115–2125.
- [7] J Fierrez-Aguilar. [2003] A comparative evaluation of fusion strategies for multimodal biometric verification,in Proc. 4th Int. *Conf.Audio-video-based Biometric Person Authentication* , 26(88):830–837.
- [8] L Hong and AK Jain. [1998] Integrating Faces and Fingerprints for Personal Identification, *IEEE Trans. on Pattern Analysis and Machine Intelligence*, 20 (2):1295–1307.
- [9] Maher K Mahmood and Jinan N Shehab.[2014] Image Encryption and Compression Based on Compressive Sensing and Chaos, *International Journal of Computer Engineering & Technology (IJCET)*, 5(1): 68 – 84.
- [10] Mahmood Al-khassaweneh, Selin Aviyente. [2008]Image Encryption Scheme Based on Using Least Square Approximation Techniques, *IEEE Transactions*, 108–111.
- [11] Suhaila O. Sharif, LI Kuncheva, SP Mansoor. [2010] Classifying Encryption Algorithms Using Pattern Recognition Techniques, *IEEE Transactions*, 168–1172.
- [12] JV Gorabal, Manjaiah DH,[2015] Multimodal Biometric Approaches to handle privacy and security issues in radio frequency identification technology, *International Journal of Computer Science and Mobile Computing*, 4(3):765–771.

FAST ANISOTROPIC FILTER BASED EM WITH SPATIAL INFORMATION FOR SEGMENTATION OF NOISY IMAGES

R. Meena Prakash* and R. Shantha Selva Kumari

¹Department of Electronics and Communication Engineering, P. S. R. Engineering College, Sivakasi, INDIA

*Department of Electronics and Communication Engineering, Mepco Schlenk Engineering College, Sivakasi, INDIA

ABSTRACT

This paper proposes a new method of Gaussian Mixture Model (GMM) based segmentation of noisy images. Gaussian Mixture model is the most widely utilized methods for segmentation of images and the parameters of GMM are calculated using the Expectation Maximization algorithm (EM). But the conventional Gaussian Mixture Model with Expectation Maximization gives poor segmentation accuracy for images with noise content. This is due to the fact that GMM considers each pixel as an independent data and calculates the distribution. It does not include the spatial data of the surrounding pixels. Many segmentation algorithms suffer from over-smoothness for segmentation and they fail to preserve the image details. Anisotropic diffusion filtering is a successful method which overcomes these undesirable effects in segmentation. In the proposed method, firstly the anisotropic diffusion filtering is applied to the image corrupted by noise to incorporate the local information. Secondly, the EM algorithm is enhanced by incorporating spatial information in the posterior probability which makes the convergence of EM algorithm also faster. The quantitative results obtained by applying the proposed anisotropic filter based EM with spatial information method on synthetic images and simulated brain images and comparison with the other methods demonstrate that the proposed method outperforms GMM by 26% and the recent method in literature by around 1%. The execution time is less compared to the other methods.

Received on: 4th-May-2016

Revised on: 15th- May-2016

Accepted on: 17th- May-2016

Published on: 20th- May-2016

KEY WORDS

Image Segmentation, Gaussian Mixture Model, Expectation Maximization, Anisotropic filter.

*Corresponding author: Email: meenaprakash73@gmail.com, Tel: +91-9442057946

INTRODUCTION

Segmentation of images intends to split the image into different parts having similar features. Segmentation finds its applications in wide areas including medical diagnosis, remote sensing and military applications. The most popular methods available for image segmentation are model based segmentation and clustering methods. Among the clustering methods, the prevalent method for image segmentation is Fuzzy c-means algorithm (FCM) [1,2]. Statistical methods such as Gaussian Mixture Model (GMM) for segmentation is another widespread method where the parameters of GMM are estimated using Expectation Maximization (EM) algorithm [3,4]. The conventional FCM and GMM work well on images without noise, but they fail to segment images corrupted by noise since they do not consider spatial related information in an image.

To integrate the spatial related information in image, the methods in the literature provide several techniques for both FCM and GMM. Blekas et al. proposed Markov Random Field priors [5] for Image segmentation to incorporate the spatial interaction among neighboring pixels. Thanh et al. [6] proposed a non-symmetric mixture model-Student's t-distribution and EM is adapted to estimate the model parameters. A self adaptive GMM [7] and neighborhood weighted GMM [8] are proposed to extend the standard GMM for suitable applications. Likewise, among the FCM based segmentation methods, Maoguo et al. [9] proposed a tradeoff weighted fuzzy factor and kernel metric to incorporate the spatial information. An RBF kernel based intuitionistic FCM replacing the Euclidean distance metric [10] is proposed to segment noisy medical images. Stelios et al. [11] proposed Fuzzy Local Information C Means Clustering (FLICM) in which he suggested the method of incorporating both spatial information and intensity information in a fuzzy manner.

Perona and Malik [12] introduced the anisotropic diffusion filter which provides an effective way of denoising images. Anisotropic diffusion based image enhancement methods are proposed in [13-17] and it is established that it is an efficient way to incorporate the local information while segmentation of noisy images. Based on the above considerations, in the proposed method, first the anisotropic diffusion filter output of the noisy image is obtained.

Then GMM based modified EM segmentation is done where the EM algorithm is enhanced by incorporating spatial information in the posterior probability. By modifying the posterior probability, the EM algorithm converges faster.

The remainder of the paper is structured as follows: Gaussian Mixture Model is detailed, the anisotropic diffusion filter is described, the details of the proposed anisotropic filter based EM with the spatial information method are explained, the experimental solutions are presented and then conclusions are given.

Gaussian mixture model and expectation maximization algorithm

The Gaussian distribution of the variable y is modelled as

$$G(y|\mu, \sigma^2) = \frac{1}{(2\pi\sigma^2)^{\frac{1}{2}}} \exp\left\{-\frac{1}{2\sigma^2}(y - \mu)^2\right\} \quad (1)$$

where μ is the mean and σ^2 is the variance.

The likelihood function for the Gaussian distribution is

$$p(x/\mu, \sigma^2) = \prod_{n=1}^N G(x_n/\mu, \sigma^2) \quad (2)$$

The Gaussian mixture distribution can be composed as a linear superposition of M Gaussian densities of the form

$$p(x) = \sum_{l=1}^M \pi_l G(x/\mu_l, \sigma_l^2) \quad (3)$$

where the variable l denotes the class and M denotes the number of classes.

Each Gaussian density $G(x/\mu_l, \sigma_l^2)$ is called a component of the mixture with its own mean μ_l and covariance σ_l^2 . The parameter π_l are called the mixing coefficients.

$$\sum_{l=1}^M \pi_l = 1 \text{ and } 0 \leq \pi_l \leq 1 \quad (4)$$

From Bayes' theorem, the posterior probabilities $p(l/x)$ are given by

$$\gamma_l(x) = p(l/x) = \frac{\pi_l G(x|\mu_l, \sigma_l^2)}{\sum_{l=1}^M \pi_l G(x|\mu_l, \sigma_l^2)} \quad (5)$$

From Equation 2, The log of the likelihood function is given by

$$\ln p(x/\mu, \sigma^2) = \sum_{n=1}^N \ln\{\sum_{l=1}^M \pi_l N(x_n|\mu_l, \sigma_l^2)\} \quad (6)$$

For maximizing the log likelihood, the derivatives of equation 6 with respect to μ_l, σ_l^2 and π_l are set to zero.

$$N_l = \sum_{n=1}^N \gamma_l(x) \quad (7)$$

The parameters are obtained as

$$\mu_l = \frac{1}{N_l} \sum_{n=1}^N \gamma_l(x) x_n \quad (8)$$

$$\sigma_l^2 = \frac{1}{N_l} \sum_{n=1}^N \gamma_l(x) (x_n - \mu_l)(x_n - \mu_l)^T \quad (9)$$

$$\pi_l = \frac{N_l}{N} \quad (10)$$

The EM algorithm is explained in the next steps.

The object is to maximize the likelihood function with regard to the parameters – mean, variance and mixing coefficient.

Step 1: The values of means μ_l , variances σ_l^2 and mixing coefficients π_l for all the classes are initialized

the initial value of the log likelihood is evaluated.

Step 2: E Step: The posterior probabilities are estimated using the current parameter values. (Equation 5).

Step 3: M Step: The parameters means, variances, and mixing coefficients for all the classes are re-calculated using the current posterior probabilities. (Equations 7-10).

Step 4: The Log likelihood is evaluated using Equation 6 and the convergence criterion is checked. If it is not satisfied, return to step 2.

The drawback existing in Gaussian Mixture Model based segmentation is that it considers each pixel as an independent data and calculates the distribution. It does not include the spatial data of the surrounding pixels. Hence the method is sensitive to noise and illumination.

Anisotropic diffusion filtering

The conventional low pass filtering and linear diffusion of an image can be obtained by convolution of the original image with a Gaussian kernel. In this method, noise can be eliminated but the edges are blurred. In anisotropic diffusion, by the proper choice of conduction coefficient, the edges are enhanced and also the noise is eliminated. The equation for anisotropic diffusion is stated as

$$\frac{\partial G(x,y,t)}{\partial t} = \text{div}[g(|\nabla G(x,y,t)|)]\nabla G(x,y,t) \quad (11)$$

where t is the time parameter, $G(x,y,0)$ is the input Gray scale image, $\nabla G(x,y,t)$ is the gradient of the image at given time t , and $h(\cdot)$ represents the conductance function. This function is selected such as to satisfy $\lim_{x \rightarrow 0} h(x) = 1$ and $\lim_{x \rightarrow \infty} h(x) = 0$. Hence, across the uniform regions, the diffusion is maximal and the diffusion is zero at the edges.

The conductance functions which are proposed in [13] are

$$h_1(x) = \exp\left[-\left(\frac{x}{T}\right)^2\right] \quad (12)$$

$$\text{and } h_2(x) = \frac{1}{1 + \left(\frac{x}{T}\right)^2} \quad (13)$$

The rate of diffusion is controlled by the gradient magnitude threshold parameter T . It acts as a threshold between the image gradients contributed by noise and those contributed by edges.

The anisotropic diffusion in discrete form is represented as

$$G_{t+1}(p) = G_t(p) + \frac{\lambda}{|\eta_p|} \sum_{s \in \eta_p} h_k(|\Delta G_{p,s}|) \Delta G_{p,s} \quad (14)$$

Where G is the input digital image, p denotes the pixel position in the image, t denotes the iteration step, h is the conductance function and K represents the gradient threshold parameter. The rate of diffusion is given by the constant λ and it lies in the interval $[0,1]$. η_p represents the 8-pixel neighborhood of pixel s . The gradient is calculated as the difference between neighboring pixels for all the directions.

$$\nabla G_{p,s} = G_t(s) - G_t(p), \quad s \in \eta_p \quad (15)$$

PROPOSED METHOD

The proposed method can be summarized as follows.

A. Apply Anisotropic Diffusion filter to the input noisy image.

Step 1: Set the number of iterations, gradient threshold parameter and the Constant λ .

Step 2: Obtain the gradient of the image in 8 directions. (Equation 15)

Step 3: Determine the conductance functions for the gradients. (Equation 13)

Step 4: Implement the anisotropic diffusion for the image. (Equation 14)

Step 5: Repeat steps 2 through 4 for the total number of iterations.

B. Apply Fast modified EM to the anisotropic filtered image

Step 1: Initialize the number of classes and convergence value of log likelihood and the parameters – mean, variance and mixing coefficient.

Step 2: Evaluate the initial log likelihood.

Step 3: Expectation Step: Estimate the posterior probabilities using current parameters. (Equation 9)

Step 4: Apply arithmetic mean filter to the posterior probabilities to incorporate the spatial information about the neighboring pixels.

Step 5: Maximization Step: Re-estimate the parameters – mean, variance and mixing coefficient using current posterior probabilities. (Equations 7-10)

Step 6: Calculate the log likelihood (Equation 6) and verify convergence. If the log likelihood value does not converge, return to step 2.

Step 7: Obtain the final model and perform segmentation based on the model.

Experimental results

The segmentation results of the method on synthetic images as well as simulated data sets is presented. The processor specification is Intel Core 2 Duo CPU @2.93GHz and the RAM specification is 4.0 GB. The algorithm is implemented with MATLAB.

Experiments on the synthetic images

The method is examined on three test synthetic images. Images similar to those used in [9] are employed. The first image with 128 x 128 pixels comprises of two classes with two intensity values - 20 and 120 as shown in **Figure-1 (a)**. The other two images are of resolution 244 x 244 and 256 x 256 pixels respectively, and shown in **Figure-2 (a)** and **Figure-3 (a)**, for which the number of clusters is 4. For the Expectation Maximization algorithm, the means of the classes are initialized by the means obtained from the K-Means segmentation of the noisy images. The threshold for the log likelihood is set as 0.01.

The parameters - Number of iterations, gradient threshold parameter and the Constant λ for anisotropic diffusion filtering are set as 25, 25 and 1/7 respectively for all the experiments on synthetic images. The conductance function given in Equation 13 is used.

The parameters of FLICM method – local window size, maximum iteration, weighting exponent of membership, threshold of the deviation between cluster centres computed at successive iterations are set as 3, 500, 2, 0.001 respectively.

The misclassification ratio (MCR) is employed to evaluate the performance of the method.

$$MCR = \frac{\text{No. of misclassified pixels}}{\text{Total number of pixels}} \quad (16)$$

In all the three synthetic images shown in **Figure-1 (a), 2 (a) and 3 (a)**, Gaussian noise by 30% is added and shown in **Figure- 1 (b), 2 (b) and 3 (b)**. The outputs of anisotropic filter are shown in **Figure-1 (c), 2 (c) and 3 (c)**. The results of Otsu's threshold segmentation method with anisotropic filtering are shown in **Figure.1 (d), 2 (d) and 3 (d)**. The results of standard EM segmentation without anisotropic filter are shown in **Figure-1 (e), 2 (e) and 3 (e)**. The results of standard EM segmentation with anisotropic filtering are shown in **Figure.1 (f), 2 (f) and 3 (f)**. The results of EM with spatial information segmentation and without anisotropic filtering are shown in **Figure-1 (g), 2 (g) and 3 (g)**. The segmentation results of FLICM are shown in **Figure-1 (h), 2 (h) and 3 (h)** and the segmentation results of the Anisotropic filter based EM with spatial information segmentation are shown in **Figure-1 (i), 2 (i) and 3 (i)**.

The qualitative and quantitative analysis of the results on synthetic images show that integrating anisotropic filtering and EM with local information segmentation provides better segmentation when compared to the methods when applied individually. Especially, the anisotropic filtering contributes more for the segmentation

accuracy while EM with local information provides better tuning in achieving good segmentation accuracy. The method of Otsu's threshold segmentation with anisotropic filtering achieves good results for synthetic image 1 and 2 but it fails to correctly segment synthetic image 3 since the method relies on bimodal histogram and does not consider the probability distribution of the pixels. The FLICM method gives better segmentation accuracy for image with two classes and with less noise. But the segmentation accuracy decreases for image with four classes and with 30% Gaussian noise. The proposed method gives better segmentation accuracy with increasing level of noise and hence the method is robust to noise.

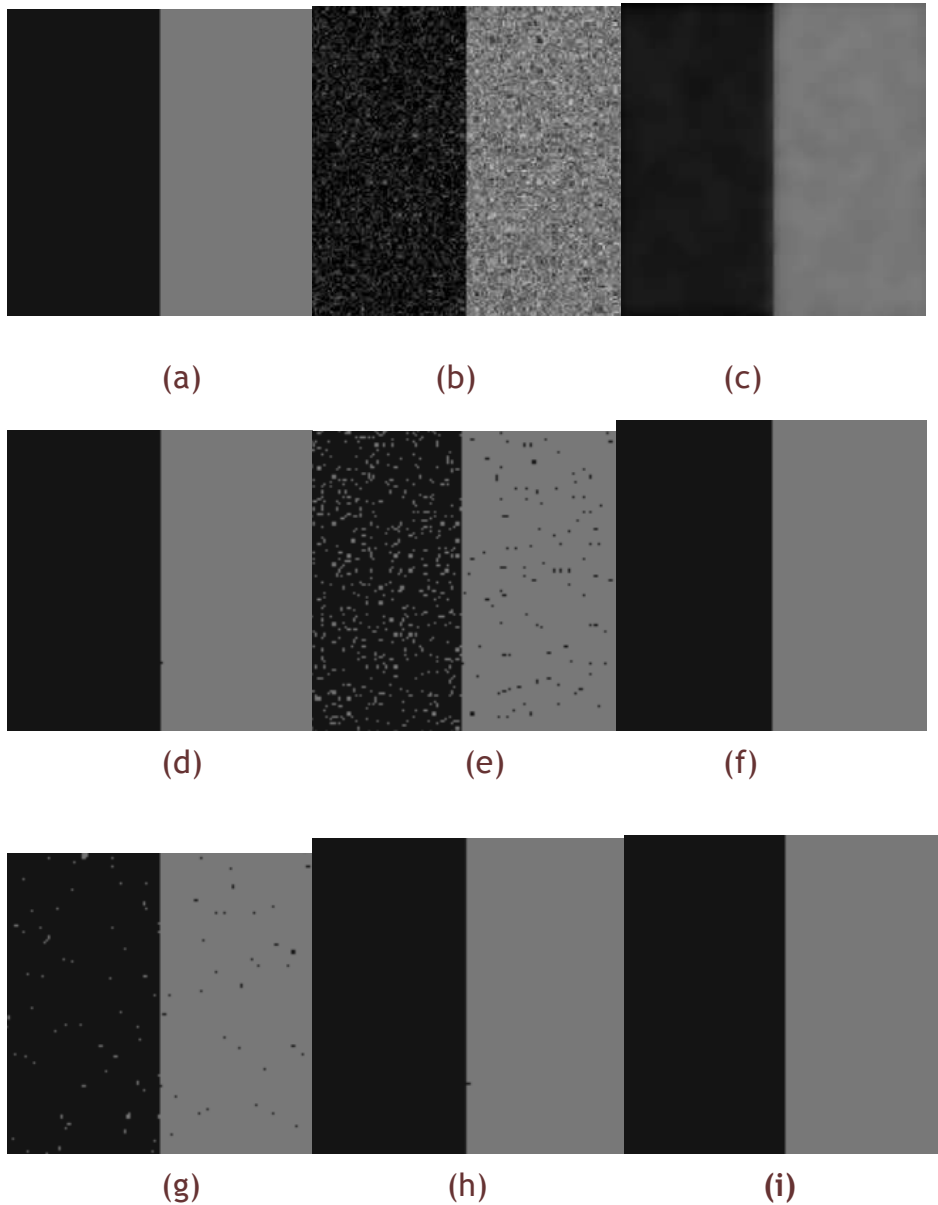


Fig: 1. Segmentation results of the Anisotropic filter based EM with spatial information method on the synthetic Image. (a) Input Image, (b) Image added with Gaussian noise (30%) (PSNR=20.18dB), (c) Anisotropic Filter Output (PSNR=32.79dB), (d) Anisotropic with Otsu's Threshold segmentation (SA=0.99988), (e) Standard EM segmentation without anisotropic filter (SA=0.9552), (f) Standard EM segmentation with anisotropic filter (SA=1.0), (g) EM with spatial information segmentation without anisotropic filter (SA=0.99377), (h) FLICM [9] (SA = 0.99994), (i) Proposed method - Anisotropic filter based EM with spatial information segmentation (SA=1.0)

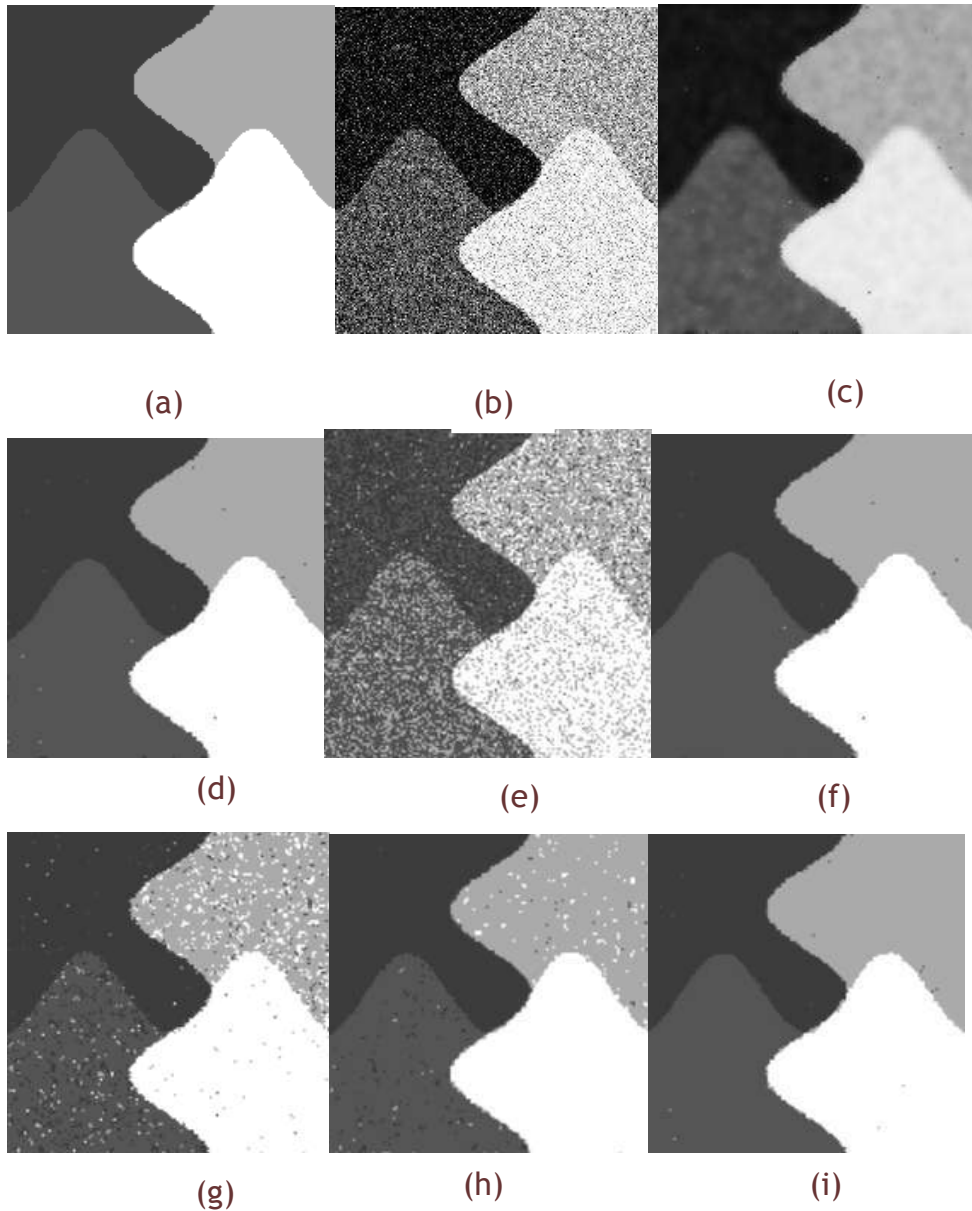


Fig. 2. Segmentation results of the Anisotropic filter based EM with spatial information method on the synthetic Image. (a) Input Image, (b) Image added with Gaussian noise (30%) (PSNR=16.89dB), (c) Anisotropic Filter Output (PSNR=24.6dB), (d) Anisotropic with Otsu's Threshold segmentation (SA=0.9913), (e) Standard EM segmentation without anisotropic filter (SA=0.6446), (f) Standard EM segmentation with anisotropic filter (SA=0.9889), (g) EM with spatial information segmentation without anisotropic filter (SA=0.9144), (h) FLICM [9] (SA = 0.0.9758), (i) Proposed method - Anisotropic filter based EM with spatial information segmentation (0.9912)

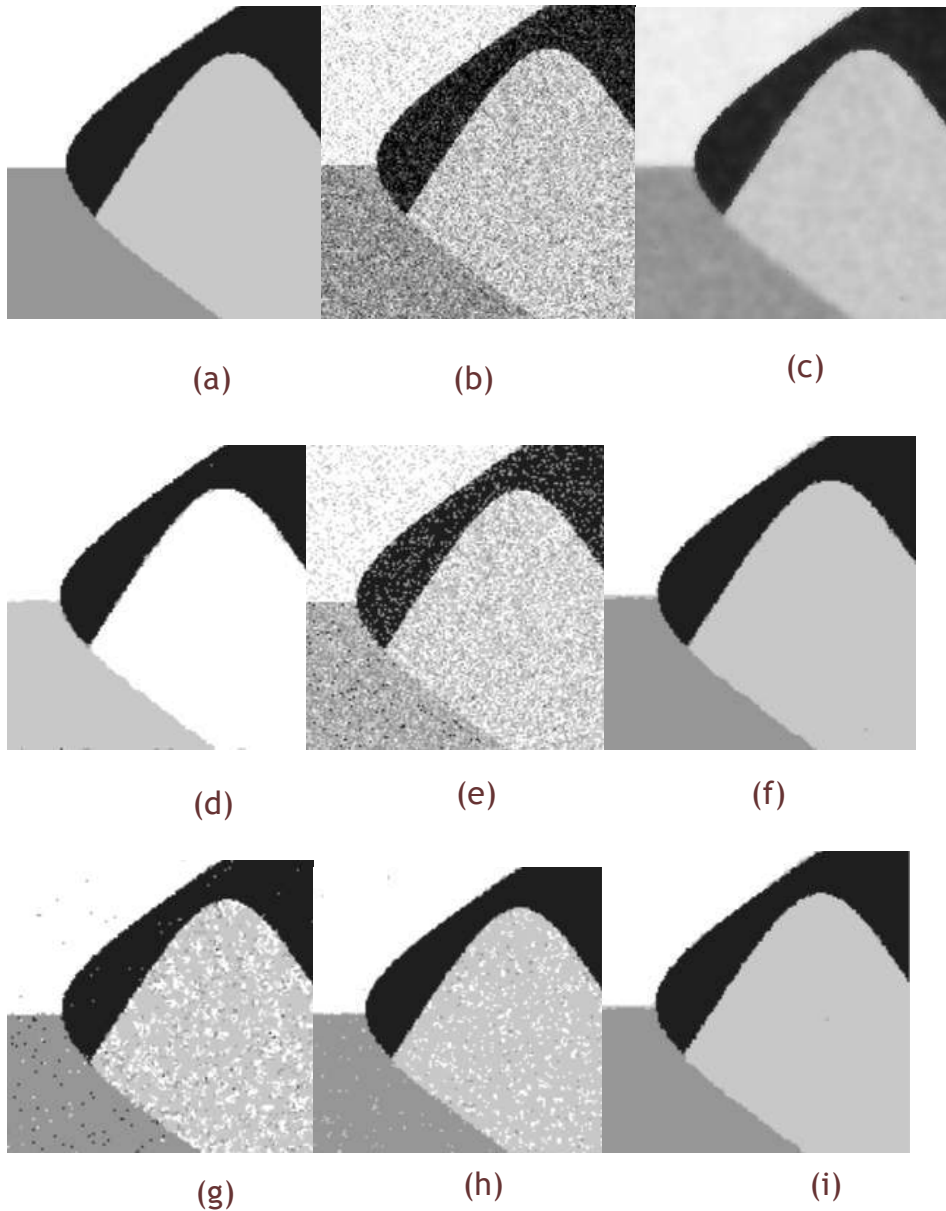


Fig: 3. Segmentation results of the Anisotropic filter based EM with spatial information method on the synthetic Image. (a) Input Image, (b) Image added with Gaussian noise (30%) (PSNR=17.27dB), (c) Anisotropic Filter Output (PSNR=28.13dB), (d) Anisotropic with Otsu's Threshold segmentation (SA=0.3842), (e) Standard EM segmentation without anisotropic filter (SA=0.6484), (f) Standard EM segmentation with anisotropic filter (SA=0.9904), (g) EM with spatial information segmentation without anisotropic filter (SA=0.8787), (h) FLICM [9] (SA =0.9412), (i) Proposed method - Anisotropic filter based EM with spatial information segmentation (0.9922)

.....

Table: 1. Comparison of Segmentation Accuracy of various methods for Synthetic Image 1

Methods	Gaussian Noise		
	15%	20%	30%
Anisotropic with Otsu's Threshold segmentation	0.99976	0.99969	0.99988
Standard EM segmentation without anisotropic filter	0.99396	0.98499	0.9552
Standard EM segmentation with anisotropic filter	1.0	1.0	1.0
EM with spatial information segmentation without anisotropic filter	0.99902	0.99756	0.99377
Fuzzy Local Information C Means Clustering (FLICM)	1.0	1.0	0.99994
Proposed method – Anisotropic filter based EM with spatial information segmentation	1.0	1.0	1.0

Table: 2. Comparison of Segmentation Accuracy of various methods for Synthetic Images 2 and 3

Methods	Synthetic Image 2			Synthetic Image 3		
	Gaussian Noise			Gaussian Noise		
	15%	20%	30%	15%	20%	30%
Anisotropic with Otsu's Threshold segmentation	0.9937	0.9934	0.9913	0.3877	0.3872	0.3842
Standard EM segmentation without anisotropic filter	0.7346	0.6976	0.6446	0.7608	0.7126	0.6484
Standard EM segmentation with anisotropic filter	0.9917	0.9907	0.9889	0.9912	0.9915	0.9904
EM with spatial information segmentation without anisotropic filter	0.9628	0.9531	0.9144	0.9612	0.9375	0.8787
FLICM	0.9923	0.9903	0.9758	0.9923	0.9828	0.9412
Proposed method – Anisotropic filter based EM with spatial information segmentation	0.9938	0.9934	0.9912	0.9926	0.9930	0.9927

Table: 3. Comparison of No. of iterations and execution Time for the methods-Standard EM segmentation with anisotropic filter, RFLCIM and Anisotropic filter based EM with spatial information method and time of execution for anisotropic filter

Images	Standard EM segmentation with anisotropic filter		RFLCIM	Anisotropic filter based EM with spatial information Method		Anisotropic Filter
	Iteration Count	Time of Execution (secs)	Time of Execution (secs)	Iteration Count	Time of Execution (secs)	Time of Execution (secs)
Synthetic Image 1	4	1.37	1.45	2	1.19	0.54
Synthetic Image 2	35	6.82	14.07	3	3.88	1.01
Synthetic Image 3	39	8.77	25.88	11	5.51	1.20

From **Table– 1, 2 and 3**, it is inferred that the performance of the Anisotropic filter based EM with spatial information method is superior to the other methods in both execution time and segmentation accuracy.

Experiments on Simulated images from Brainweb

The proposed anisotropic filter based EM with spatial information method is also tested on T1-weighted MR brain images from the BrainWeb database. The method is validated on simulated images with 40% in-homogeneity and 9% noise 181 x 217 x 181 dimension 1 x 1 x 1 mm³ spacing.

The ground truth for the Brain Web dataset is the phantom atlas used to generate the simulated scans. The Dice Similarity Index (DSI) is used as the performance metric. The Dice Similarity Index DSI is given by

$$DSI = \frac{2(P \cap G)}{P + G} \quad (17)$$

Where P represents the sum of pixels classified by the proposed method and G represents the sum of pixels classified by the ground truth and $P \cap G$ represents the sum of pixels classified by both the proposed method and the ground truth.

Two simulated images (#91 and #120) from Brainweb dataset are taken. The brain image is segmented into three classes – Cerebro-spinal Fluid with pixel value 128, Gray matter with pixel value 192 and White matter with pixel value 254. The original images are shown in **Figure–4 (a)** and **Figure– 5 (a)**. The ground truths of the images are shown in **Figure– 4 (b)** and **Figure–5 (b)**. The segmentation results of standard GMM and the anisotropic filter based spatial EM method are shown in **Figure–4 (c), (d)** and **Figure–5(c), (d)**.

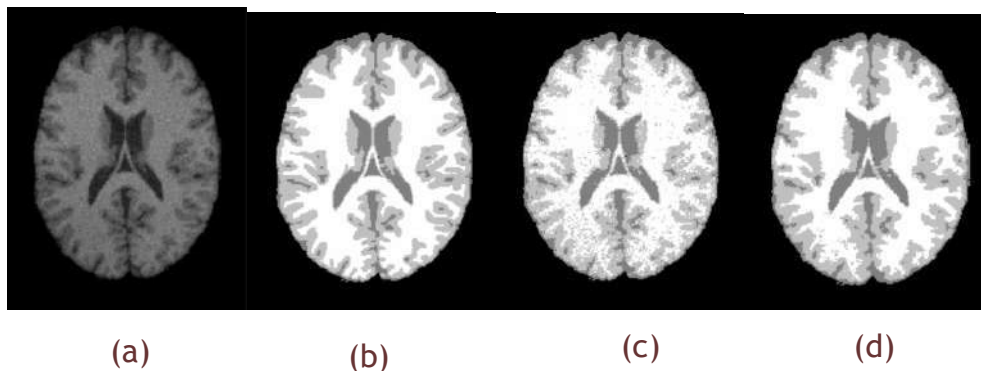


Fig: 4. Segmentation results of the proposed anisotropic filter based EM with spatial information on the MR brain image slice #91. (a) Input Image, (b) Ground truth Image, (c) Standard EM, (d) Anisotropic filter based EM with spatial information method

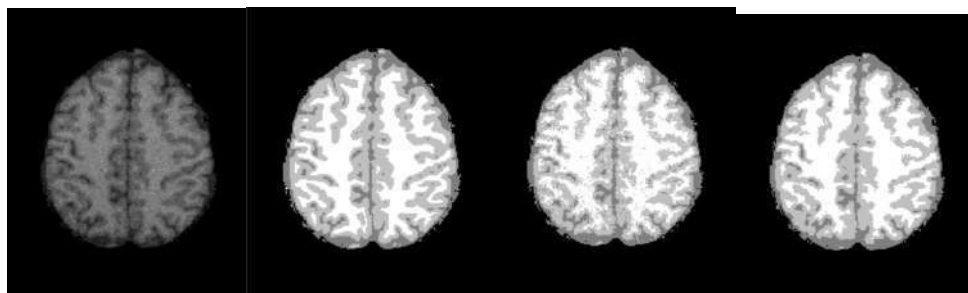


Fig: 5. Segmentation results on the MR brain image slice #120. (a) Input Image, (b) Ground truth Image, (c) Standard EM, (d) Anisotropic filter based EM with spatial information method.

Table 3. Performance Comparison of the Proposed Method to Standard EM Method for Brainweb T1 weighted Images with 40% in-homogeneity and 9% noise slices #91 and #120.

Class	Dice Similarity Index	
	Standard GMM	Proposed Method
GM (#91)	0.8305	0.8702
WM (#91)	0.8973	0.9339
CSF(#91)	0.9070	0.9067
GM (#120)	0.8549	0.8801
WM (#120)	0.8756	0.9037
CSF(#120)	0.8965	0.9078

From **Table-3**, it is inferred the proposed method provides good results for simulated brain images from the Brain web.

CONCLUSION

A new method for segmentation of noisy images based on Gaussian Mixture Model is presented. Anisotropic filter is used for details preserving smoothing. To incorporate the spatial data among the neighboring pixels, the posterior probability is weighted with arithmetic mean filter. The proposed method has been tested on various synthetic and simulated brain images. It is demonstrated that the proposed Anisotropic filter based EM with spatial information method is more efficient both quantitatively and qualitatively compared to the methods in the literature for noisy images. The method is simple and has less computational cost.

ACKNOWLEDGEMENT

None

CONFLICT OF INTEREST

Authors declare no conflict of interest.

FINANCIAL DISCLOSURE

No financial support was received to carry out this project

REFERENCES

- [1] J Bezdek.[1981] Pattern Recognition with Fuzzy Objective Function Algorithms, New York, Plenum
- [2] J Dunn.[1974] A fuzzy relative of the ISODATA process and its use in detecting compact well-separated Clusters, *Journal of Cybernetics*, 3(3):32–57
- [3] Asghar CM Bishop.[2006] Pattern Recognition and Machine Learning. New York: Springer,
- [4] Dempster AP, Laird NM, and Rubin DB.[1977] Maximum Likelihood from Incomplete Data via the EM Algorithm, *Journal of the Royal Statistical Society* 39(1): 1–38,.
- [5] K Blekas, A Likas, N P Galatsanos, and IE Lagaris.[2005] A Spatially Constrained Mixture Model for Image Segmentation, *IEEE Trans. Neural Netw*, 16(2) Mar.
- [6] MNThanh, and QMJ Wu.[2013] A Nonsymmetric Mixture Model for Unsupervised Image Segmentation, *IEEE Trans. Cyber*, 43(2) :751–765
- [7] Zezhi Chen, Tim Ellis. “A self-adaptive Gaussian mixture model, *Computer Vision and Image Understanding*, 122:35–46,
- [8] Hui Tang, Jean-Louis Dillenseger, Xu Dong Bao, Li Min Luo.[2009] A vectorial image soft segmentation method based on neighborhood weighted Gaussian mixture model, *Computerized Medical Imaging and Graphics*, 33: 644–650.
- [9] Maoguo Gong, and Yan Liang.[2013] Fuzzy C-Means Clustering With Local Information and Kernel Metric for Image Segmentation ”, *IEEE Trans. Image Process*, 22(2):573–584.
- [10] Prabhjot Kaur, A.K.Soni, Anjana Gosain.[2013] A robust kernelized intuitionistic fuzzy c-means clustering algorithm in segmentation of noisy medical images”, *Pattern Recognition Letters*, 34:163–175.
- [11] Stelios Krinidis and Vassilios Chatzis.[2010]A Robust Fuzzy Local Information C-Means Clustering Algorithm, *IEEE Transactions on Image Processing*, 19(5):1328–1337, May
- [12] Pietro Perona and Jitendra Malik, “Scale-Space and Edge Detection Using Anisotropic Diffusion”, *IEEE Transactions on Pattern Analysis and Machine Intelligence*, vol.12, No.7,pp.629–639, July 1990.
- [13] Sumathi K and Anandh KR.[2014]Anisotropic Diffusion Filter based Edge Enhancement for the Segmentation of Carotid Intima-Media Layer in Ultrasound Images Using Variational Level Set method without Re-initialisation”, *IEEE Trans.*,238–241,

- [14] Tudot Barbu.[2014] Robust anisotropic diffusion scheme for image noise removal, *Procedia Computer Science*, 35: 522–530.
- [15] Chenchen Tong, Ying Sun, Nicolas Payet, Sim-Heng Ong.[2012] A general strategy for anisotropic diffusion in MR image denoising and enhancement, *Magnetic Resonance Imaging*, 30: 1381–1393.
- [16] Gui Gao, Lingjun Zhao, Jun Zhang, Diefei Zhou, Jijun Huang.[2008] A Segmentation Algorithm for SAR images based on the anisotropic heat diffusion equation, *Pattern Recognition*, 41: 3035–3043
- [17] Tsiotsios C, Petrou M. [2012] On the choice of the parameters for anisotropic diffusion in image processing., *Pattern Recognition*, 46(5): 1369–1381.

AUTOMATED IMAGE ENHANCEMENT USING GREY-WOLF OPTIMIZER ALGORITHM

Murali K.* and Jayabarathi T.

School of Electrical Engineering, VIT University, Vellore, INDIA

ABSTRACT

Application of Grey-wolf optimizer algorithm for image enhancement is the objective of this paper. Here Image enhancement is considered to be an optimization problem and it is solved using Grey-wolf optimizer algorithm. The process is automated by using entropy and edge information of the image. The superiority of the proposed technique is established by statistically analyzing the results of 50 independent trails of the algorithm. Additionally, PSNR are used to evaluate the performance of the algorithm. The results are compared with classical Histogram Equalization (HE) and evolutionary Particle Swarm Optimization (PSO) algorithm.

Received on: 12th-May-2016

Revised on: 1st -June-2016

Accepted on: 9th – June-2016

Published on: 24th – June-2016

KEY WORDS

Image Enhancement (IE); Grey-wolf optimizer; Metaheuristic algorithms; Particle Swarm Optimization (PSO)

*Corresponding author: Email: muralikmurali@yahoo.in

INTRODUCTION

Digital image processing is of great relevance to researches both in academia and in the industry as it involves many practical projects leading to various applications. Being an indispensable field, Vision and image processing techniques have become a part of our daily lives. One of the most critical and crucial parts of image processing is image enhancement. It is one of the important pre-processing techniques. According to Gonzalez et al, enhancement techniques may be branched into four groups: a) Point operation; b) Spatial operation; c) Transformation and d) Pseudo-coloring; [1]. This paper is based on spatial operation.

Automation of image enhancement is notoriously a difficult task in image processing [2]. However, these automation algorithms find many application in various fields such as automation engineering, medical imaging [3,4] etc; They help to enhance the image in a complex manner, by reducing the cumbersome job. The aim of this paper is to enhance images without intervention of humans. It could possibly pave way to artificial vision, machine learning & classification etc.[5] in the near future. Recently some of the image quality metrics such as edge intensity, sum of the edges, entropy etc., have been used for image enhancement.

One of the classical methods for image enhancement is Histogram equalization [HE][1]. Being one of the simplest methods, it creates a uniform distribution of cumulative density function of input image [6]. The major drawback of HE is that the mean-brightness of the HE image is considered as the middle gray-level and the mean of the image is not considered. So it is important to consider alternatives for image enhancement. One such alternative is metaheuristic algorithms, which is simple and time efficient. Some of the metaheuristic algorithms reported for image enhancement are Genetic Algorithm (GA) [7,8], Artificial Bee colony Algorithm(ABC)[9], Particle Swarm Optimization (PSO) [10,11], Black hole algorithm [12] etc.

The better performance of the above algorithms motivated me to apply “Grey-wolf optimizer” (GWO) algorithm [13] on image enhancement problem. The results are compared with HE and PSO for validation of IE. The remainder of the paper is organized as follows; Section II provides the problem formulation for IE; In section III,

Grey-wolf optimizer algorithm is described. The results along with the discussion are given in section IV. The conclusion is drawn in section V.

PROBLEM FORMULATION

In this paper, image is mapped to an objective value. The objective value is determined by parameters such as entropy and edge information. In order to increase the value of this objective function, value of each and every pixel of the image is altered. They are altered in such a way that the image does not lose its information, while enhanced [9,12]. To evaluate the image, an objective function is created.

Local Information

For a local user defined window $n \times n$, the local mean $m(i,j)$ is defined as,

$$m(i, j) = \frac{1}{n \times n} \sum_{p=i-(n-1)/2}^{i+(n-1)/2} \sum_{q=j-(n-2)/2}^{j+(n-2)/2} f(p, q) \quad (1)$$

Global Information

The Global mean of the image is defined as

$$D = \frac{1}{M \times N} \sum \sum f(x, y) \quad (2)$$

The Global variance of the image is given by

$$\sigma(i, j) = \sqrt{\frac{1}{n \times n} \sum \sum (f(x, y) - m(x, y))^2} \quad (3)$$

Therefore the total global information would be extracted as given in eqn. (4). With the above equation the total transformation function can be summarized as the following

$$K(i, j) = \frac{k D}{\sigma(i, j) + b} \quad (4)$$

$$g(i, j) = K(i, j)[f(i, j) - c \times m(i, j)] + m(i, j)^a \quad (5)$$

In eqn (5), there are four constants “ a, b, c and k ”, that are varied for altering the values of the pixels. They produce large variations to create $g(i,j)$, from which the best image is taken as the ‘enhanced’ image.

Objective function:

In order to automate the image enhancement process, we need to create objective function that will be used for determining the quality of the image. According to [9], an image is said to be enhanced if a) the number of edges are high; b) It is uniformly distributed; It is known that when an image is uniformly distributed, the entropy of the image is high [10]. So, to determine the objective function or the evaluation criterion, we take parameters such as entropy, number of edges and sum of edge intensity into consideration [8].

Thus, the “Objective function” which also called as fitness function is formulated as

$$Max.F(I_e) = \log(\log(E(I_s))) \times \frac{n_{edgels}}{MXN} \times H(I_e) \quad (6)$$

Where,

$E(I_s)$ is the edge intensity of image after Sobel operator is used as edge detector [1].
 n_{edges} is the number edges above threshold in sobel operation.
 $H(I_c)$ is the entropy of the transformed image[1].

IMPLEMENTAION OF GREY-WOLF OPTIMIZER ALGORITHM

The Grey-Wolf Optimizer (GWO) algorithm is a nature inspired algorithm introduced by Mirjalili et al.[13]. It mimics the leadership hierarchy and hunting mechanism of the Canis lupus (i.e Grey-wolves). The effectiveness of the algorithm makes it to have a wide variety of applications in the fields of Economic dispatch [14,15], neural networks in training multi-trainer perceptron's [16], harmonic elimination in inverters [18], Software reliability growth modelling [19] etc. The Particle Swarm Optimization (PSO) algorithm is implemented as given in [17]. The mathematical model by which the Grey-wolf optimizer algorithm works is briefed below.

Grey-Wolf Optimizer - Algorithm

The best position of the swarm or search agents is called alpha wolf or the leader wolf [13]. The next two best solutions are considered as Beta (β) and delta (δ) respectively. These three α , β and δ wolves play a crucial role in determining the optimal or near-optimal solution. All the other solution are assumed as omega solution (ω), which are made to change with reference to the above three solutions.

The position of the omega solutions are updated by the following equations

$$\vec{D} = |\vec{C} \cdot \vec{X}_p(t) - \vec{X}(t)| \quad (7)$$

$$\vec{X}(t+1) = \vec{X}_p(t) - \vec{A}\vec{D} \quad (8)$$

Here, 't' indicates the current iteration,

\vec{X}_p denotes the position of the prey/ solution

\vec{X} denotes the position of grey-wolf.

The vectors \vec{A} and \vec{D} are given by

$$\begin{aligned} \vec{A} &= 2 \cdot \vec{a} \cdot \vec{r}_1 - \vec{a}; \\ \vec{C} &= 2 \cdot \vec{r}_2 \end{aligned} \quad (9 \& 10)$$

Where \vec{a} is linearly decreased from '2' to a very small value near zero.

The position of α , β and δ wolves are updated as follows

$$\vec{D}_\alpha = |\vec{C}_1 \cdot \vec{X}_\alpha - \vec{X}| \quad (11)$$

$$\vec{D}_\beta = |\vec{C}_2 \cdot \vec{X}_\beta - \vec{X}| \quad (12)$$

$$\vec{D}_\delta = |\vec{C}_3 \cdot \vec{X}_\delta - \vec{X}| \quad (13)$$

$$\vec{X}_1 = \vec{X}_\alpha - \vec{A}_1 \cdot (\vec{D}_\alpha) \quad (14)$$

$$\vec{X}_2 = \vec{X}_\beta - \vec{A}_2 \cdot (\vec{D}_\beta) \quad (15)$$

$$\vec{X}_3 = \vec{X}_\delta - \vec{A}_3 \cdot (\vec{D}_\delta) \quad (16)$$

$$\vec{X}(t+1) = \frac{\vec{X}_1 + \vec{X}_2 + \vec{X}_3}{3} \quad (17)$$

Where, \vec{D} gives the distance;

\vec{X} is the position;

While, $\vec{X}(t+1)$, gives the updated position using eqn.(17).

Pseudocode for implementation

```

Initialize the grey-wolf population
Initialize a, A and C
Calculate the fitness of each search agent / grey-wolf
For each iteration
Use best search agent as 'X $\alpha$ ';
Use the second best search agent as 'X $\beta$ ';
Use the third best search agent as 'X $\delta$ ';
While(t<Max no. of iterations)
If search agent =  $\omega$ 
Use eqn.(7) and (8) for position updation
If search agent =  $\alpha/\beta/\delta$ 
Use eqn.(11)-(16) for position updation
t=t+1;
end while;
return;

```

Implementation of Algorithm

The GWO, implanted for image enhancement were initialized with 20 search agents. The values of 'a', which is linearly decreasing from '2' to '0' is initialized. The maximum number of iterations is fixed as 20. After first iteration, the best solution as given by eqn.(6) is taken as " α -wolf", while next two best solutions are taken as " β " and " δ " wolves respectively. The other solutions become ω wolves. Using (7) and (8), positions of all the wolves are updated.


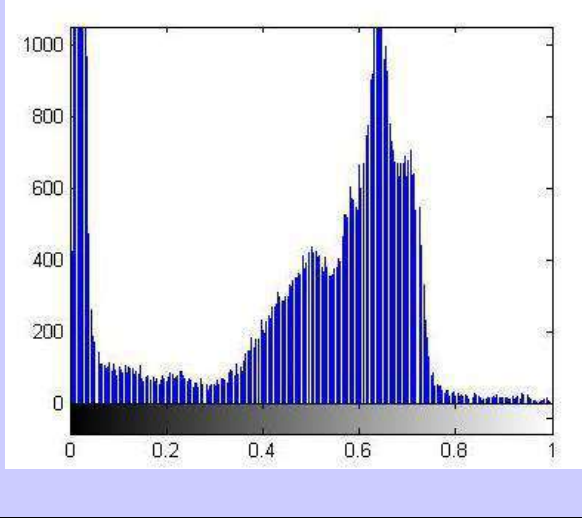

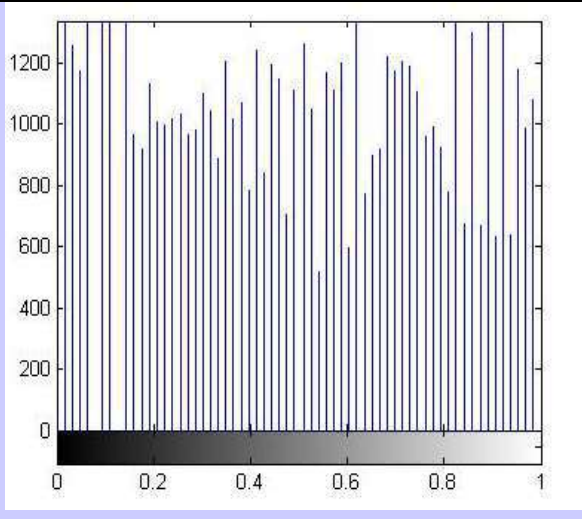

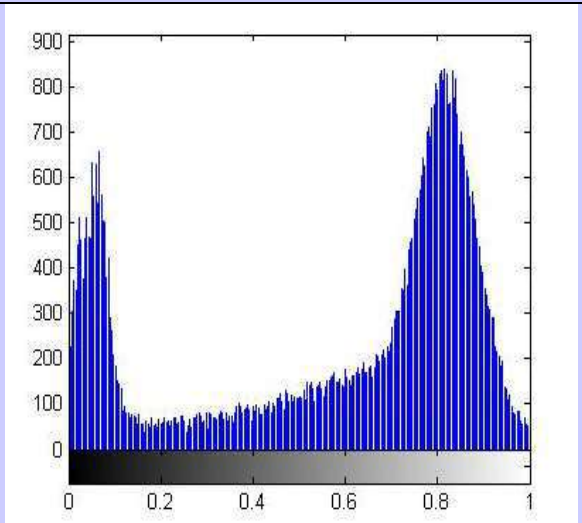
RESULTS AND DISCUSSIONS

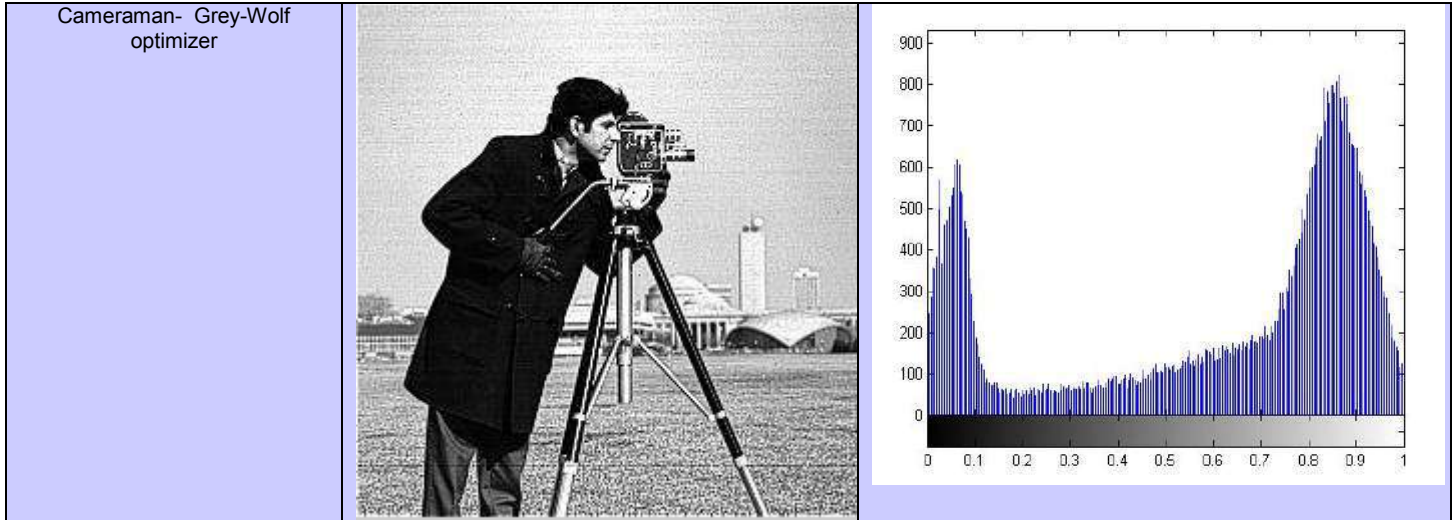
The above proposed method is evaluated with many gray-level images. However, due to space limitations, results of four benchmark images and two medical images are shown. The four decision variables $a \in (0, 1.5)$; $b \in (0, Total\ mean/2)$; $c \in (0, 1)$ and $k \in (0.5, 1.5)$ are initialized in their limits [10]. The four decision variables are then used by eqn. (5) to transform the image. Then the objective or fitness value is calculated according to eqn. (8).

Table: 1. Results from various methods

S.No	Image	Size	Fitness	HE	PSO	Proposed method (Grey-wolf)
1	Tire	205 X 232	0.2707	0.4776	0.8178	0.8192
2	Cameraman	256 X 256	0.2677	0.4501	0.8257	0.8282
3	Rice	256 X 256	0.5303	0.6169	1.2993	1.3003
4	Plane	512 X 512	0.2288	0.4338	0.6912	0.6930
5	Medical image 1 – X-Ray	224 X 253	0.2850	0.2192	0.4343	0.4362
6	Medical image 2 - Mammogram	558 X 563	0.2832	0.2187	0.3545	0.3639

Table: 2. Visual analysis of 'Cameraman' image and its histograms

Image / Algorithm	Image	Histogram
Cameraman- Original Image		
Cameraman- HE		
Cameraman- PSO		



The visual results with the respective histograms are given in Table- 2. From the table it can be visually concluded that PSO and Grey-wolf optimizer algorithms give better results than HE. In order to evaluate the effectiveness of the algorithm, each algorithm was made to run for 50 independent trail runs and statistical data is presented. From Table- 3 and 4, it can be seen that, entropy and number of edges of Grey-wolf optimizer algorithm are slightly higher than PSO. The standard deviation of GWO is less than that of PSO showcasing the consistency of GWO algorithms. This clearly indicates that GWO algorithm can be treated at par or even better when compared to PSO.

Table: 3. Comparison of statistical results of Entropy of ‘Cameraman’ Image

Cameraman/ Entropy	Mean	Best	Worst	Standard deviation
Original Image	NA	7.0097	NA	NA
HE	NA	5.9106	NA	NA
PSO	7.3215	7.4159	6.9125	0.2485
GWO	7.3521	7.4032	7.0102	0.2252

Table: 4. Comparison of statistical results of number of edges of ‘Cameraman’ Image






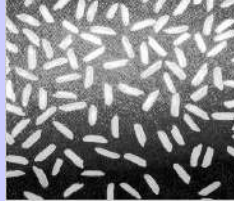

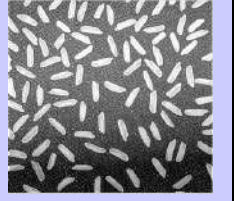








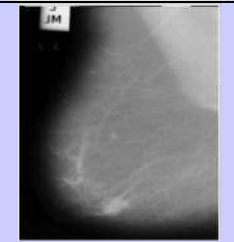

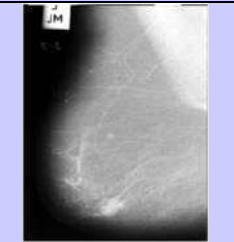

Cameraman/ No. of edges	Mean	Best	Worst	Standard deviation
Original Image	NA	2503	NA	NA
HE	NA	2430	NA	NA
PSO	3442	3482	3352	142
GWO	3452	3484	3395	95

Table: 5. Comparison of results of fitness and PSNR of ‘Plane’ Image with that of GA[7][8]

Plane	GA[7]	GA[8]	PSO	GWO
Fitness value	NA	0.5702	0.6912	0.6930
PSNR	17.92	17.89	20.68	21.35

Table 5 presents the comparison of fitness and PSNR of ‘Plane’ image with that of other state-of-art algorithms such GA[7]and [8] with that of PSO and GWO. From the table, the superiority of GWO can be clearly seen. In addition, the visual results of all other images are presented in Table -6.

Table: 6. Visual Results of Images enhanced

Image Name	Original Image	HE	PSO	GWO
Tire				
Rice				
Plane				
Medical image 1 - X-ray				
Medical image 2 - Mammogram				

The statistical analysis of all the images 1-6 also reiterates that GWO and PSO are superior to classical HE technique. The images when visually inspected also prove the same. It can also be seen from the above tabulations that GWO is comparable and superior to PSO both in terms of solution quality and computational time. It should also be noted that GWO has relatively less steps when compared to PSO, reducing the computational time.

The exploration of search space of GWO is because of the fact that all solutions are based on alpha, beta and delta positions. This is mathematically modelled in eqn.(9), where, the A is random with values, greater than ± 1 or less than -1 , causing exploration in the search space. In addition, eqn.(10), randomly generates the value of C , in the range of $[2,0]$, which makes the algorithm more stochastic, thereby increasing its exploitation ability. It also decreases the chance of local convergence. The use of ' a ' in the range of $[2,0]$, by linearly decreasing them paves way for exploitation, i.e. local search. This eventually increases the chance of convergence, when A is in the range of $[-1,1]$.

CONCLUSION AND FUTURE WORK

In this paper, we have used Grey-wolf optimizer for deducing a technique for automated image enhancement, an optimization problem. The output images and the corresponding metrics of the images produced by classical HE and PSO algorithm are used for comparison. The visual and mathematical results prove the superiority of GWO and PSO over HE. The statistical analysis of 50 independent trail runs of PSO and GWO algorithms shows that GWO is at par comparable or superior to that of PSO, for image enhancement problem. In future, hybridization of the grey-wolf algorithm is to be done to improve its performance. The algorithm will also be extended for enhancement of colour images.

FINANCIAL DISCLOSURE

There is no financial support for this work.

ACKNOWLEDGEMENT

The author is grateful to Chancellor, Vice-Chancellor and Vice-Presidents of VIT University, for providing excellent infrastructure facilities and encouragement which have made this work possible.

CONFLICT OF INTERESTS

There are no conflicts of interests.

REFERENCES

- [1] Gonzalez RC, Woods RE. [2002] Digital image processing.
- [2] Jain AK. [1989] Fundamentals of digital image processing. Prentice-Hall, Inc..
- [3] Rangayyan RM. [2004] Biomedical image analysis. CRC press.
- [4] Rangayyan RM, Acha B, Serrano C. [2011] Color image processing with biomedical applications. Bellingham: SPIE Press.
- [5] Jagannath, M., & Adalarasu, K. Diagnosis of diabetic retinopathy from fundus image using Fuzzy C-Means clustering algorithm
- [6] Chen SD, Ramli AR. [2003] Minimum mean brightness error bi-histogram equalization in contrast enhancement. *Consumer Electronics, IEEE Transactions on*, 49(4):1310–1319.
- [7] Hashemi S, Kiani S, Noroozi N, Moghaddam ME. [2010] An image contrast enhancement method based on genetic algorithm. *Pattern Recognition Letters*, 31(13):1816–1824.
- [8] Verma A, Goel S, Kumar, N. [2013] Gray level enhancement to emphasize less dynamic region within image using genetic algorithm. In *Advance Computing Conference (IACC), 2013 IEEE 3rd International* (pp. 1171–1176). *IEEE*.
- [9] Draa A, Bouaziz A. [2014] An artificial bee colony algorithm for image contrast enhancement. *Swarm and Evolutionary Computation*, 16: 69–84.
- [10] Gorai A, Ghosh A. [2009] Gray-level image enhancement by particle swarm optimization. In *Nature & Biologically Inspired Computing, 2009. NaBIC 2009. World Congress on* (pp. 72–77). *IEEE*.
- [11] Yaghoobi S, Hemayat S, Mojallali H. [2015] Image gray-level enhancement using Black Hole algorithm. In *Pattern Recognition and Image Analysis (IPRIA), 2015 2nd International Conference on*, 1–5 *IEEE*
- [12] Murali K, Jayabarathi T. [2013] Automated Image enhancement using Evolutionary Algorithms, *Proceedings of Seventh International Conference on Science Engineering and Technology*, 7b., VIT University.
- [13] Mirjalili S, Mirjalili SM, Lewis A. [2014]. Grey wolf optimizer. *Advances in Engineering Software*, 69: 46–61.
- [14] Wong LI, Sulaiman MH, Mohamed MR, Hong MS. [2014] Grey Wolf Optimizer for solving economic dispatch problems. In *Power and Energy (PECon), 2014 IEEE International Conference on* (pp. 150–154). *IEEE*.
- [15] Song HM, Sulaiman MH, Mohamed MR. [2014] An application of grey wolf optimizer for solving combined economic emission dispatch problems. *International Review on Modelling and Simulations (IREMOS)*, 7(5): 838–844.
- [16] Mirjalili S. [2015] How effective is the Grey Wolf optimizer in training multi-layer perceptrons. *Applied Intelligence*, 43(1):150–161.
- [17] Eberhart RC, Kennedy J. [1995] A new optimizer using particle swarm theory. In *Proceedings of the sixth international symposium on micro machine and human science* 1: 39–43
- [18] Dzung PQ, Tien, NT Tuyen, ND, Lee HH. [2015] Selective harmonic elimination for cascaded multilevel inverters using Grey Wolf Optimizer algorithm. In *Power Electronics and ECCE Asia (ICPE-ECCE Asia), 2015 9th International Conference on* (pp. 2776–2781). *IEEE*.
- [19] Alaa and Amal Abdel-Raouf. [2016] Estimating the Parameters of Software Reliability Growth Models Using the Grey Wolf Optimization Algorithm, *International Journal of Advanced Computer Science and Applications*.

ANONYMISING THE SPARSE DATASET: A NEW PRIVACY PRESERVATION APPROACH WHILE PREDICTING DISEASES

V. Shyamala Susan* and T. Christopher

PG and Research Department of Computer Science, Government Arts College, Udumalpet, Tamil Nadu, INDIA

ABSTRACT

Data mining techniques analyze the medical dataset with the intention of enhancing patient's health and privacy. Most of the existing techniques are properly suited for low dimensional medical dataset. The proposed methodology designs a model for the representation of sparse high dimensional medical dataset with the attitude of protecting the patient's privacy from an adversary and additionally to predict the disease's threat degree. In a sparse data set many non-zero values are randomly spread in the entire data space. Hence, the challenge is to cluster the correlated patient's record to predict the risk degree of the disease earlier than they occur in patients and to keep privacy. The first phase converts the sparse dataset right into a band matrix through the Genetic algorithm along with Cuckoo Search (GCS). This groups the correlated patient's record together and arranges them close to the diagonal. The next segment dissociates the patient's disease, which is a sensitive value (SA) with the parameters that determine the disease normally Quasi Identifier (QI). Finally, density based clustering technique is used over the underlying data to create anonymized groups to maintain privacy and to predict the risk level of disease. Empirical assessments on actual health care data corresponding to V.A. Medical Centre heart disease dataset reveal the efficiency of this model pertaining to information loss, utility and privacy.

Received on: 19th-May-2016

Revised on: 21st -June-2016

Accepted on: 29th - June-2016

Published on: 29th - June-2016

KEY WORDS

Privacy Preservation, Clustering, sparse high dimensional dataset, band matrix, health care data, anatomisation, Genetic Algorithm (GA) and Cuckoo Search Algorithm (CSA).

*Corresponding author: Email: shyamalasusan@gmail.com, Tel: +91-9916913776

INTRODUCTION

In the recent days, data mining techniques play a primary role within the healthcare domain [1] and medical industry, with the aim of improving the health and preserving the patient's privacy. Heart disorder is among the predominant causes of mortalities in several countries, inclusive of India. So there is a need for medical practitioners to predict heart disease earlier than they occur in patients. At the same, time anonymizing the heart disease data set is a task with a large undertaking given that of unstructured or semi-structured datasets. For instance, within the case of relational data (e.g., gender, age, BMI), records consists of only one value for every attribute. On the contrary, set-valued data (e.g., diagnostic codes and lab tests) have one or more values (cells) for every attribute.

Many data mining techniques such as naïve bayes algorithm, bagging algorithm, the neural network algorithm, decision tree, kernel density, k-mean clustering, etc were used for diagnosing of heart disease [2-4]. Anonymisation is managed through various techniques such as k-anonymity [5], l-diversity [6] and t-closeness [7]. T-closeness is the upgraded variant of k- anonymity and l- diversity qualities. These methods anonymise the dataset by generalization and attribute suppression, but the end result is the data loss. In the recent works, permutation technique stick to a procedure of Anatomy [8] where it groups the distinctive sensitive data from a transaction, and later permute them to dissociate the relationship. However, this method failed to provide its significance for high dimensional data.

The objective of this research attempts to be equipped to predict the probability of getting affected with heart disease with the given sparse patient dataset and to preserve the patient's disease from an adversary.

BACKGROUND STUDY

Health information systems have largely helped to increase the possibility of constructing the medical documents available to researchers, public health organizations, and the others who hold interest in medical data. However, health care data generally includes a large amount of patient privacy. Sharing this kind of data directly will be a great threat in the case of patient privacy. Hence it becomes a necessity for practical techniques to be developed

for balancing the healthcare data sharing and privacy preservation. In recent times, the relevance concerned with Privacy-Preserving Data Mining (PPDM) methods is analyzed thoroughly and studied by Mat win [9]. Usage of certain techniques showed their capability of avoiding the discriminatory utilization of data mining. Few techniques provided a proposal that any stigmatized group must not be focused over a number of generalization of data compared over the common population.

Recently, K Anonymization technique additionally utilized for ensuring the assurance of patient information [7] [9][10]. Once the security of protection is pertinent, the information is readied for investigation and the learning which helps choice making is extricated. It is confused, misfortune in utility of data [7] [9]. Zhu and Peng [11] initially depicted obviously the present state of China Restorative informatization level and clarified the need of cross-authoritative data sharing. [10] The specific issue known as connecting assault is additionally considered. The K-anonymity is then again integrated with data mining technique for protecting the identity disclosure of the. Once the protection of privacy is applicable, the data is prepared for analysis and the knowledge which assists decision making is extracted. It is complicated, and there is loss in utility of data. Zhu and Peng [11] first described clearly the current condition of China Medical informatization level and explained the need of cross-organizational information sharing. The particular problem known as linking attack is also studied. Then a respective K Anonymization model is formulated along with Suppression techniques which are utilized for preserving privacy.

Machanavajjhala et al [6] proposed l-diversity which, not like k-anonymity, had the knowledge of the distribution of values pertaining to the sensitive attributes and regarding the impacts of background knowledge. l-diversity, a framework which provides stronger privacy assurance is employed to Inpatient Micro data that is gathered from adult dataset samples. They help in protecting the privacy of the user, either by making changes to quasi identifier values or through the addition of noise. The identity of patients has to be protected while the patient data are shared.

Gal et al [12] introduced a privacy model which is an upgraded version of K anonymity and l-diversity along with multiple sensitive attributes. Here the patient data set is got from the Kentucky Cancer Registry. But this model finds difficulty in distinguishing QIs and SAs.

T-closeness which is the upgraded variant of k- anonymity that is introduced by Soria-Comas et al [13] is highly correlated with ϵ - differential privacy. This approach is useful in improving the quality of anonymity and minimization of the loss of information for Patient Discharge Data.

Soria-Comas et al [14] introduced new kind of refinements with respect to k-anonymity, in which t-closeness performs better as the one providing with the guarantees of strictest privacy. It depends on generalization and suppression and the benefits of micro aggregation are examined, and then multiple micro aggregation algorithms for the purpose of k-anonymous t-closeness are proposed and later evaluated empirically.

Loukides and Gkoulalas-divanis [15] presented a new mechanism for anonymizing the data by meeting the data publishers' utilization requirements with a low information loss experience. A measurement of accurate information loss and an efficient anonymization algorithm are brought into use for minimizing the information losses. Experimental investigations related to on click-stream and medical data exposed that the new technique permitted more robust query answers rather than the state sophisticated techniques that are equal to them in terms of efficiency. The need for privacy is imposed by implementing a partition in the patient record dataset **PR** into sets patient records which are disjoint that are called as anonymized groups. The probability of the association of any kind of transaction in G with that item amounts to half [16].

CBA[17] presented an efficient technique to preserve privacy with minimal information loss by modifying prognosis codes and measured the data loss due to generalization and suppression and anonymise the patient's identity thro Clustering-established Anonymizer (CBA).However this clustering approach is not suitable for high dimensional data and suffers from high information loss and fails to protect against l-diversity. Biomedical researchers anonymise the data with improved utility, but it doesn't help in high dimensionality problem. In DRC[18] approach, utility metrics were particular to the data recipient's requirements. Utility loss is observed to increase with the variation in the data recipient's requirement.

The problem that exists with the available methods is that a big portion of the initial terms are typically absent from the anonymized dataset and every other method is applicable to low dimensional dataset samples. In Anatomy [10], the quasi identifiers are isolated from sensitive values and are provided protection against attribute disclosure. As it generates and issues the quasi identifiers directly it also renders a compromise over data utility.

Protection of privacy employing disassociation is observed as a complex issue in [10]. There are only less works [18-19] which aid in preserving the original data, without the addition of noise, on the basis of an anatomy [10] idea.

PROBLEM SPECIFICATION

The proposed approach designs a model for the case of representation of sparse high dimensional medical data with a perspective of shielding the patient's privacy and in addition to aid the sufferers in having skills over the sickness's threat degree. The heart disease dataset comprises less number of SA that determines the risk stage of heart disease as well as QI values which are the parameters that identify the disease. As the dataset are arbitrarily distributed over the complete area, the task lies in efficiently grouping patients' records with similar QI values collectively to predict the hazard stage and anonymising the patient record with the disease to preserve privacy that has no sensitive value. The distinct contribution of this work is given beneath:

The first segment minimises the bandwidth of the sparse patient report by Genetic algorithm with Cuckoo Search (GCS). This permutes the and thus yields the adjacent rows correlated and brings them near to the diagonal. As it gets hold of the correlation well, it maximizes the utility and reduces the search space. When the patients' records are regrouped as a band matrix, the subsequent step is the construction of anonymised group of the patient with a view to guard the privacy and to predict the sickness. Anatomisation method is used over the regrouped band with the intention to dissociate the QI values with SA. This results in two tables which are the QIT and ST. Then the density based clustering algorithm anonymises the Sensitive attributes in ST with QI values in QIT through the clustering the closest non-sensitive QI values with SA. This helps in protecting the privacy and each group predict the risk level of the patient. Empirical assessments on original health care data corresponding to V.A. Medical Centre heart disease dataset illustrate the efficiency of this model corresponding to information loss, utility and privacy.

Case study

The V.A. Medical Centre database is the well-known heart disease data set extensively used by ML researchers for dealing with heart diseases. This database comprises of 76 attributes; nonetheless all the experiments that are published refer about making use of a subset of 14 among them.

The **Table- 1** below is the sample test report of the patients used by the medical practitioner for determining the measure of heart disease earlier than they occur in patients. Every one of these attributes can be grouped into three kinds:

1. Identifier attributes: a minimal set of attribute which can make the explicit identification of individual records.
2. Sensitive Attributes (SA): The sensitive attribute are regarded to be a privacy breach in case related to a specified individual, and are provided in the right of the Table.
3. Quasi Identifiers (QI) attributes: The remaining of the attributes that are non-sensitive, are utilized for determining the level of heart disease and can also is utilized by an adversary for re-identifying individual patient record.

These Experiments has been carried out with the V.A. Medical Centre database on determining the probability related to the existence of values 1 and 2, for the case of the non-sensitive classes. In this work, only 14 attributes are considered by the ML researchers that are given below

Age, sex, type of chest pain (Cpt), blood pressure at rest (Rbp), serum Scestoral (Sc), blood sugar at fasting (Fbs), electrographic at rest (Recg), maximum heart rate (Thalach), ST depression made by exercise corresponding to rest (Old peak), exercise induced angina (Exang), slope of the peak exercise ST (Slope), number of major vessels (Ca), blood disorder (Thal), the predicted attribute (Class).

Eight patients' treatment history records are considered for evaluation as depicted in **Table- 2** and **Table- 3** indicates the ranges for diagnosing the diseases. In **Table- 2** only two patients' disease (P1 and P8) are diagnosed. Now the challenge is to predict heart risk level for the other patients and at the same time to preserve privacy of the patient (P1 and P8) by anonymising the table.

The initial phase removes the attributes Recg, Exang and slope as they have no values in **Table-1**. **Table- 4** is replaced with "1" on the basis of the range specified in **Table- 3** and 0 if not in the range or else it is left blank

Table: 1. Samples of Sparse heart disease dataset

Age	Sex	Cpt	Rbp	Sc	Fzs	Recg	Thalah	Exang	Oldpeak	Slope	Ca	Thal	Claas
66	1	1					120	0					
67			160	226	0				2.5			3.5	
67			175	290	0		129						
47		2	130		0		172		1.4	1	0	3	
56	1	2		236	0	0	178		0.8		0	3	
57	0				3						0		
63	1		130		0		147		1.4		1	7	2
44	1	2		289									
52	1		120						1.9			8	
57	1					2					2		
54	1		143		3				1.7			3	1

Table: 2. Eight patients' Samples of heart disease dataset

Patient id	Quasi Identifiers (QI)								Sensitive Attributes
	Cp	trestbps	chol	fbf	Thalach	oldpeak	ca	thal	
P1	1				120				2
P2		160	226	0		2.5		3.5	
P3		175	290	0	129				
P4				3			0		
P5	2		289						
P6		120				1.9		8	
P7				2			2		
P8		143		3		1.7		3	1

Table: 3. Attributes ranges of V.A.Medical Centre heart disease dataset

Attributes	Class one-severe	Second class-moderate
Cpt	2	1
Rbp	140-160	160-180
Sc	200-230	230-290
Fbs	0-2	2-4
Thalach	130-155	110-130
Old peak	2.5-3	1-2
Ca	1	2
thal	8	3

Then the patient's record is reorganized as a band matrix by employing GCS approach on the basis of their correlation which is depicted in **Table- 5**. The subsequent step improves the quality of anonymisation by employing disassociation is carried out that outputs two Tables namely QIT and ST which discloses privacy. QIT indicates the patient history of records and ST refers to the patient's level of heart disease. This is provided in Table 6.

Table: 4. Converted sparse heart disease dataset

Patient id	QI								SA
	Cpt	Rbp	Sc	Fbs	Thalach	Old peak	Ca	thal	
P1	1	0	0	0	1	0	0	0	2
P2	0	1	1	0	0	1	0	1	
P3	0	1	1	0	1	0	0	0	
P4	0	0	0	1	0	0	1	0	
P5	1	0	1	0	0	0	0	0	
P6	0	1	0	0	0	1	0	1	
P7	0	0	0	1	0	0	1	0	
P8	0	1	0	1	0	1	0	1	1

Table: 5. Final Reorganized Table

Patient id	QI								SA
	ca	fbs	thal	oldpeak	Trestbps	chol	thalach	Cp	
P7	1	1	0	0	0	0	0	0	
P4	1	1	0	0	0	0	0	0	
P8	0	1	1	1	1	0	0	0	1
P6	0	0	1	1	1	0	0	0	
P2	0	0	1	1	1	1	0	0	
P3	0	0	0	0	1	1	1	0	
P5	0	0	0	0	0	1	0	1	
P1	0	0	0	0	0	0	1	1	2

Table: 6. Final Published groups

Patient id	QIT									ST
	ca	fbs	thal	oldpeak	trestbps	chol	thalach	Cp		
P7	1	1	0	0	0	0	0	0		
P4	1	1	0	0	0	0	0	0		
P8	0	1	1	1	1	0	0	0		1
P6	0	0	1	1	1	0	0	0		
P2	0	0	1	1	1	1	0	0		
P3	0	0	0	0	1	1	1	0		
P5	0	0	0	0	0	1	0	1		
P1	0	0	0	0	0	0	1	1		2

Then Modified Density Based Clustering (MDBSCAN) is performed over QIT and ST in Table 6 which again gives the anonymised Table as result by splitting the medical records into two clusters as illustrated in Table- 7 and Table- 8. This protects the privacy in such way that P7, P4, P6, P3, P1 patients' are groups as one cluster and P2, P5, P8 in other. In a similar manner, the diseases are predicted in such a manner that p7, p4, p6, p2 are more susceptible to type 2 and p2 p5 may be vulnerable to type 1 and the patients are advised to meet the clinicians before the disease becomes worsened. The GCS approach with clustering approach proved its efficiency in terms of utility, information loss and execution time.

Table: 7. Anonymised patient record

Patient id	QI								SA
	Ca	Fbs	thal	Old peak	Rbp	Sc	Thalach	Cpt	
P7	1	1	0	0	0	0	0	0	2
P4	1	1	0	0	0	0	0	0	
P6	0	0	1	1	1	0	0	0	
P3	0	0	0	0	1	1	1	0	
P1	0	0	0	0	0	0	1	1	

Table: 8. Anonymised patient record

Patient id	QI								SA
	Ca	Fbs	thal	Old peak	Rbp	Sc	Thalach	Cpt	
P8	0	1	1	1	1	0	0	0	1
P2	0	0	1	1	1	1	0	0	
P5	0	0	0	0	0	1	0	1	

PRELIMINARIES

Notation and description

The goal of the paper is the anonymization of the V.A.Medical Centre heart disease data which comprises of a set of patient records $PRD = (P_1, \dots, P_n)$, $n = |T|$, Each patient record $P \in PRD$ contains attributes that are received from an attribute set $A = (a_1, \dots, a_d)$ $d = |A|$. The data is specified as a binary matrix A with n number of rows and d number of columns. For example Table- 1 has 16 patient records with 14 attributes which is discussed elaborately again in the section that follows.

$$A[i][j] = \begin{cases} 1 & a_j \in P_i \\ 0 & a_j \notin P_i \end{cases} \tag{1}$$

For instance, the matrix for heart disease data shown in table 4 is expressed as

$$A[8][8] = \begin{pmatrix} 1 & 0 & 0 & 0 & 1 & 0 & 0 & 0 \\ 0 & 1 & 1 & 0 & 0 & 1 & 0 & 1 \\ 0 & 1 & 1 & 0 & 1 & 0 & 0 & 0 \\ 0 & 0 & 0 & 1 & 0 & 0 & 1 & 0 \\ 1 & 0 & 1 & 0 & 0 & 0 & 0 & 0 \\ 0 & 1 & 0 & 0 & 0 & 1 & 0 & 1 \\ 0 & 0 & 0 & 1 & 0 & 0 & 1 & 0 \\ 0 & 1 & 0 & 1 & 0 & 1 & 0 & 1 \end{pmatrix} \tag{2}$$

In the set of attributes $A[i][j]$ for the patient records $PR = (P_1, \dots, P_n)$, some are sensitive to privacy, such as the heart disease is severe or medium condition seen in running example [Table -1].

Definition 1 (Sensitive Attributes (SA)): The set $SA \in A$ having the attributes denoting a privacy threat if they are associated with certain patient records, renders the sensitive attributes, $S = \{sa_1, \dots, sa_m\}$ $m = |S|$. The rest of the attributes in the table indicated as Quasi Identifiers (QIs) are insensitive, which means that their association with a specific individual is not dangerous. In contrast, these items that are harmless can be used by an adversary for re-identification of individual patient records, as shown in the introductory section. These items are specified by QID attributes.

Definition 2 (Quasi Identifier (QI) attributes): The collection of attributes in A that an attacker can get knowledge about, for re-identifying separate patient records comprise the set of QIs. Typically, any attribute that is non-sensitive is QIs, therefore $QI = A \setminus SA$, $QI = (qi_1, qi_2, \dots, qi_m)$. The records constituting of attributes from SA

are represented as Sensitive Attributes (SA), again the one having just the attributes from QI are regarded as non-sensitive.

Definition 3 (Privacy): A transformation that is privacy-preserving of patient set PR is said to contain privacy degree p if the probability corresponding to the association of any patient records $pr \in PR$ with a particular sensitive item $sa \in SA$ does not exceed $1/p$. This is same as thinking that the respective patients records of a patient data can have correlation to a specific sensitive item having probability at the most $1/p$ within $p - 1$ other patient records. It has to be noticed that, the having an association of an individual patient data with an item in QI could not be considered as a privacy breach. A

Permutation-based technique is used same as [10], for achieving privacy preservation.

The need for privacy is imposed by implementing a partition in the patient record dataset PR into sets patient records which are disjoint that are Called as anonymized groups. For each group G, the exact QI attributes of the patient records are exposed, in addition to a summary corresponding to the frequencies of sensitive items which are in G. The probability of the association of any kind of transaction in G with that item amounts to half [16]. In general, let $f_1^G \dots f_m^G$ represent the number of occurrences with respect to the sensitive items $sa_1 \dots sa_m$ seen in group G. Hence group G gives the privacy degree,

$$p^G = \min_i |G|/f_i \quad (3)$$

The privacy degree with respect to a whole partitioning \mathcal{P} of PR is expressed by

$$p^{\mathcal{P}} = \min_G p^G$$

PROPOSED METHODOLOGY

Data Reorganization By Genetic With Cuckoo Search Algorithm

The V.A.Medical Centre heart disease data set that is used in this work involves sparse patient record. As the heart diseases data is less dense, it is randomly spread in the overall set. In the first phase, the sparse patient set is represented as a matrix format for the arrangement of band matrix. The Band matrix organization has been accepted as an advantageous mode to denote the sparse data in different scientific applications [20].

For the matrix A, a graph $G = (V, E)$ is constructed where V has one vertex for every patient record there exists an edge from vertex v_i to vertex v_j for the entire non-zero elements. If matrix A is symmetric, and then G can be inferred to be undirected. GCS algorithm is based on the observation that indicates that a permutation pertaining to the patient records of the matrix is linked with a vertices re-labeling for G. For the transformation of heart diseases data matrix is required to reduce the distance 'b' between non-zero elements by doing a permutation of the rows and columns from the diagonal.

Reverse Cut hill-McKee Algorithm best deals with the symmetric matrices for the purpose of bandwidth reduction. This method is usually inexpensive, even though the result got may not have good quality, specifically if the original matrix is far from symmetric. Computing $[A \times A]^T$ is an additional computational overhead; although the quality corresponding to the solution is far better (i.e. the resultant bandwidth is very much lesser). For the purpose of providing a solution to this issue, GCS is presented for the reduction of band matrix for both the case of symmetric and unsymmetric matrices.

To minimize the band width of the matrix A, GCS traversal begins from an initially selected patient records as root node. Each patient record lying at the same distance from the root inside the traversal path constitutes a level set. Each node in the traversal is considered as chromosomes. Nonetheless, the genetic algorithm can get easily slipped off in local optima. With a purpose to remedy this, a Cuckoo Search Algorithm (CSA) [21] is employed for searching for the nearby identical distance patient records from the initial patient records matrix 'A' which is generated by GA. The cuckoo bird lays one egg at a point of time and after which leaves this egg in any randomly chosen nest. The number of available nearest distance value corresponding to the patient records is pre-determined, and the probability $Pa(0,1)$ is computed. Here, in this case the current patient records are selected as same and the rest of the rows are permuted in case it gives zero elements. The best nest patient records along

with the diagonal element (eggs) will be carried over to the next n generation when it is a good one or if it is stopped.

For the global optimal finding of the non-zero elements to patient records distance value is computed and rearrangement is also carried out between records exploiting genetic operations such as Multipoint crossover, and K swap mutation.

The Multipoint Crossover operator is employed for the initial band matrix solution hoping to generate a new better band matrix solution population by the interchange of many cross sections that are either odd or even.

K swap mutation operator is then applied over a parent patient records chromosome by randomly choosing 2 labels and then swapping them. Then swap operation is carried out k times.

The entire process is continued iteratively till no improvement is seen. At each step, the vertices that are in the same level which share the same parent (attributes such as $asca$, Sc etc.,) are ordered in an increasing sequence on the basis of the vertex degree. By reversing the order obtained, the permutation that needs to be applied over the patients of matrix A is used.

Genetic Cuckoo Search (GCS)

```

Encode population of heart disease data points as chromosomes
Set population size, chromosome, max-gen, gen=0
Generate
Initial a population of  $n$  host
nests by randomly picking
samples ( $A_i$ ,  $i=1,2,3,\dots,n$ );
In each patient records population fitness value( $FT$ ) is evaluated;
While (gen < max-gen)
If ( $FT_i < FT_j$ )
  Replace row  $j$  by new patient record
End
Perform genetic operations
Get number of cuckoos randomly by Levy flights
Choose a nest as patient records among  $n$  randomly
Host birds abandon
 $P_a$  in  $(0,1)$ nests, and search  $P_a$  with non-zero elements
Select fitness( $FT$ ) with high  $P_a$ 
perform permutation
  Bandwidth reduced matrix  $B$ 
  Gen=gen+1
End while
  
```

Anonymization method

When the data in the sparse patient records is reorganized the subsequent step is the creation of anonymized groups. Within the first part, the relationship dissociation between QI and SA is finished and produced as two new Tables that might be the QIT and SAT that is involved in disclosing the privacy. The next phase is the anonymisation mechanism [22] in which the non-sensitive attributes gets organized with different sensitive attributes for the preservation of privacy in such a way that the degree of privacy is way much below $1/p$ in every one of the grouping.

Modified Density Based Clustering Method (MDBSCAN) [23] is employed to the anatomised QIT and ST for performing the anonymisation. The DBSCAN clustering approach has the dilemma of border objects. The border features often don't take into account foremost QIT and ST data points. So here MDBSCAN is offered which normally considers the core QIT and ST data points while clustering. At first, a group is created for every distinct touchy attributes by way of on the grounds that a collection of facets (P) within the ST . This sensitive values' QI is then mapped to the identical team and eliminated from the QIT . A point P is considered as a core point if it comprises at the least $minPts$ facets that consists three or 4 quasi identifiers in distance ϵ (degree of privateness) of it, and additionally, these facets can also be reached directly from $p..$ Now the rest of the QI values in the QIT

Table are mapped to the group on the basis of the distance ϵ along with the sensitive attributes QI value. This procedure goes on till all the QI values are mapped onto the group.

Each group helps in assisting the patient by identifying the risk level of the disease. With the objective of preservation of privacy, each QIT with none of the sensitive value has to be grouped with sensitive transactions in such a way that the privacy degree is below $1/p$ in each one of the group.

MDBSCAN needs two parameters: ϵ and the minPts required in order to create a dense region. It begins with random sensitive attributes (unclassified) that has not been come across to be visited. This sensitive attributes ϵ -neighborhood is then regained to each QI, and in case it has adequately several points, a cluster is created. Else, the QI point is then labeled as outliers to SAT. This process is carried on till all the QI values are mapped onto the group. During the last step of the MDBSCAN, each core object is now allocated to its best density-reachable chain when all density-reachable chains that reach to the core object are known. Just in case any one of the clusters contains only one single QIT, the clusters are merged employing a linkage or amalgamation rule which determines when the 2 clusters are similar enough to be connected together.

Anonymization (Band matrix B)

Perform disassociation using anatomy
 Release new two namely QIT and SAT

Clustering
 (set of patients records (PESAT) , Eps, MinPts ,i \in QIT)

```

ClusterId := nextclusterId(outlier);
For(i=1;i<n; i++) DO
  Point := P.get(i);
  If Point. CIId = UNCLASSIFIED then
    If Expand Cluster(P, ClusterId, Eps, MinPts) then
      ClusterId := nextclusterId(ClusterId)
    End If
  End If
End For
End; // MDBSCAN
For x_border in the border list
  result.size(x_border)=Retrieve Neighbours(x_border,Eps)
  Assign x_border to CIId
End for
End
  
```

The entire patient record is represented as SetOfPoints.The global density parameters that are determined manually are represented as Eps and MinPts. The function P.get(i) returns the i-th element of QIT. Given below ExpandCluster is the important function utilized by MDBSCAN .

```

Expand Cluster(set of patients records(P) CIId, Eps, MinPts) : Boolean;
seeds:=P.regionQuery(P,Eps);
If seeds. size<MinPts then // no core point
Else // all patient records in seeds are density- reachable from Point
P.changeCIIds(seeds,CIId);
seeds. Delete(P);
While seeds <> Empty Do
current P := seeds. first();
result := P.regionQuery(current P, Eps);
If result.size>= MinPts then
P.changeCIId(P,NOISE);
Return False;
Add all UNCLASSIFIED then seeds. Append(result P);
Label UNCLASSIFIED and NOISE as BORDER DATAPOINTS
End If; // If result.size>= MinPts then
End While; // seeds <> Empty RETURN True;
End If ;//If seeds. size<MinPts then
  
```

End; // Expand Cluster

EXPERIMENTALEVALUATION

The heart disease dataset that is available at <ftp://ftp.ics.uci.edu/pub/machine-learning-databases/heart-disease/processed.va.data> is used to evaluate the GCS technique with MDBSCAN. The data set contains 76 raw attributes. However, the most published experiments best has reference to 14 of them with classification.

The data set comprises of 200 rows. The efficiency of this methodology is checked with respect to utility and effectiveness and proved that this method performs better than the existing techniques like Clustering-Based Anonymizer (CBA) [17], Data Recipient Centered (DRC) [18] approach.

Utility: The anonymized data set Utility is measures by calculating the distance present between the original and estimated pdf over all cells. It is measured by KL-divergence [24] as a metric which provides meaning for the evaluation of the amount of data loss endured by data anonymization.

$$KL_Divergence(Act,Est) = \sum_{(C)} (\forall cell C) \left[(Act_C^S \log_{\frac{Act_C^S}{Est_C^S}} \left[\frac{Act_C^S}{Est_C^S} \right]) \right] \quad (5)$$

The actual pdf value of Sensitive Attribute (SA) for a cell C is expressed by

$$Act_C^S = (\text{Occurrences of } S \text{ in } C) / (\text{Occurrences of } S \text{ in } PR) \quad (6)$$

The estimated pdf Est_C^S is Calculated in a similar way, excepting that the numerator consists of equ(5) that is summed over all groups intersecting cell C

$$a \cdot b / |G| \quad (7)$$

The number of occurrences of the item s in G is represented by a, and the number of transactions that match the QIT selection predicate (last line of (5)) are denoted by b. For each (p, r) setting, 100 group-by queries gets generated by means of the random choice of SA and q1 . . . qir from this the average reconstruction error is computed. The reconstruction error is measured with the following query.

```
SELECT COUNT (*) FROM T WHERE (Sensitive Item sa is present) AND (q1l = val1) ^ . . . ^ (qir= valr)
```

The reconstruction error is measured by changing the p the degree of privacy, m is the number of sensitive item that is arbitrarily selected, and r is the number of QI values that varies. More than 100 group-by queries are created by arbitrarily choosing q1,q2,q3...qnand s1,s2,s3.....sm. The average reconstruction error is determined and the clustering accuracy is measured. The experimental result is illustrated in the **Figure- 1**.The clustering algorithm preserves correlations in a better manner between the patient records for better utility.

Figure-2 illustrates the execution time of CBA, DRC and MDBSCAN for p = 20, that is the most important factor possessing influencing on runtime performance. MDBSCAN is time-effective, with completion time ranging at most 16 sec for the heart disease dataset. A more considerable overhead is suffered by GCS execution, which needs 185 sec for the heart disease dataset. Nevertheless, this overhead is only observed for the input transformation only once, regardless of p values. However the execution time corresponding to the new MDBSCAN with GCS is less compared with the other clustering methods. Since the MDBSCAN that has high dimension problem is solved by using of GCS.DRC only has the capability of dealing with execution times that are in in the range of 300 sec for the heart disease dataset.

The efficiency of QI is evaluated in terms of clustering accuracy. For this p=10 is fixed upon and the number of QI is varied in {2,4,6,8}. **Figure-3** illustrated the results on learning a QI attribute. It can be observed that clustering accuracy reduces only with a slight increase of QI, as the most correlated attributes are yet in the same column. In every case, MDBSCAN with GCS is seen with better clustering accuracy in comparison with other clustering techniques.

Figure-4 indicates the utility loss vs. privacy loss with regard to various privacy requirements (p=10 and p=20). The results that are affected in terms of privacy and utility are measured. If one selects a different measure for privacy (or utility), then the figure may appear in a different way. From the figure, GCS outperforms compared to other privacy requirements. The results indicates that GCS yields considerable better data utility rather than RCM and RCM with greedy (RCMG), as in the GCS method unsymmetric band matrix reconstruction is also taken into consideration.

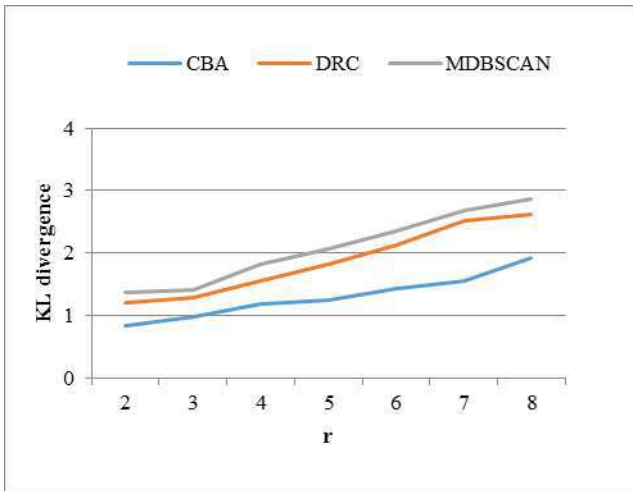


Fig. 1. Reconstruction Error vs r (p = 10)

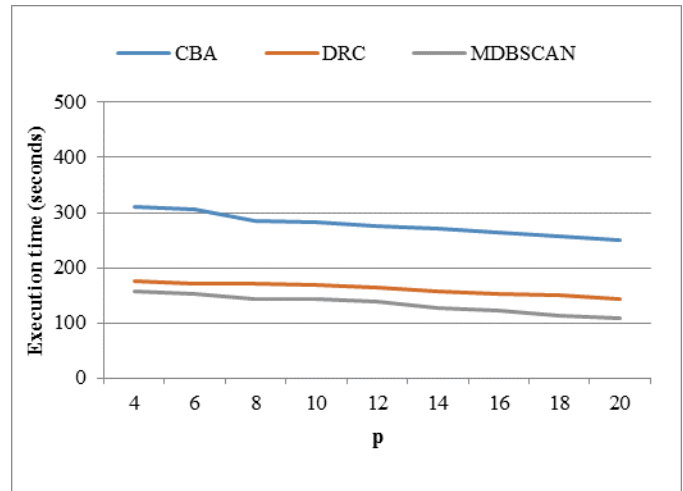


Fig. 2. Execution Time

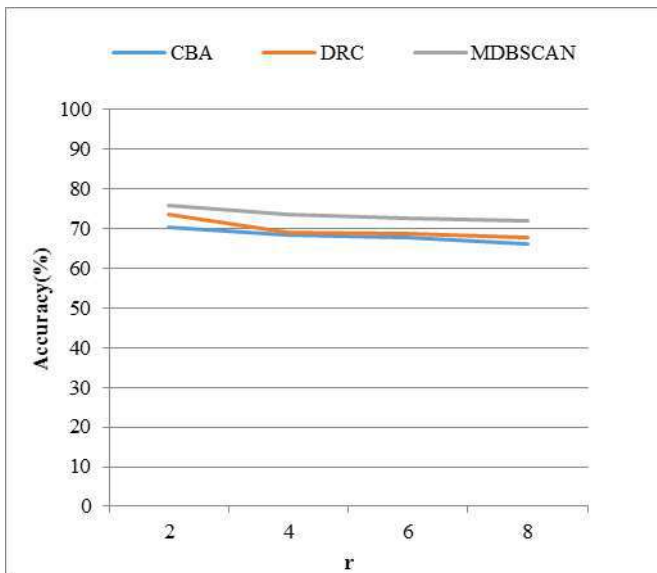


Fig. 3. Clustering accuracy (r=8 ,p=10)

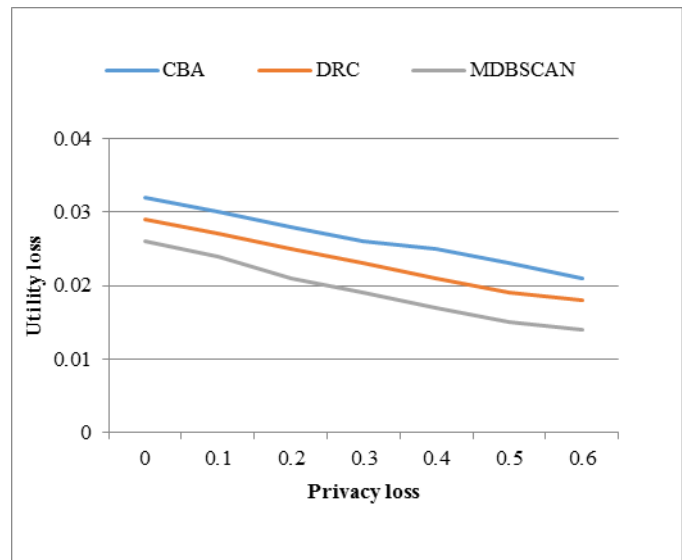


Fig. 4. Privacy-Utility Trade-off by Varied privacy requirements Clustering accuracy (r=8, p=10)

CONCLUSION

The proposed methodology designs a model for the representation of the sparse high dimensional medical dataset obtained from V.A. Medical Centre heart disease dataset with the attitude of protecting the patient's privacy from an adversary and additionally to predict the disease's threat degree. The CGS algorithm converts the sparse high-dimensional heart disease data set as a band matrix that limits the search space and maximizes the utility.

Anatomizations technique reduces the data loss and discloses privacy. The Modified Density Based Clustering (MDBSCAN) Method proved its resourcefulness through the minimization of the time, privacy and complexity in comparison to the available highly performing techniques like CBA,DRC and it also renders a reduction in the computational overhead.

COMPETING INTEREST

The authors hereby declare that they possess no competing interest.

AUTHORS' CONTRIBUTION

The author V.Shyamala Susan conceived the idea and developed the algorithm on the data set. The author Dr.T.Christopher analyzed the result and provided suggestions to modify the algorithm. Both the authors read and approve the final submission.

ACKNOWLEDGEMENT

None

FINANCIAL DISCLOSURE

The work has been supported by the University Grants Commission (UGC)-New Delhi,India and the grant number is MRP-5711/15(SERO/UGC)January 2015.

REFERENCES

- [1] Asghar MH, Mohammadzadeh N, Negi A.[2015] Principle application and vision in Internet of Things (IoT), in Computing, Communication & Automation (ICCCA), 2015 International Conference on.,427–431, 15–16 May.
- [2] Luigi Atzori, Antonio Iera, Giacomo Morabito.[2010]The Internet of Things: A survey, Computer Networks, 54(15): 2787–2805, ISSN 1389–1286.
- [3] Hicks D, Mannix K, Bowles HM, Gao BJ.[2015] SmartMart: IoT-based In-store mapping for mobile devices, in Collaborative Computing: Networking, Applications and Worksharing (Collaboratecom), 616-621, 20-23 Oct. 2013.
- [4] Al Nuaimi, K Kamel, H. [2011]A survey of indoor positioning systems and algorithms, in Innovations in Information Technology (IIT), 2011 International Conference on185–190, 25–27 April
- [5] Pereira PP, Jens E, Rummen K, Jerker D, Asma R, Mia J.[2013] Enabling cloud connectivity for mobile internet of things applications. In: Proceeding of the IEEE 7th international symposium on service oriented system engineering (SOSE), pp 518–526.
- [6] Asghar MH, Mohammadzadeh N, Negi A.[2015] Principle application and vision in Internet of Things (IoT), in Computing, Communication & Automation (ICCCA), 2015 International Conference on, 427–431, 15–16 May.
- [7] Hicks D, Mannix K, Bowles HM, Gao BJ.[2015] SmartMart: IoT-based In-store mapping for mobile devices, in 9thInternational Conference onCollaborative Computing: Networking, Applications and Worksharing (Collaboratecom), 616-621, 20-23 Oct. 2013.
- [8] Al Nuaimi, K Kamel H. [2011]A survey of indoor positioning systems and algorithms, in Innovations in Information Technology (IIT), 2011 International Conference on, 185–190, 25–27 April
- [9] Luigi Atzori, Antonio Iera, Giacomo Morabito.[2010]The Internet of Things: A survey, Computer Networks, 54(15) : 2787–2805, ISSN 1389–1286.

ABOUT AUTHORS

V Shyamala Susan, received her post graduate degree in MCA from Coimbatore Institute of Technology, Coimbatore and M.phil degree is earned from M.S University, Tirunelveli. At present, she is working as the Head, Department of Computer Science in A.P.C. Mahalaxmi College for women, Thoothukudi, India. She has published 5 papers in international/national journal s. She has got eleven years of teaching experience and her area of interest is data mining.

Dr. T. Christopher is presently working as Asst Professor, PG and Research department of Computer Science, Government Arts College, Coimbatore. He has published 20 papers in international/national Journals; His area of interest include Data mining, Network security. He has to credit 23 Yearsof teaching and research experience

COMBINING MULTIPLE COLOR AND SHAPE FEATURES FOR IMAGE RETRIEVAL

Mussarat Yasmin¹, Muhammad Sharif¹, Isma Irum¹, Waqar Mehmood¹, Steven Lawrence Fernandes²

¹COMSATS Institute of Information Technology, Department of Computer Science, Wah Cantt, PAKISTAN

²Department of Electronics and Communication Engineering, Sahyadri College of Engineering & Management, Mangalore, Karnataka, INDIA

ABSTRACT

Image retrieval has been getting importance and popularity in the field of information retrieval since the last decades. Systems have been developed to retrieve image on the basis of its contents for indexing, matching, searching and browsing the image databases. In this study, an effective CBIR system has been proposed by defining a shape feature extraction model named symmetry, area, direction angle and arc length features (SADAF) model. SADAF introduces a new shape features model which is generic in nature. In the proposed approach, objects are first located with image segmentation. SADAF model is then applied to extract visual shape contents of the image. After matching, searching and retrieval process, the retrieved results are arranged according to the distance of color from query image to those of retrieved images, calculated through color histogram. Qualitative analysis for proposed technique has been performed with widely accepted quantification measures precision and recall rates. Comparison of the method proposed with other existing descriptors of shape has also been done to prove its supremacy and reliability over the techniques already in literature.

Received on: 7th- Aug- 2016

Revised on: 17th- Aug- 2016

Accepted on: 22nd - Aug-2016

Published on: 31st- Aug-2016

KEY WORDS

Boundary Extraction, CBIR, Feature Extraction, High Level Features, Image Segmentation, Image Information, Low Level Features, Matching, Searching, Shape Descriptor.

*Corresponding author: Email: steven.ec@sahyadri.edu.in

INTRODUCTION

With the growing popularity and advancing technology in image acquisition, electronic archives of image have also increased considerably due to the emergence of devices with high speed processors and cheapest memories. For proper organization of these electronic archives, implementation of database is amongst strongly recommended approaches. Hence Content Based Image Retrieval (CBIR) has remained most popular database image manipulator for the indexation, matching, searching and retrieval of images [1-8].

With the emergence of CBIR, color features have gained greater popularity for image recognition visually but the semantic gap [9] has often resulted in compromised or poor performance of the system. This is due to the fact that color features only recognize the color of image and not its visual contents. This has created a difference between meanings of images. For example, in Figure 1 both images have same colors visually but their meaning is completely different.

To minimize the semantic gap, a state of the art technique has been presented in [10] which uses evolutionary programming to extract shape, texture and color features of image. Color features do not include spatial information of image and hence fail to completely describe the contents of image. But fuzziness can overcome the absence of color features as introduced in Fuzzy Color Histogram (FCH) [11], Self Organization Map (SOM) and Subtractive Fuzzy Clustering [12].

Within the context described above and keeping in view the fact that shape descriptors are more stronger in describing an image semantically in comparison with features of image like color and texture [13], a shape descriptor is required which can fully describe the contents of image i.e., what the image is comprised of. There are many descriptors of shape mentioned in existing literature which are divided as *shape descriptors based on region* and *shape descriptors based on contour*. Information about boundary is only considered in contour based

shape descriptors whereas all image pixels are taken in region based shape descriptors [14]. Fourier descriptor (FD) is contour based shape descriptor and suitable for character recognition application. Fourier transform is applied on complex vector of image boundary to obtain FD [15]. The curvature scale space descriptor (CSS) performs analysis of image boundary as a 1D signal in scale space [16]. Adopted in MPEG-7, the ART is a 2D descriptor which is based on both moment and region [17]. Image moments (IM) are useful in recognition problems and also have the capability of coping with geometric transformations like scaling, translation and rotation as well as general affine transformations [18].



Fig. 1. Semantic Gap

Image segmentation allows combination of same pixels due to their coherent visual characteristics; therefore, it is considered essential for various standard applications as it tends to semantic approach for image analysis [19]. A new shape descriptor has been demonstrated in this paper which follows a newly defined shape features model SADAF in combination with color features calculated through color histograms.

The sections of paper are arranged like this. Proposed work complete description is mentioned under Section 2 whereas Section 3 demonstrates the results along with discussion of proposed approach at length. Section 4 concludes the method described and Section 5 presents the references.

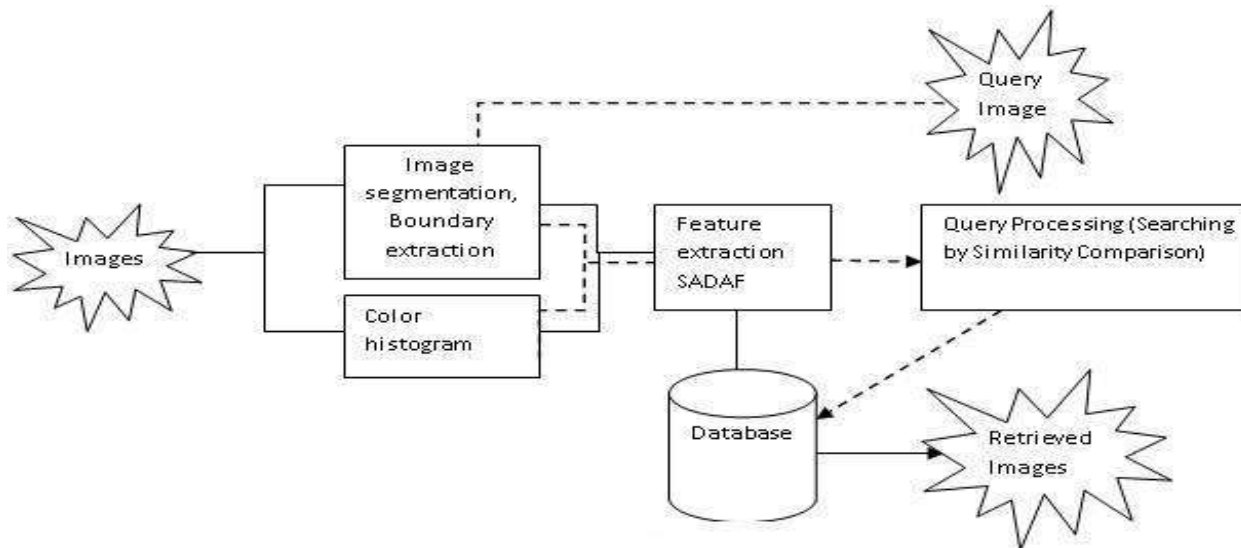


Fig. 2. Architecture of Proposed Method

METHODS

Proposed CBIR System

A new CBIR system has been proposed in this paper based on the idea that similar images contain same features. Figure 2 presents general architecture of the system. First, color histogram is calculated for database population and image segmentation for boundary extraction is then performed. To these boundary images, the new proposed features extraction model SADAF is applied to extract the shape features. Numerical values of these features are saved in database. When query image is presented, the same process is performed for features calculation and distance of features for both images is calculated. As a result, images with less distance are selected as retrieved images and sorted according to distance in color from the query image. This process is further described in the succeeding sections.

Segmentation of Image

Segmentation of image based on edges is adopted for the proposed approach. For this purpose, canny edge descriptor [20] is used because strong edges are needed for boundary extraction and canny edge operator fully detects the strong edges. Figure 3 shows the input and gradient images.



Fig: 3. Input Image is on the Left, Gradient Images on the Right

The operator performs convolution with original image and 3×3 kernels for horizontal and vertical derivatives approximation calculation. The horizontal gradient G_x and vertical gradient G_y can be computed as follows if I be the original image [21].

$$G_x = \begin{bmatrix} -1 & 0 & +1 \\ -2 & 0 & +2 \\ -1 & 0 & +1 \end{bmatrix} * I \quad (1)$$

$$G_y = \begin{bmatrix} -1 & -2 & -1 \\ 0 & 0 & 0 \\ +1 & +2 & +1 \end{bmatrix} * I \quad (2)$$

Here * means the 2-dimensional convolution operation. Towards the right, the x-coordinate increases whereas towards down, the y-coordinate increases. The gradient magnitude can be calculated by combining both gradient approximations as follows:

$$G = \sqrt{|G_x|^2 + |G_y|^2} \quad (3)$$

Boundary Extraction

In this section, boundary of objects contained in the image is extracted by tracing the continuous edges. For this eight connected neighbors, as specified in Figure 4, are used. The image at hand is a binary edge image in which a 0 is a non edge pixel and 1 is an edge pixel. By image scanning from top to bottom and from left to right, we look at its eight connected neighborhood pixels if a pixel is 1 and if a pixel is found to be 1 in the neighborhood then we trace its neighborhood recursively. In this manner, solid and continuous edges are traced out.

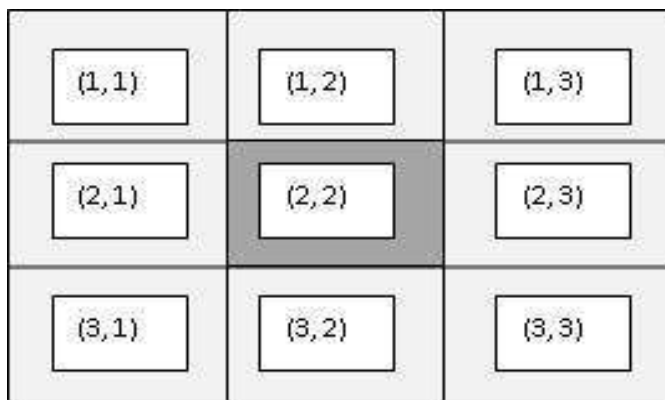


Fig: 4. Eight Connected Neighbors

Features Extraction Model: SADAF

Features extraction has been performed by defining a new features extraction model SADAF in which four features namely symmetry, area, direction angle, and arc length have been specified by treating image as a function $f(x, y)$ in a plane surface. These features are discussed in detail one by one respectively in the following sections.

Symmetry

Following expression defines an image $I(m, n)$ with rows m and columns n as its dimensions in plane surface.

$$I(m, n) = f(x, y) \quad (4)$$

By setting up the central point of extracted boundary image at the origin of plane surface, very useful characteristics of an image are obtained, one of them being Symmetry. Symmetry is a property that specifies the spatial layout of an image i.e., in which quadrant that part of image lies. Figure 5 shows some examples of extracted boundary images in a plane surface.

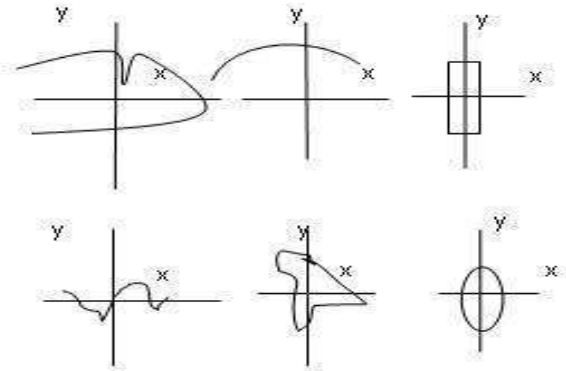


Fig: 5. Examples of Traced Boundaries in the Plane Surface

Symmetry can be defined by the following expressions.

$$f(x, -y) = f(x, y) \tag{5}$$

$$f(-x, y) = f(x, y) \tag{6}$$

$$f(y, x) = f(x, y) \tag{7}$$

$$f(-x, -y) = f(x, y) \tag{8}$$

Expressions 5 to 8 specify that the image is in 1st& 4th, 1st& 2nd, 1st, 1st& 3rd quadrants respectively.

Area

Assuming that $f(x, y) \geq 0$, area under the curve in Figure 6 has to be determined.

Let $x_0, x_1, x_2, \dots, x_{k-1}, x_k$ be a partition of $[m, n]$ such that length of each subinterval $[x_{r-1}, x_r] = \frac{n-m}{k}$.

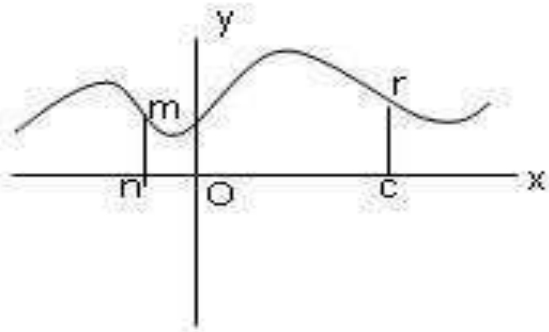


Fig: 6. Area under an Image

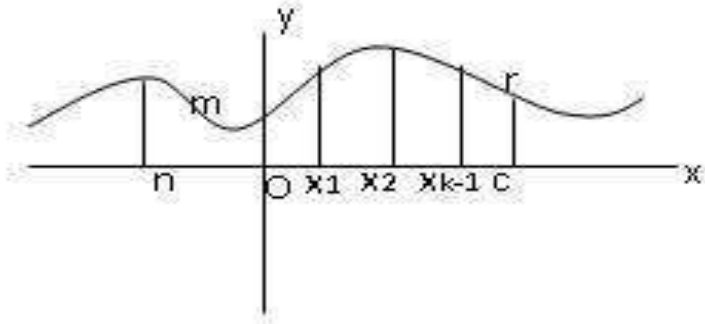


Fig: 7. Partitioning into K Rectangles

Drawing vertical lines from each of the points $x_r, r = 1, 2, 3, \dots, k$ to the graph of $y = f(x, y)$, partitions are made into n smaller areas. Let a_r be any point of $[x_{r-1}, x_r]$. Corresponding to a_r the ordinate of point on $y = f(x, y)$ graph is $f(a_r, b_c)$. On each sub interval $[x_{r-1}, x_r]$ we construct rectangle with the closed interval as its base and $f(a_r, b_c)$ as its height. The rectangle on $[x_{r-1}, x_r]$ is shown in greater detail in Figure 7. Its area is $f(a_r, b_c)$ and sum of all k rectangles = $\sum_{r=1}^k \sum_{c=1}^k f(a_r, b_c) \Delta x = S(p, f)$ (9)

Thus by putting the limit, area of an image $I(m, n) \setminus r \leq m \leq 1, c \leq n \leq 1$ in plane surface is defined by the expression.

$$A = \int_{m=1}^r \int_{n=1}^c f(x, y) dy dx \tag{10}$$

Direction Angle

If different points are taken on the image and vectors are drawn from those points to the origin of graph $y = f(x, y)$, the direction angle can easily be determined. From this the angle of orientation is calculated for any image under consideration as shown in Figure 8.

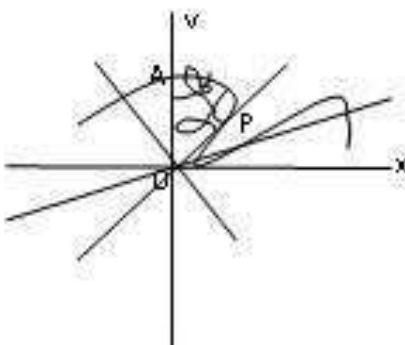


Fig: 8. Computing Direction Angle

Let $v = [x, y]$ be a vector, the direction angles α, β of v are defined as:

$$\alpha = \Theta(v, x) \tag{11}$$

$$\beta = \Theta(v, y) \tag{12}$$

By definition each of these angles lies between 0 and π from the right ΔOAP .

$$\cos \alpha = \frac{x}{OP} = \frac{x}{\sqrt{x^2 + y^2}} \tag{13}$$

$$\cos \beta = \frac{y}{OP} = \frac{y}{\sqrt{x^2 + y^2}} \tag{14}$$

From Eqs.13 and 14:

$$\alpha = \cos^{-1} \left(\frac{x}{\sqrt{x^2 + y^2}} \right) \tag{15}$$

$$\beta = \cos^{-1} \left(\frac{y}{\sqrt{x^2 + y^2}} \right) \tag{16}$$

Arc Length

Let $x_0, x_1, x_2, \dots, x_{n-1}, x_n$ are points such that $a = x_0 < x_1 < x_2, \dots < x_{n-1} < x_n = b$ is a partition of $[a, b]$. Then the arc AB is divided into n smaller arcs by the points

$$P_0(x_0, f(x_0, y_0)), P_1(x_1, f(x_1, y_1)), \\ P_2(x_2, f(x_2, y_2)), \dots, P_{r-1}(x_{r-1}, f(x_{r-1}, y_{c-1})), \\ P_r(x_r, f(x_r, y_c)),$$

By definition rth chord passes from the point P_{r-1} to P_r

$$|P_{r-1}P_r| = \sqrt{(x_r - x_{r-1})^2 + (y_c - y_{c-1})^2 + (f(x_r, y_c) - f(x_{r-1}, y_{c-1}))^2} \tag{17}$$

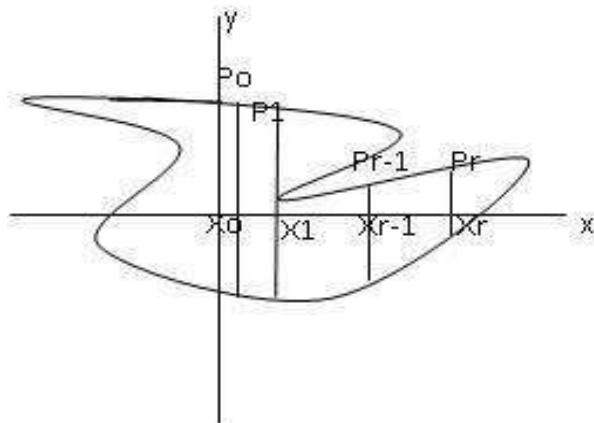


Fig: 9. Computing the Length of Arc

From Figure 9, the total length for image can be calculated by summing up all the lengths as follows:

$$s = \int_{x=1}^r \int_{y=1}^c \sqrt{1 + \left(\frac{dy}{dx}\right)^2 \left(\frac{dx}{dy}\right)^2} dy dx \quad (18)$$

Color Extraction

For color extraction, color histograms are computed and saved in database as color features because of the reason that color histogram is easy to compute and indexed in database. On the basis of above four features, images are selected and presented according to the distance of their histograms from the query image. In this way, sorting of retrieved images is done according to query image color i.e., image nearer to query image in color is presented first and so on.

RESULTS AND DISCUSSION

To provide quantification results, 9 images have been provided as query image one by one from 9 random categories. The database used is COREL database [22, 23] of 10,000 images from which a set of 60 images per category is constructed to form a 540 images testing database.

Belonging to the same category of query image, a retrieved image is considered as relevant.

Table 1 list nine categories from which query images have been provided. All categories contain images having the content as mentioned in category name. Widely accepted quantification measures precision rate and recall rate have been computed to demonstrate the strength of proposed solution. Precision and recall rates have been computed with the help of following expressions.

$P = \text{Relevant retrieved images} / \text{Total retrieved images}$

$R = \text{Relevant retrieved images} / \text{Total images in that category}$

Table1. Categories of Test Images

S. No.	Name of Category
1	Butterfly
2	Voyage
3	Sunset
4	Flowers
5	Building
6	Food
7	Vehicle
8	Horses
9	Beach

A tradeoff has always been observed between precision and recall as ratio of retrieved images to total images is defined as recall and ratio of accurate images to retrieved images of that category is defined as precision. A good balance can be maintained by retrieving a maximum number of accurate images according to the image provided as query image.

The proposed method is intended to retrieve 50 images per search but due to space limitations top 20 results of first 3 categories have been presented in Figure 10.

Query Image



Retrieved Images



a) Results of first 20 Retrieved Images of Butterfly, On the top is Query image of Butterfly

Query Image



Retrieved Images



b) Results of first 20 Retrieved Images of Voyage, On the top is Query image of Voyage

Query Image



Retrieved Images



c) Results of first 20 Retrieved Images of Sunset, On the top is Query image of Sunset

Fig: 10. Top 20 Retrieved Results

For comparison, contour based shape descriptors FD [7], CSS [8] and Smallest Rectangle Distance (SRD) [14] have been used. These three shape descriptors have been tested in the same environment as that of proposed method i.e., Intel Core i3 processor, 2.8 GHz processor speed, 2 GB RAM, Windows OS and Matlab 7.0 as a tool used with the same database. Average precision results have been shown in Table 2 and plotted in Figure 11.

Table 2. Comparison of Average Precision

No. of Retrieved Images	FD	CSS	SRD	SADAF
10	0.68	0.62	0.67	0.79
20	0.58	0.6	0.58	0.72
30	0.56	0.49	0.52	0.7
40	0.52	0.44	0.48	0.65
50	0.5	0.4	0.36	0.63

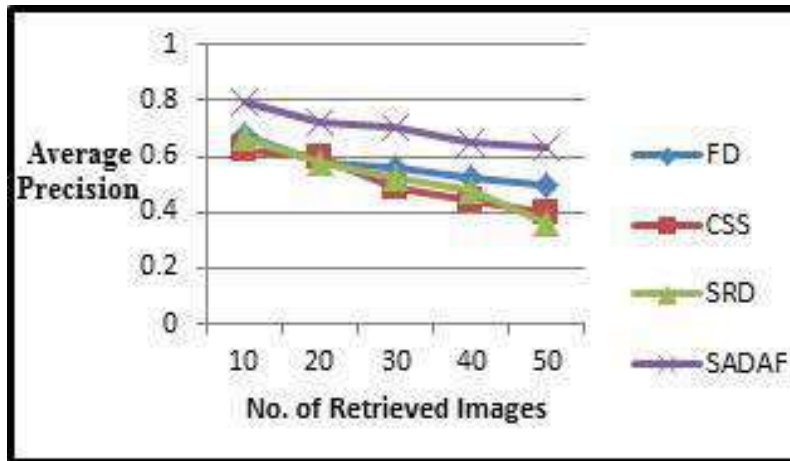


Fig: 11. Comparison Results of Average Precision Rates, Test Image Categories: Butterfly, Voyage, Sunset, Retrieved Images 10, 20, 30, 40 & 50

It is clear from Table 2 and Figure 11 that the proposed solution presents best retrieval performance. As FD and CSS are contour based descriptors, the proposed descriptor is also contour based but it performs much better than both existing contour based descriptors. If features are properly extracted from the image, image matching becomes simpler. Moreover, the system is robust to image alterations like changes in size, scale and orientation. Rotation is controlled through feature direction angle; if the area is less distant from the area of query image and angle is different, in this case the images are same but rotated at the rate of direction angle. Similarly, arc length serves as an identification of change in size and symmetry in change of position. These changes can be observed in Figure 10; all changes are present in retrieved images. System successfully identifies these changes and accurately retrieves the relevant images. Image segmentation simplifies image matching because it narrows down the search space and decreases the processing overheads because in identifying a major or strong object, there is no need to take into account less information presented in the image and wasting the time. Processing speed of proposed solution is very high. It takes 1.5 seconds to calculate the query image features and get them matched with database images. Distance is calculated with Euclidean distance formula and images are sorted. From these sorted images, top 50 images are selected as retrieved images because proposed system is intended to retrieve 50 images per search.

Recall and precision for all nine categories is given in Table 3.

Table3. Proposed System Precision and Recall (%)

No. of Retrieved Images	Category	Precision	Recall
50	Butterfly	79.4	68.1
50	Voyage	78.9	68.8
50	Sunset	78.1	68.2
50	Flowers	78.4	69.9
50	Building	79.8	68.0
50	Food	78.3	69.5
50	Vehicle	79.6	69.6
50	Horses	79.0	69.7
50	Beach	79.9	68.1

From each of nine categories one by one, the system receives a query image to record recall and precision for performance evaluation of system proposed. Total images to be retrieved are selected as 50. Precision and recall of butterfly are 79.4 & 68.1, voyage-78.9 & 68.8, sunset-78.1 & 68.2, flowers-78.4 & 69.9, building-79.8 & 68.0, food-78.3 & 69.5, vehicle-79.6 & 69.6, horses-79.0 & 69.7 and beach-79.9 & 68.1 respectively. This is also plotted in Figure 12. The systems shows an overall mean precision of 79 and mean recall of 68. This shows that the system balances the tradeoff between precision and recall.

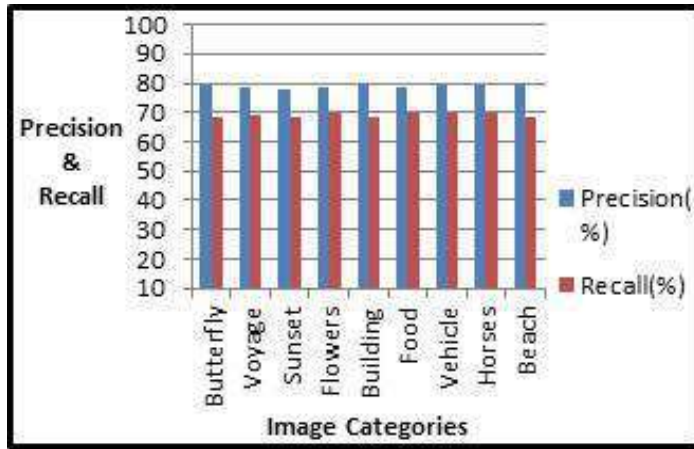


Fig: 12. Precision and Recall (%) of Proposed System

Next, the system receives an image from all nine categories as query image. Desired images which are required to be retrieved are selected as 10, 20, 30, 40 and 50. Precision and recall are recorded which are given in Table 4 and Table 5 respectively.

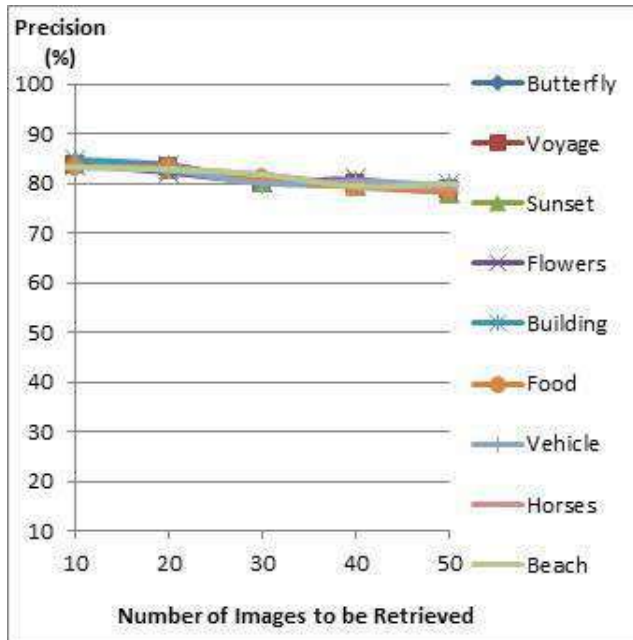
Table4. Precision (%) for No. of Images to be retrieved 10, 20, 30, 40 & 50

Category	No. of Images to be Retrieved				
	10	20	30	40	50
Butterfly	83.7	83.7	80.1	79.9	79.4
Voyage	83.5	83.1	80.4	79.9	78.9
Sunset	84.6	83.0	80.2	79.6	78.1
Flowers	83.8	82.2	80.3	80.8	78.4
Building	84.8	83.7	80.4	79.7	79.8
Food	83.3	83.2	80.8	79.2	78.3
Vehicle	83.5	82.7	80.0	80.5	79.6
Horses	83.2	83.0	81.8	79.7	79.0
Beach	83.2	82.8	81.8	79.4	79.9

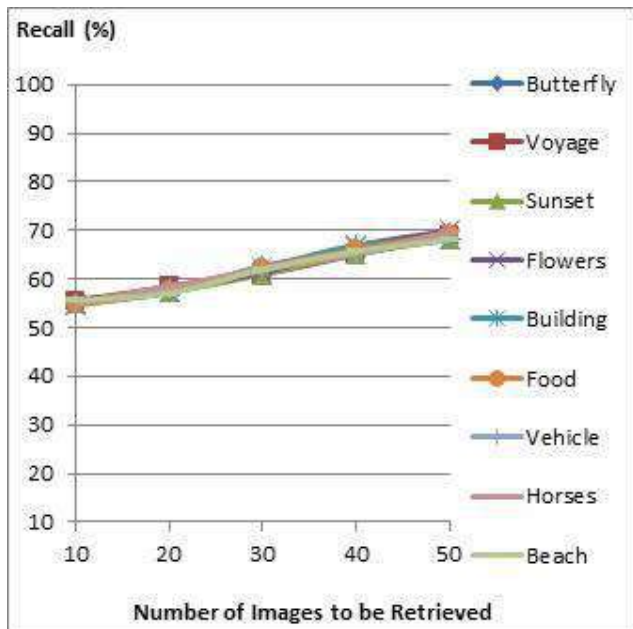
Table 5. Recall (%) for No. of Images to be retrieved 10, 20, 30, 40 & 50

Category	No. of Images to be Retrieved				
	10	20	30	40	50
Butterfly	55.8	57.5	62.6	65.8	68.1
Voyage	55.5	58.4	61.0	65.1	68.8
Sunset	54.9	57.3	61.0	65.2	68.2
Flowers	54.8	58.3	61.3	66.8	69.9
Building	54.8	57.3	62.2	66.9	68.0
Food	54.6	57.7	62.4	66.1	69.5
Vehicle	55.0	58.2	62.2	65.1	69.6
Horses	55.0	58.5	61.9	65.4	69.7
Beach	55.6	57.1	62.0	65.7	68.1

As could be observed from Table 4 and Table 5, when the number of images to be retrieved is low, precision increases and recall decreases. It is due to the fact that recall falls when low number of images is to be retrieved because the relevant retrieved images to total relevant images ration is on the higher side due to high number of relevant images in the database. Whereas the relevant retrieved images and total number of retrieved images ratio decreases in case the number of images to be retrieved is low hence the system retrieves most relevant images efficiently. So, relevant images retrieval needs to be in maximum number for balancing the system. In Figure 13(a) & (b) respectively, precision as well as recall of each category for 10, 20, 30, 40 and 50 images to be retrieved is plotted.



(a) Precision(%) for All Categories for Number of Images to be Retrieved 10, 20, 30, 40 & 50



(b) Recall (%) for All Categories for Number of Images to be Retrieved 10, 20, 30, 40 & 50

Fig: 13. Precision and Recall (%) of Proposed System

CONCLUSION

A new scheme for features extraction has been presented in this study which ensures a fast and accurate retrieval of images on the basis of their shape and color contents. The system is based on the idea of presenting a query image to the system. On the basis of such query image, the system filters out images which are similar in shape and color. Like any other CBIR system, the proposed system also takes into consideration the fact that similar

images have some common features. The features extraction model SADAF selects features in a way that it can recognize image well in case of any image alterations like scaling, translation and rotation. System speed is implementable i.e., it can be implemented in a real time system of CBIR. Image segmentation speeds up the process of features extraction and image matching. The descriptor proposed is a simple and small descriptor that outperforms the existing descriptors.

CONFLICT OF INTEREST

Authors declare no conflict of interest.

ACKNOWLEDGEMENT

None.

FINANCIAL DISCLOSURE

No financial support was received to carry out this project.

REFERENCES

- [1] Rehman, et al; "Content Based Image Retrieval: Survey". *World Applied Sciences Journal*, vol.19, no.3, pp. 404-412, 2012.
- [2] Yasmin, et al; "Use of Low Level Features for Content Based Image Retrieval: Survey". *Research Journal of Recent Sciences ISSN*, vol.2277, p. 2502, 2013.
- [3] Yasmin, et al; "IMAGE RETRIEVAL TECHNIQUES USING SHAPES OF OBJECTS: A SURVEY". *Sci. Int (Lahore)*, vol.25, no.4, pp. 723-729, 2013.
- [4] Yasmin, et al; "Powerful Descriptor for Image Retrieval Based on Angle Edge and Histograms". *Journal of applied research and technology*, vol.11, no.5, pp. 727-732, 2013.
- [5] Mussarat, et al; "Content Based Image Retrieval Using Combined Features of Shape, Color and Relevance Feedback". *KSII Transactions on Internet and Information Systems (TIIS)*, vol.7, no.12, pp. 3149-3165, 2013.
- [6] Mussarat Yasmin, Muhammad Sharif, Sajjad Mohsin, Isma Irum, "An Efficient Content Based Image Retrieval Using El Classification and Color Features", *Journal of Applied Research and Technology*, Vol. 12, 877-885 (October 2014).
- [7] Mussarat Yasmin, Sajjad Mohsin, Muhammad Sharif, "Intelligent Image Retrieval Techniques: A Survey", *Journal of Applied Research and Technology*, Vol. 12, 87-103 (February 2014).
- [8] REHMAN M, SHARIF M, RAZA M. Shape Features Extraction Method for Content based Image Retrieval, *Sindh University Research Journal-SURJ (Science Series)*. 2016 Mar 30; 48(1).
- [9] Rui and Huang: "Optimizing learning in image retrieval," in *Proc. of Computer Vision and Pattern Recognition, 2000. Proceedings. IEEE Conference on* pp. 236-243, 2000.
- [10] Singh and Sontakke; "Neutralizing the Semantic Gap in the Content Based Image Retrieval (CBIR) System". *European Journal of Scientific Research*, vol.75, no.4, pp. 536-549, 2012.
- [11] Han and Ma; "Fuzzy color histogram and its use in color image retrieval". *Image Processing, IEEE Transactions on*, vol.11, no.8, pp. 944-952, 2002.
- [12] Alnihoud; "Content-based image retrieval system based on self organizing map, fuzzy color histogram and subtractive fuzzy clustering". *Int. Arab J. Inf. Technol.*, vol.9, no.5, pp. 452-458, 2012.
- [13] Yasmin, et al; "Content based image retrieval by shape, color and relevance feedback". *Life Science Journal*, vol.10, no.4s, 2013.
- [14] Amanatiadis, et al; "Evaluation of shape descriptors for shape-based image retrieval". *Image Processing, IET*, vol.5, no.5, pp. 493-499, 2011.
- [15] Zhang and Lu; "Shape-based image retrieval using generic Fourier descriptor". *Signal Processing: Image Communication*, vol.17, no.10, pp. 825-848, 2002.
- [16] Jalba, et al; "Shape representation and recognition through morphological curvature scale spaces". *Image Processing, IEEE Transactions on*, vol.15, no.2, pp. 331-341, 2006.
- [17] Bober; "MPEG-7 visual shape descriptors". *IEEE Transactions on circuits and systems for video technology*, vol.11, no.6, pp. 716-719, 2001.
- [18] Flusser and Suk; "Pattern recognition by affine moment invariants". *Pattern recognition*, vol.26, no.1, pp. 167-174, 1993.
- [19] Chen, et al; "Object segmentation of database images by dual multiscale morphological reconstructions and retrieval applications". *Image Processing, IEEE Transactions on*, vol.21, no.2, pp. 828-843, 2012.
- [20] Canny; "A computational approach to edge detection". *Pattern Analysis and Machine Intelligence, IEEE Transactions on*, no.6, pp. 679-698, 1986.
- [21] Li and Wang; "Automatic linguistic indexing of pictures by a statistical modeling approach". *Pattern Analysis and Machine Intelligence, IEEE Transactions on*, vol.25, no.9, pp. 1075-1088, 2003.
- [22] Wang, et al; "Simplicity: Semantics-sensitive integrated matching for picture libraries". *Pattern Analysis and Machine Intelligence, IEEE Transactions on*, vol.23, no.9, pp. 947-963, 2001.
- [23] Eini, et al: "A new Fourier shape descriptor using smallest rectangle distance," in *Proc. of Computer and Knowledge Engineering (ICCKE), 2012 2nd International eConference on* pp. 39-43, 2012.